AFCRL-70-0593
28 OCTOBER 1970
ENVIRONMENTAL RESEARCH PAPERS, NO. 335

ECOM - 5339
RESEARCH AND DEVELOPMENT TECHNICAL REPORT

AIR FORCE CAMBRIDGE RESEARCH LABORATORIES
L. G. HANSCOM FIELD, BEDFORD, MASSACHUSETTS

ATMOSPHERIC SCIENCES LABORATORY
U. S. ARMY, WHITE SANDS MISSILE RANGE, NEW MEXICO

Fog Modification by use of Helicopters

VERNON G. PLANK
ALFRED A. SPATOLA
JAMES R. HICKS

United States Army

United States Air Force

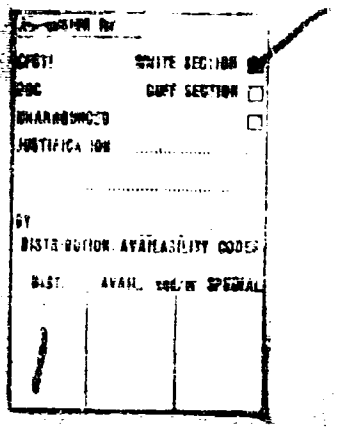

AFCRL-70-0593
28 OCTOBER 1970
ENVIRONMENTAL RESEARCH PAPERS, NO. 335

ECOM - 5339
RESEARCH AND DEVELOPMENT TECHNICAL REPORT

METEOROLOGY LABORATORY PROJECT 7605

AIR FORCE CAMBRIDGE RESEARCH LABORATORIES
L. G. HANSCOM FIELD, BEDFORD, MASSACHUSETTS

ATMOSPHERIC MODIFICATION TECHNICAL AREA, TASK ITO.61102.B53A.20

ATMOSPHERIC SCIENCES LABORATORY
U. S. ARMY, WHITE SANDS MISSILE RANGE, NEW MEXICO

Fog Modification by use of Helicopters

VERNON G. PLANK
ALFRED A. SPATOLA
JAMES R. HICKS *

A joint U.S. Army - U.S. Air Force project in warm fog modification is reported in this document.

*Cold Regions Research and Engineering Laboratory
Hanover, New Hampshire

United States Army

United States Air Force

AIR FORCE (1) 30 DECEMBER 1970 - 1350

Abstract

Results of helicopter clearing experiments conducted at the Greenbrier Valley Airport, Lewisburg, West Virginia, during the period 7 to 29 Sept 1969, are presented and discussed. Thirty-five hover experiments and 18 runway-clearing experiments were performed on 10 separate days with fog layers ranging from 125 to 525 ft in depth. The hover experiments, which were successful in virtually all cases, yielded clearings that varied from 400 to 2800 ft in length extent. The largest clearings occurred with the shallowest fog during tests conducted within one hour or so of the natural dissipation time of the fog. The runway-clearing experiments were successful in clearing the full 6000 foot extent of the runway on two occasions, were partially successful on four occasions and were unsuccessful on 12 occasions. Six helicopter landings were accomplished through artifically-created clearings.

Particular quantitative results of the hover experiments are described. The wake penetration distance of the helicopters ranged from about 700 to 1000 ft. The steady-state clearing times varied from approximately 150 to 260 sec. The total entrainment (mixing) of environmental air into the wake air during the steady-state period was between 350 and 1050 percent. The clearing ratios, the ratios of cleared volume to down-transported volume, had values of 1.8 to 8.7. The clearing persistence, following helicopter departure from the test sites, varied with fog depth, and with the convective state of the fog, from as little as 1 to 2 min to as much as 25 to 30 min. The cleared zones at the surface level were characterized by temperatures 0.3 to 3.0^{o}C warmer than ambient, by relative humidities near 100 percent, by specific humidities that were 0.1 to 1.2 gm/kg

larger than the saturated specific humidities of the fog surroundings, and by downwash-groundwash wind velocities of 6 to 20 mph with peak gust speeds of as much as 50 mph.

Conclusions about the wake characteristics and fog-clearing capabilities of helicopters are discussed in a separate appendix. The conclusions are based on existing theory and on the totality of the findings of the Lewisburg Program, as well as those of the Thule AFB Program (conducted previously by CRREL) and the Eglin AFB and Smith Mountain Programs (conducted previously by AFCRL).

Optimum flight procedures for fog-clearing are discussed and reoommendations are made for future research efforts.

Contents

Contents

Illustrations

Illustrations

Tables

Tables

Fog Modification By Use of Helicopters

1. INTRODUCTION

The cloud and fog-clearing capabilities of helicopters have been demonstrated for particular flight and cloud physics conditions by Hicks (1965). Plank and Spatola (1969), and Plank (1969). In the reported experiments, cleared zones of 500 to 5000 ft length extent were created in stratus clouds and ground fog within time periods of 5 to 15 min.

The data acquired in these experiments were mostly of a qualitative type, obtained simply to demonstrate the feasibility of the helicopter clearing technique. Hence, as an extension of these prior tests, and in an attempt to secure quantitative rather than qualitative clearing information, the U.S. Air Force (Air Force Cambridge Research Laboratories) and the U.S. Army (Atmospheric Sciences Laboratory) conducted a joint helicopter-fog-clearing-program at the Greenbrier Valley Airport, Lewisburg, West Virginia, during the period 7 to 29 Sept 1969. The U.S. Marine Corps (Development and Education Command) also participated in the program.

This program, referred to as the "Lewisburg Program," is described in this report. The official title assigned to the program was "Project Downwash."

Before proceeding to this description, it might be pointed out that the theoretical basis for this type of cloud or fog clearing with helicopters rests primarily

(Received for publication 28 September 1970)

on the principle of downwash mixing. No seeding agents are employed whatsoever. The helicopter, during clearing, either hovers or moves slowly forward in the clear air above the cloud layer. This clear air at flight altitude has a relative humidity of some value less than 100 percent and is, of course, devoid of liquid water. The downwash action of the helicopter rotor(s) forces this clear air downward into the cloud or fog layer, to distances of the order of 500 to 1000 ft, the exact distance being dependent on the atmospheric conditions and the type of helicopter employed. The wake air, on descending, entrains and mixes with the cloudy air of the surroundings and the cloud droplets along the course of the wake are totally or partially eliminated by evaporative mixing. The dimensions of the clearings created by the helicopter wake are generally much larger than those of the helicopter itself, usually some 10 to 20 times larger. This too is a product of the entrainment-mixing process.

2. THE LEWISBURG PROGRAM

2.1 Program Objectives

The Lewisburg Program was undertaken to ascertain quantitatively the fog-clearing capabilities of helicopters of different types (CH-46, CH-47 and CH-54 types) under various cloud physics conditions. Specifically, the objectives were (1) to determine the volumetric size of the clearings that could be created in the fog layers within particular time periods by means of (a) hovering the helicopters above the fog top at different altitudes, and (b) flying the helicopters across the top of the fog at different altitudes and airspeeds; (2) to ascertain the most practical and efficient modes of flying helicopters to achieve an optimum, continuous clearing over a particular ground location or along an airport runway; (3) to establish the "persistence times" of the clearing created under objectives (1) and (2); and (4) to acquire information about the types of flight aids needed for safe and effective clearing operations.

2.2 Plans for Accomplishing Objectives

To accomplish these objectives, plans were made in the Spring and Summer of 1969 to select an appropriate airport field site which had a high incidence of occurrence of radiation-type fog and to provide the observational-measurement facilities to permit the conduct of two basic types of experiments, hover experiments and runway-clearing experiments.

The hover experiments were considered to be the best means for acquiring quantitative data concerning the "clearing effectiveness" of helicopters. Clearing

effectiveness, neglecting definition details, is described in terms of a volumetric ratio which specifies the volume amount of cloud clearing that is produced (in any particular experiment during a given time period) relative to the total volume amount of air that is down-transported across the rotor disk area of the helicopter during this same period. The denominator parameter of the ratio, the down-transport volume, can be readily determined from aerodynamic theory for a hovering helicopter, where the helicopter suspension force is supplied solely by rotor (propeller type) lift. But the down-transport volume, that is, the downward volumetric component of the total wake circulations, cannot, at present, be reliably determined for a helicopter in forward flight, where part of the suspension force is supplied by rotor lift and part by aerodynamic (moving wing type) lift. Existing observational-theoretical knowledge of helicopter wakes, in their totality, is inadequate to permit such determination (refer to Appendix D).

The hover experiments were also emphasized in the program planning because a mathematical model had been developed to describe the helicopter fog-clearing situation of the hover mode. Experimental verification of the model was desired to permit its later use for extrapolation-prediction purposes, to forecast the particular meteorological conditions under which helicopters could clear fog operationally, and those under which they could not. This model will be described in a separate report.

The runway-clearing experiments were designed to obtain semi-quantitative data concerning the meteorological conditions for which runway-clearing was possible, or impossible, concerning the number of helicopters and flight patterns that had to be employed, concerning the airspeeds and flight altitudes required to achieve optimum effects, and concerning the sizes, wind-drift characteristics and persistence of the cleared zones produced.

2.3 Selection of the Test Airport and Base Airport

As pointed out by Plank (1969), the type of fog that is most amenable to clearing by the helicopter downwash technique is radiation fog of thickness less than about 500 ft. Other particular types of fog can also be cleared by the technique, for example, shallow maritime-advection-fog, Hicks (1965), steam fog, hillside stratus; but radiation fog is undoubtedly the most-frequently-occurring clearable type.

The classic fog study by Stone (1936) shows that radiation fog of Appalachian Valley type has a maximum annual frequency of occurrence over the region of the State of West Virginia. From a climatological study of 9 years of data for White Sulphur Springs, West Virginia, conducted as part of the advance planning work of the Lewisburg Program, Spatola (1970) found that this type of fog occurred

most frequently during the months of August and September. There were 13 days with visibilities equal to or less than 1/8 mile during the early morning period after sunrise in August, and during the month of September there were 12 days.

Based on the results of these studies, the Greenbrier Valley Airport, at Lewisburg, West Virginia, (located about 8 miles NW of White Sulphur Springs, see the map of Figure 1.) was selected as the "test airport" for the fog-clearing program and the month of September was chosen as the month for the program operations. September was chosen, rather than August, because the variability of the fog conditions during September, primarily the variability of fog thickness and of the upper-air properties above the fog layers, was greater, climatologically, than in August. A greater diversity of fog situations appeared to be available for experimentation in September; and this was desirable for the purposes of the program.

The helicopters themselves could not be based at the test airport, since the fog conditions there would prohibit flight operations, that is, would prevent take-offs and landings. They had to be based at some nearby airport which normally remained clear of fog and open for flying, and which also had the necessary facilities (navigational aids, fuel, parking space, maintenance) required to support the helicopter operations. Woodrum Field, in Roanoke, Virginia, was selected as the "base airport." This airport is located about 46 miles SE of the test airport.

2.4 The Helicopters and Observational Aircraft

The U.S. Army provided four helicopters for the purposes of the program. A CH-54A (Flying Crane) helicopter was supplied by the 291st Aviation Company, Fort Sill, Oklahoma. This helicopter was employed during the period 7 to 13 Sept but became inoperative on the latter date due to a mechanical malfunction for which repair parts were not readily available. It was replaced by a second CH-54A helicopter, from the same organization, which was present during the period 23 to 29 Sept. A CH-47A (Chinook) helicopter was furnished by the 177th Aviation Company, Fort Benning, Georgia, and was utilized during the period 11 to 27 Sept. A CH-47C helicopter was provided by the Aviation Detachment, U.S. Army Electronics Support Command, U.S. Naval Air Station, Lakehurst, New Jersey, and was flown during the period 23 to 29 Sept.

The U.S. Marine Corps (Marine Corps Squadron One, Marine Corps Air Station, Quantico, Virginia) furnished a CH-46 (Sea Knight) helicopter for the period 23 to 29 Sept.

The U.S. Air Force (103rd Special Operations Group, West Virginia Air National Guard, Charleston, West Virginia) supplied a C-119 (Packet) aircraft

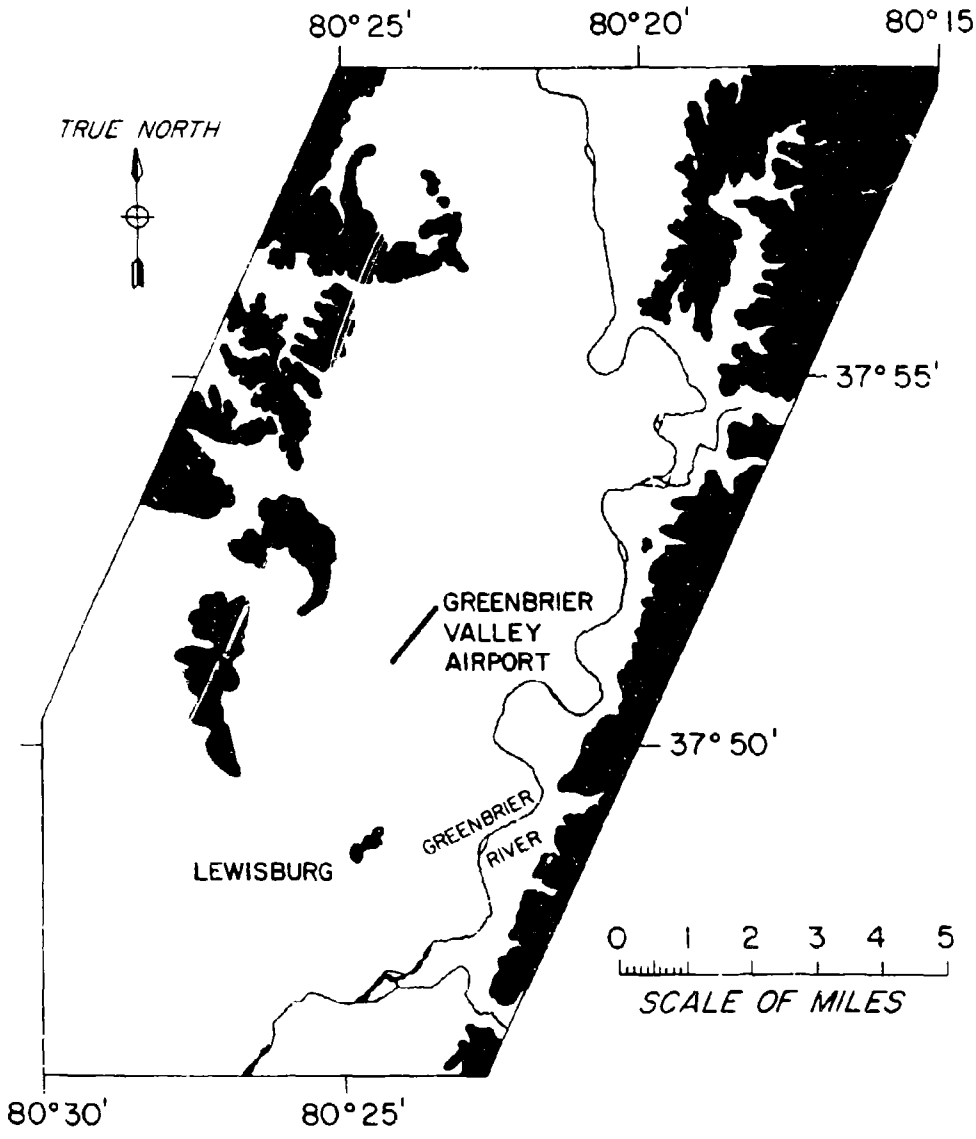

Figure 1. Topographical Map of the Greenbrier Valley Showing Airport Location. Terrain with elevation exceeding 2350 ft is indicated in solid black. The airport field elevation is 2301 ft

that was employed throughout the program for the purpose of command, observation and aerial photography.

Photographs of these helicopters and aircraft are shown in Figure 2. The weight, rotor-diameter and fuel consumption specifications of the helicopters, are given in Table 8 which is described later.

A listing of project and flight personnel who were based at Roanoke, Virginia, and who were involved in the flight-operations part of the Lewisburg Program is provided at the end of the report.

2.5 Special Aircraft Instrumentation

A Cambridge-System dew-point recorder, a Johnson-Williams liquid-water content (LWC) meter and a time-event recorder were installed and operated in the CH-54A helicopter during the period 7 to 12 Sept, in the CH-47A helicopter during the period 13 to 22 Sept; and in the CH-47C helicopter during the period 23 to 29 Sept. The upper left hand photograph of Figure 3 shows how the instrument sensors were mounted outboard of the helicopter.

A time-event recorder and a Mitchell motion-picture camera were installed in the C-119 aircraft and were operated on each of the missions.

Professional motion-picture photographers were employed aboard one, and sometimes two, of the helicopters and the C-119 aircraft to photograph the results of the clearing experiments. One photographer was provided by the U.S. Army Cold Regions Research and Engineering Laboratory, Hanover, New Hampshire; two others were provided by Detachment 5, Aerospace Audio and Visual Services, Andrews AFB, Virginia. The methods of photography (downward and rearward-directed from the helicopters and sideward-directed from the C-119) are illustrated in Figure 3.

2.6 Surface and Upper-Air Measurements and Observations at the Test Airport

The Greenbrier Valley Airport is situated along the approximate centerline of the Greenbrier Valley and lies about 5 miles North of the town of Lewisburg. The general valley topography and location of the airport are indicated in Figure 1. The runway at this airport is 6000 ft long, oriented 040 to 220° magnetic, as shown in Figure 4.

Surface and tethered-balloon measurements of the fog and meteorological conditions at this airport were made on each day that clearing missions were flown. Temperature, humidity, wind speed and direction, visibility, drop-size-distribution and liquid-water-content (LWC) were measured at the surface level. Profiles of the first four parameters were obtained through the fog layer to altitudes 100 to 500 ft above the fog top.

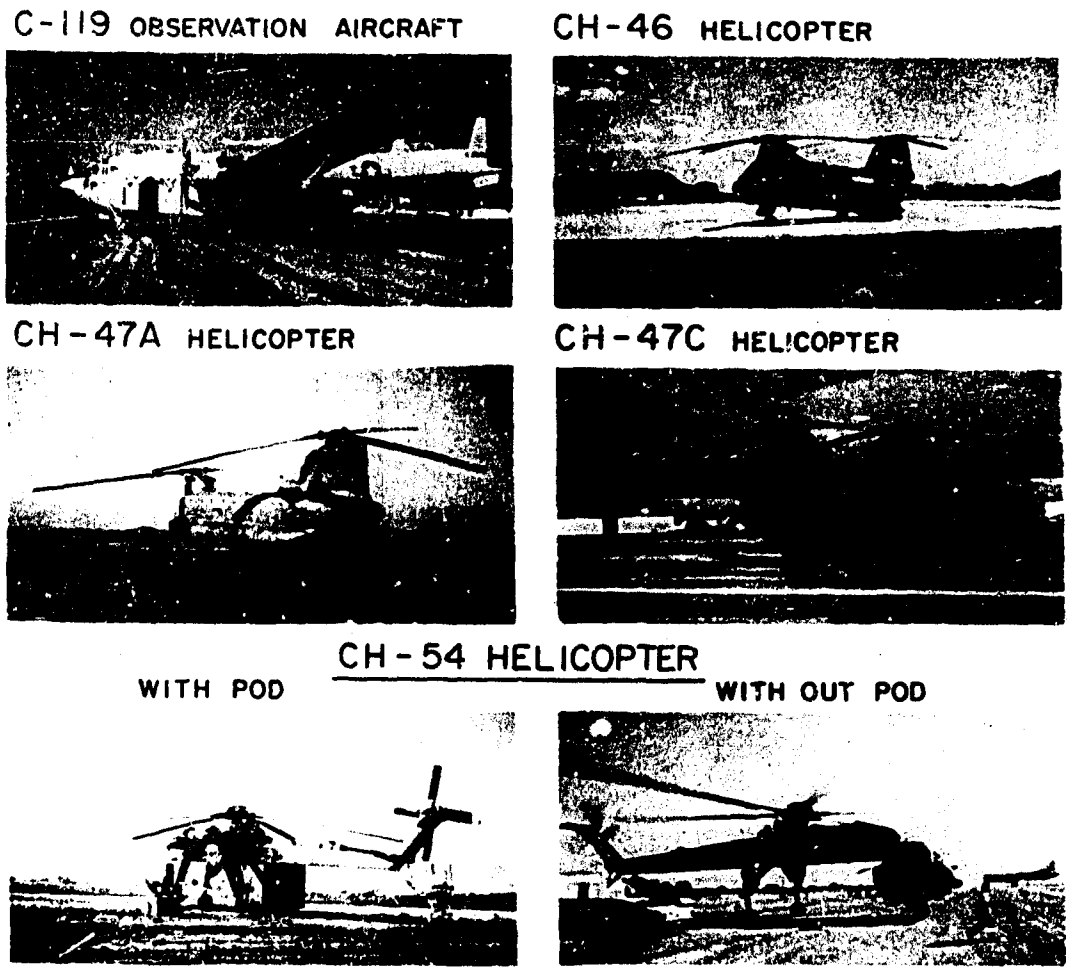

Figure 2. Photographs of Observational Aircraft and Helicopters used in Lewisburg Program. The weight, rotor diameter, and fuel consumption rate specifications of the helicopters are listed in Table 8

Surface observations with standard instruments were made at 30 min intervals throughout the periods of fog from the Site 1 location at the NE end of the runway (refer to Figure 4). Numerous visibility markers were erected at particular distances from the Site 1 location to provide means of estimating visibilities within the fog. Drop-size and LWC measurements were made at approximate hourly intervals, using a whirling-arm, slide-sampling device, from a site near the airport terminal building.

Two standard wiresonde instruments were operated from Sites 1 and 2 to obtain profiles of temperature and humidity through the fog layer to altitudes of about 700 ft. Wiresonde ascents were usually made during the periods 0300 to 0400

Figure 3. Photographs Illustrating Methods of Aerial Photography and of Mounting Temperature-Dew Point Sensor in the Helicopter. The boom-mounting of the sensor is shown at the upper left. The same photograph also reveals how the photographer positioned himself to secure down pointing photographs of the clearing events. Rearward-pointing photography was accomplished from the helicopter as illustrated at the lower left, looking out the open back ramp of the helicopter. Motion pictures were acquired from the C-119 observational aircraft from the rear door position indicated in the photograph at right

and 0600 to 0700 EDT. No soundings were made after the latter time, because the fog-clearing operations customarily commenced at sunrise and because the balloons, elevated above the fog, were then employed as site location markers for the helicopter and aircraft personnel flying aloft. No wiresonde ascents could be made from the airport at any time other than when the airport was closed due to fog. FAA regulations prohibit tethered balloon flights near an active runway.

The wiresonde balloons were also used to obtain wind direction information within the fog layer. The balloons had aerodynamic flight characteristics* and the wind direction was determined (as a function of height) by observing and recording both the ballon pointing direction, where the vertical visibilities in the

*See footnote on following page

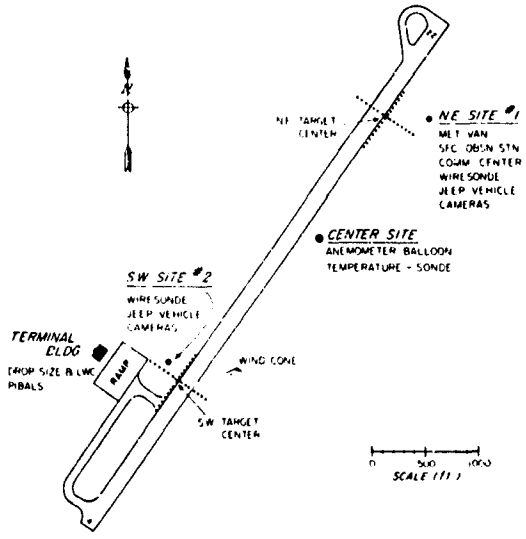

Figure 4. Map Diagram of the Greenbrier Valley Airport, Showing Runway Test Sites and Instrument Locations. Refer to text for description of measurements performed

fog permitted, and the azimuth direction of the "lean" of the balloon-tether cable.

Another, smaller "temperature-sonde" unit was used to obtain temperature sounding information to a height of about 175 ft at 1 to 2 hr intervals. These soundings were made mostly from the center-site location, but sometimes were made from near the terminal building. The temperature readings from this instrument were judged to be more accurate than those of the other wiresonde instruments.

A Schjeldahl balloon (Figure 5), 30 ft long and with aerodynamic flight characteristics*, was elevated from the center site and was used to carry an anemometer aloft. The wind speed readings of this anemometer were telemetered to the ground and recorded. Thus, wind speed profiles through the fog layer and above it were obtained at times corresponding to those of the wiresonde ascent times. Wind direction information from above the fog top was also obtained from this balloon by the flight personnel aloft, who noted and recorded the pointing direction of the balloon at different balloon altitudes.

A pibal ascent was made on each day of operation immediately after the fog layer dissipated and it became possible to track the pibal balloon. Wind readings were made at 500 ft intervals, from the surface to an altitude of about 5000 ft.

Two "target sites" for the helicopter hover experiments were established near the Site 1 and Site 2 locations, see Figure 4 for the precise locations. Orthogonally-oriented lines of small, tethered balloons (10 g size, helium-filled, spaced 50 ft apart, tethered on cords approximately 5 ft long) were set up at the sites before experiments began. One line of balloons was oriented parallel to the runway, the other normal to the runway. There were 14 balloons in each line, excluding the common, central one, and the terminal balloons were located 350 ft

*These aerodynamic characteristics were that the balloon had a streamlined shape and had tail fins, which kept the nose of the balloon always pointed in the approximate direction of the flight altitude wind.

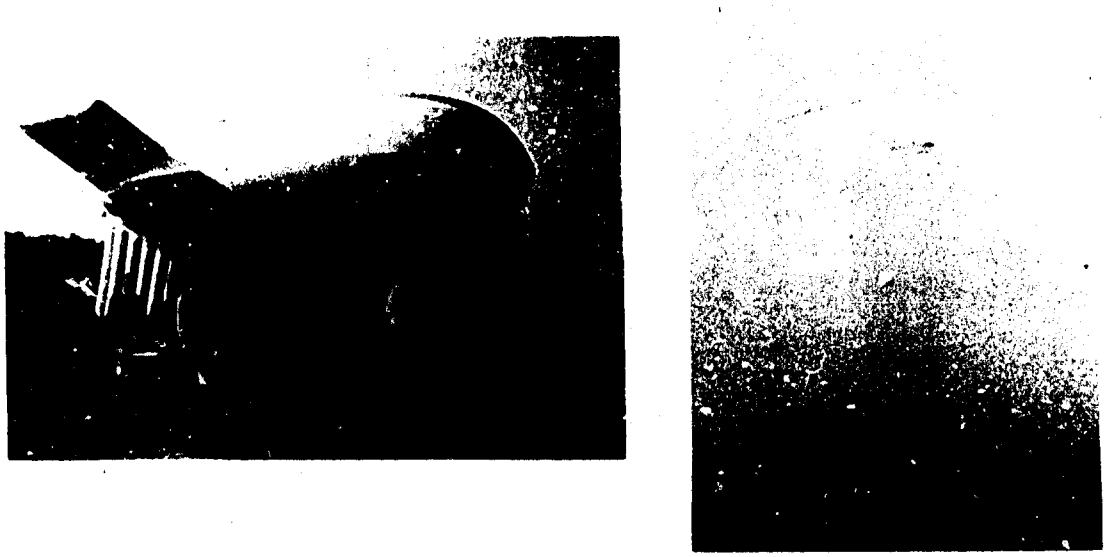

Figure 5. Photographs of Schjeldahl Anemometer Balloon. Wind speed measurements within the fog layers were obtained and telemetered to the ground using this low-level sounding balloon of the U.S. Army. A close-up view of the balloon and readout equipment is presented at the left. The right hand photograph shows the balloon ascending into the fog on one of the test days

from the target center. Red balloons were used, primarily because they were readily available. Photographs showing one line of these balloons before and during helicopter clearing are presented in Figure 6.

The balloons at the target sites were employed to indicate, by their swaying, bouncing motions, the approximate speed and area extent of the helicopter downwash. They also served as indicators of visibility-enhancement effects. For example, while only the second balloon from center might have been visible before downwash clearing, the seventh balloon from center might have been visible during clearing.

Time-lapse cameras, mounted on eye-level swivel bases, were set up at each of the target centers to record the downwash and visibility-enhancement events revealed by the tethered balloons (Figure 7). The cameras were swung manually in the direction of the predominant fog-clearing events. The cameras were also operated during periods before and after the experiments, to record the normal wind and visibility events.

Portable, hand-held anemometers were used during certain experiments to obtain measurements of the speed of the horizontal "ground-wash wind" of the helicopter wake.

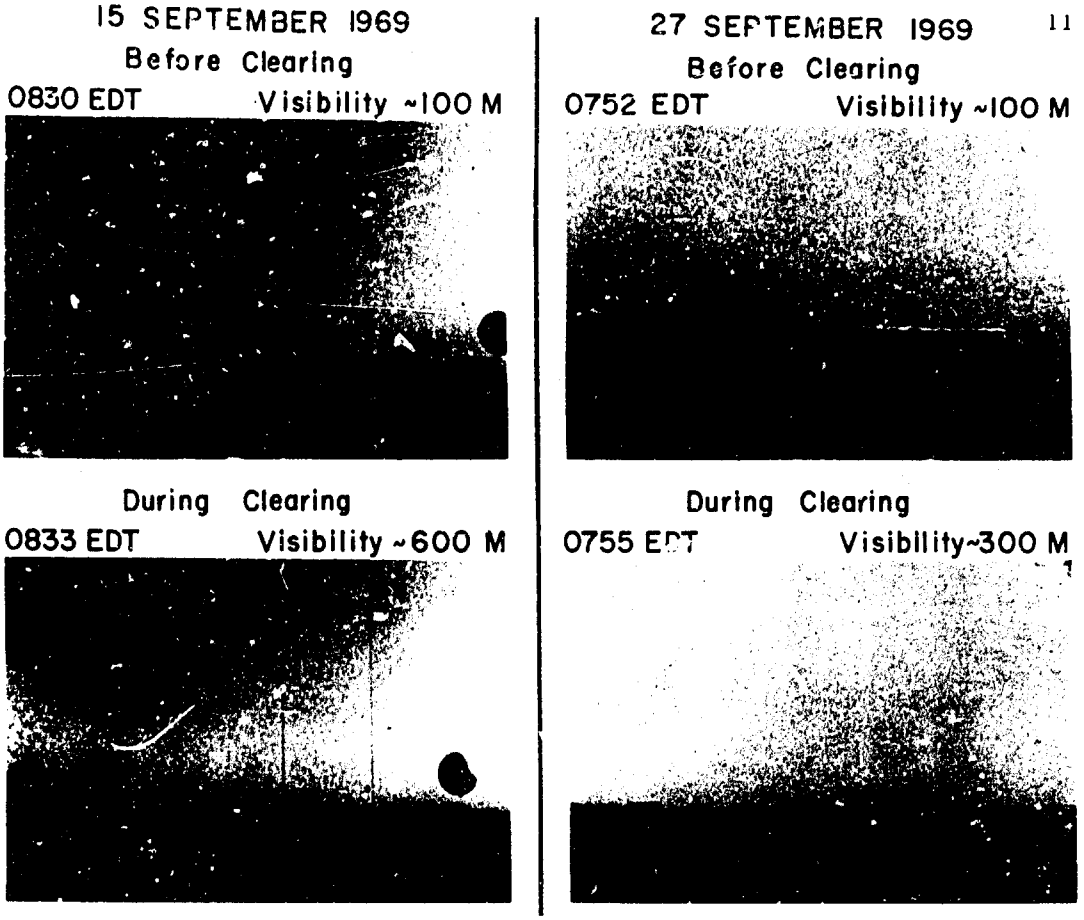

Figure 6. Before-Clearing and During-Clearing Photographs of One of the Lines of Tethered Balloons at the NE Site. The photographs show clearings produced in Test 1 of 15 Sept 1969 (at left) and in Test 1b of 27 Sept 1969 (at right). The balloons farthest from view in the latter test have been carried, and are being held, close to the ground by the helicopter downwash

Cambridge Systems dew-point recorders were mounted in two jeep vehicles that were employed at the target sites during hover experiments, to obtain horizontal profiles of temperature and dew-point across approximate diameter lines of the circular downwash zones. The jeeps were stopped periodically during their travel to obtain stable instrument readings at particular places within the zones. The measurement technique was quite successful and much useful data were acquired. A photograph of one of the jeep vehicles is shown in Figure 8.

Professional photographers with Aeroflex motion-picture cameras were stationed near each of the target sites to record the downwash clearing events that occurred in their vicinities during the experiments. A clock was photographed

Figure 7. Photograph of One of the Time-Lapse Cameras. These cameras were used at the NE and SW sites to record the visibility-enhancement and downwash events of the helicopter tests. The cameras were pointed manually in the direction of the predominant effects that were revealed by the tethered balloons of the two target networks. Pictures were obtained at 1.5 sec intervals

at the beginning and end of each continuous sequence of motion picture footage and the framing rate of each of the cameras was accurately established. Hence, the occurrence time of any particular event shown in the photographs could be determined later.

Air-ground communication between the field site and the aircraft aloft was maintained by VHF and UHF radio. Communication between the various ground stations, including the mobile jeep vehicles, was accomplished by walkie-talkie radio and by land-line telephone. All air-ground communications were recorded on tape. The tapes were timed and transcribed later, to provide a time history of all pertinent voice conversations concerning the experiments.

Field operations for the U.S. Army at the test airport were directed by Dr. Emily M. Frisby, who was also the co-director of the overall program. Field operations for the U.S. Air Force at the test airport were managed by Mrs. Elizabeth L. Kintigh. Surface meteorological measurements and observations were made by nine observers of the Meteorological Support Activity, Fort

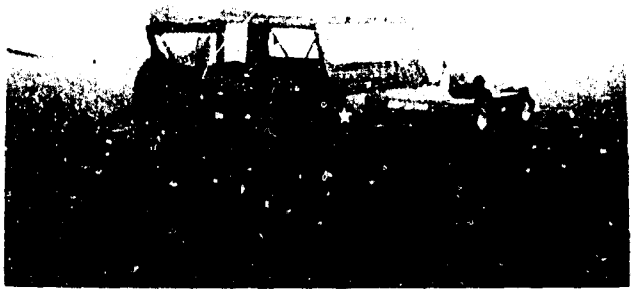

Figure 8. Photograph of Jeep Vehicle used to Obtain Temperature-Dew Point Information within Cleared Zones. The instrument sensor is shown mounted on the pipe that slopes upward from the back of the jeep. The power-supply, amplifier and recorder were carried in and monitored from the rear seat location

Huachuca, Arizona. Wiresonde, pibal and tethered balloon support was furnished by five persons from the 6th Weather Squadron, Mobile, Tinker AFB, Oklahoma. The "anemometer balloon" was supplied by the Engineering Development Technical Area, Atmospheric Sciences Laboratory, Fort Monmouth, New Jersey, and was operated by two of its personnel. The drop-size and LWC measurements were made by an individual from the U.S. Army Cold Regions Research and Engineering Laboratory, Hanover, New Hampshire, which also furnished the small "temperature-sonde" unit. Two jeep vehicles and drivers were provided by the Transport Office, Fort Monmouth, New Jersey. Motion-picture photography was accomplished by two persons from Detachment 5, Aerospace Audio and Visual Services, Andrews AFB, Virginia.

A list of the particular participants in the field site operations is presented in Section 13 of this report.

3. TYPICAL OPERATIONAL DAY

The nature of the Lewisburg program can perhaps best be summarized by describing the events of a typical operational day.

The fog situation at the Greenbrier Valley Airport (Lewisburg Airport) was monitored throughout the evening and early-morning hours by the project personnel at this airport. The synoptic weather situation was monitored by the project personnel stationed at Roanoke, Virginia. The facilities of the U.S. Weather Bureau Office at Woodrum Field were employed.

A decision to begin, or not begin, field measurement operations at the Lewisburg Airport was made at about 0230 EDT, by telephone conference between the Roanoke and Lewisburg personnel. A second, final decision, to conduct or not conduct a fog-clearing mission, was made approximately 0430 EDT, also by telephone conference.

On days with missions the C-119 aircraft departed Woodrum Field at about 0630 EDT and arrived over the Lewisburg Airport at about 0650 EDT, some 10 min before sunrise. The C-119 reconnoitered the airport, and the project flight crew obtained initial photographs of the fog situation and checked the positioning and altitudes of the marker balloons that had been elevated from the ground to indicate the locations of the test sites and runway.

The helicopters, one or several, departed Woodrum Field at about 0640 EDT and arrived over the Lewisburg Airport at about 0700 EDT.

The hover experiments were conducted first. If only a single helicopter was present, it hovered initially over one of the target sites, the pilot maintaining his position by reference to the marker balloon. Then, after steady-state clearing conditions had been attained and all ground measurements completed, it moved to the second target site and hovered there, usually at a different altitude than at the first site. If two helicopters were present, they hovered simultaneously over the two sites, sometimes at the same altitude, sometimes at different altitudes. If more than two helicopters were present, separate sets of experiments were conducted involving all of the helicopters.

The runway-clearing experiments were performed next. The marker balloons were shifted back from the immediate runway vicinity and were aligned parallel to the runway. The helicopters, singly or in formation, flew various kinds of clearing patterns across the fog top, (a) racetrack patterns, (b) 90 to 270° loop-turn patterns, and (c) back-and-forth, hover-turn patterns.* Sometimes these patterns encompassed the full 6000 ft extent of the runway; sometimes they included only a portion of the runway.

On particular days, following the runway-clearing experiments, attempts were made to create clearings by hovering, through which the helicopters could land at the fog-enshrouded airport. These "hover-to-land" experiments were conducted when the fog situation was appropriate.

After the performance of these several types of experiments, the helicopters and observational aircraft returned to Roanoke, Virginia. A pibal ascent was made at the test airport and the field operations were terminated for the day. Termination time was usually about 0830 to 0930 EDT.

---

*The 90 to 270° turn is a standard turn wherein the pilot first turns right, climbs and then circles around to the reciprocal heading of his former, before-turn heading. The back and forth pattern cited above is described in Section 6.

4. METEOROLOGICAL CONDITIONS ON DAYS OF OPERATIONS

4.1 Initial Conditions and Time Cross Sections

Helicopter fog-clearing operations were conducted on 10 separate days during the September period. The specific dates and times of the clearing missions and individual experiments conducted are identified in Appendix A and in Tables 1 and 6. Pertinent information about fog depth, top appearance, surface visibility and helicopter flight altitudes is provided in these tables.

Photographs illustrating the initial appearance of the fog layers over the Lewisburg Airport, prior to the commencement of the tests, are presented in Figure 9. The approximate, mean-sea-level altitude of the fog-top at the time of photography is indicated.

The time history of the fog situations and associated meteorological conditions is summarized in the time cross sections of Figure 10. The drafted information and diagram isolines are explained in the caption. It can be seen that the fog over the airport which customarily formed about 0200 to 0400 EDT progressively deepened with time until about 1 hr after sunrise time (0650 to 0710 EDT), that its depth during the test periods on the different days ranged from 125 to 525 ft, and that it usually dissipated naturally sometime during the period 0930 to 1230 EDT. The manner of the natural dissipation of this fog on one of the days (29 Sept) has been investigated by Plank and Spatola and is described in a report that has been submitted for Journal publication.

The temperature, humidity and wind measurements made in the upper air were obtained mostly before 0700 EDT. As noted earlier, such measurements could not be obtained during experimental periods because the wiresonde and anemometer balloons were required as site-location markers.

Certain of the acquired upper-air data were of dubious accuracy for a variety of reasons which will not be discussed in detail. Data were eliminated from analytical consideration when they failed to compare logically with other synoptically-acquired data. The data of the second wiresonde ascents of most of the days, obtained under conditions of dense fog, were considered to be erroneous. It was speculated that the errors resulted from some type of instrumental "wet bulb effect," or "damp cable effect." Difficulties with these second ascents of the morning were recognized at the time they were made, but the reasons for the troubles were never satisfactorily resolved. Hence, whereas the temperature-dewpoint profiles for these ascents have been drafted on the Figure 10 diagrams, because they indicate the approximate stability-structure of the lower atmosphere, it should be noted that the diagram isotherms for most days were not drawn to conform to the particular temperature values of these

Table 1. Hover Tests, Description and Summary of Results

Date	Time Period EDT	Test No.	Site	Helicopter(s)	Fog Characteristics: Depth ft	Top Appear.	Surface Vis mi	Surface LWC gm/m³	Wind in Fog Layer (Mean): Dir. θ	Speed mph	Hover Level ft	Comments about Plan-View Shape and Sizes of Clearings Produced	Area Extent of Clearing at Surface Level ft² x 10⁶	Time Required to Create Clearing min	Persistence Time of Clearing after Test min
7 Sept	0743-0757	5	NE	CH-54ˣ	500-550	Stable, Hazy	180	---	300	3.1	~700	Circular depression, or hole ~500 ft. dia. (TD)			
11 Sept	0717-0723	2	NE	CH-54ˣ	250-300	Stable	160	---	342	3.0	~500	Elliptical hole, 700x1100 ft. (SD)	0.61		
11 Sept	0817-0830	6a	NE	CH-47A	300-350	Mildly Conv.	90	---	342	3.0	~500	Elliptical hole, 700x800 ft. (SD), 400x450 ft. (TD)	0.44		
11 Sept	0830-0843	6b	NE	CH-47A	300-350	Mildly Conv.	90	---	342	3.0	400-500	Circular depression, or hole, ~500 ft. dia. (TD)			
11 Sept	0857-0910	7	SW	CH-47A	300-350	Mildly Conv.	90	---	342	3.0	~400	Elliptical hole, 500x650 ft. (SD), 300x700 ft. (TD)	0.33		
12 Sept	0706-0720	1	NE	CH-47A	200-250	Stable	115	0.20	269	2.6	~300	Cleared trail, 1000x2800 ft. (SD), 650x2000 ft. (TD)	2.2	~7	5 to 10
12 Sept	0706-0720	1	SW	CH-54ˣ	200-250	Stable	115	0.20	269	2.6	475-575	Cleared trail, 800x3000 ft. (SD), 700x2500 ft. (TD)	1.9	~7	5 to 10
12 Sept	*0743-0750	3	SW	CH-47A & CH-54ˣ	250-300	Mildly Conv.	140	0.09	269	2.6	~350 / ~350	Cleared trail, 700x2500 ft. (SD)	1.4	6	> 3
13 Sept	0715-0732	1	NE	CH-54ˣ	200-250	Mildly Conv.	115	0.11	360	5.4	~300	Elliptical hole, 500x1000 ft. (SD), 400x600 (TD)	.39	8	3 to 4
13 Sept	0715-0732	1	SW	CH-47A	200-250	Mildly Conv.	115	0.11	360	5.4	300-450	Elliptical hole, 600x950 ft. (SD), 400x600 (TD)	.45	5 to 6	3 to 4
13 Sept	*0757-0802	4	SW	CH-47A	200-300	Mildly Conv.	140	0.08	360	5.4	350-400	Elliptical hole, 500x950 ft. (SD), 350x550 (TD)	.37	~9	4 to 5
13 Sept	0812-0824	5	NE	CH-47A	200-300	Mildly Conv.	90	0.08	360	5.4	350-400	Elliptical hole, 450x800 ft. (SD), 350x750 ft. (TD)	.28	~7	4 to 5
14 Sept	0835-0900	1a	NE	CH-47A	500-550	Conv.	90	0.21	343	5.7	575-625	Elliptical hole, 350x700 ft. (SD), 250x300 ft. (TD)	.19	~11	1 to 2
14 Sept	0908-0910	1b	SW	CH-47A	500-550	Conv.	90	0.21	343	5.7	625-675	Elliptical hole, 350x600 ft. (SD), ~250 ft. dia. (TD)	.17		1 to 2
16 Sept	0712-0729	1	NE	CH-47A	175-225	Stable	90	0.17	345	4.5	325-375	Elliptical hole, 700x1300 ft. (SD), 450x1000 ft. (TD)	.71	13	5 to 6
16 Sept	0730-0743	2	SW	CH-47A	200-250	Stable	90	0.17	345	4.5	275-325	Elliptical hole, 900x1300 ft. (SD), 700x900 ft. (TD)	.92	12	5 to 6
16 Sept	*0822-0838	4	SW	CH-47A	200-300	Mildly Conv.	115	0.10	345	4.5	350-450	Circular Hole, 1000 ft. dia. (SD)	.79	10	3 to 4

SYMBOLS KEY

*	Tests conducted for purpose of accomplishing helicopter landing(s)
NE	Northeast site at Greenbrier Valley Airport
SW	Southwest site at Greenbrier Valley Airport
C	Central site at Greenbrier Valley Airport
CH-46	Sea Knight Helicopter, double rotor, weight ~18,000 lb
CH-47	Chinook Helicopter (A and C Models used), double rotor, weight ~26,000 lb
CH-54	Sky Crane Helicopter, single rotor, without cargo pod, weight ~31,000 lb
CH-54ˣ	Sky Crane Helicopter, single rotor, with cargo pod, weight ~37,000 lb
SD	Surface-level dimensions of clearings, determined photogrammetrically from series of photographs or motion picture film by establishing map boundaries of the cleared zone.
TD	Fog-top-level dimensions of clearings or depressions, determined photogrammetrically from knowledge of helicopter dimensions and spacings of marker balloons.

Table 1. Hover Tests, Description and Summary of Results (Cont'd)

Date	Time Period EDT	Test No.	Site	Helicopter(s)	Fog Characteristics: Depth ft	Top Appear.	Surface Vis. m	Surface LWC gm/m³	Wind in Fog Layer (Mean): Dir. 0	Speed mph	Hover Level ft	Comments about Plan-View Shape and Sizes of Clearings Produced	Area Extent of Clearing at Surface Level ft² x 10⁵	Time Required to Create Clearing min	Persistence Time of Clearing after Test min
23 Sept	0726-0746	1	NE	CH-46	250-300	Mildly Conv.	230	0.11	330	5.4	~500	Elliptical hole, 450x1000 ft. (SD), 250x700 ft. (TD)	0.35	2 to 3	
23 Sept	0726-0746	1	SW	CH-47C	250-300	Mildly Conv.	230	0.11	330	5.4	550-650	Elliptical hole, 600x1200 ft. (SD), 400x800 ft. (TD)	0.57	7	
23 Sept	0748-0756	2	NE	CH-54	300-350	Conv.	205	0.09	330	5.4	~700	Elliptical hole, 600x900 ft. (SD), 300x400 ft. (TD)	0.42	~6	4 to 8
23 Sept	0748-0756	2	SW	CH-47C	300-350	Conv.	205	0.09	330	5.4	600-650	Elliptical hole, 600x1400 ft. (SD), 350x1000 ft. (TD)	0.66	5 to 6	4 to 8
23 Sept	0822-0829	5	SW	CH-46 &CH-47A	350-400	Conv.	160	0.09	330	5.4	~450 ~450	Two separate, circular holes, 700x800 ft. dia. each (SD)	~0.44 ~0.44	4 to 6 4 to 6	
23 Sept	*0829-0840	6a	SW	CH-46, CH-47A &CH-54	350-400	Conv.	160	0.03	330	5.4	~450 ~450 ~450	Trail, 800x2200 ft. (SD), at landing time of CH-54 at 0840 EDT	1.4	11	
23 Sept	*0838-0843	6b	SW	CH-46 &CH-47A	350-400	Conv.	160	0.03	330	5.4	~450 ~450	Trail, 1300x2600 ft. (SD), at landing time of CH-47C at 0843 EDT	2.7		
23 Sept	*0843 0845	6c	SW	CH-46	350-400	Conv.	160	0.03	330	5.4	~450	Trail, 1100x2400 ft. (SD), at landing time of CH-47A at 0845:30 EDT	2.1		2½ to 4½
27 Sept	0741-0751	1a	NE	CH-54	450-500	Stable, Hazy	115	0.14	280	4.1	~700	Elliptical hole, 400x600 ft. (SD), 200x400 ft. (TD)	.19	4 to 9	1 to 3
27 Sept	0741-0751	1a	SW	CH-47A	450-500	Stable, Hazy	115	0.14	280	4.1	~600	Elliptical hole, 400x800 ft. (SD), 200x400 ft. (TD)	.25	4 to 9	1 to 3
27 Sept	0751-0802	1b	NE	CH-54	450-500	Stable, Hazy	115	0.14	280	4.1	450-500	Elliptical hole, 450x750 ft. (SD), 200x400 ft. (TD)	.27	5 to 11	1 to 3
27 Sept	0751-0802	1b	SW	CH-47A	450-500	Stable, Hazy	115	0.14	280	4.1	~600	Circular hole, ~700 ft. dia. (SD), residual haze within	.39		
27 Sept	0902-0927	4	NE	CH-47A	450-500	Stable, Hazy	180	0.15	280	4.1	~700	Elliptical hole, 400x600 ft. (SD), 200x400 ft. (TD)	.19	5 to 15	1 to 3
27 Sept	0902-0927	4	C	CH-47C	450-500	Stable, Hazy	180	0.15	280	4.1	575-675	Elliptical hole, 400x600 ft. (SD), 150x350 ft. (TD)	.19	5 to 10	1 to 3
27 Sept	0902-0927	4	SW	CH-46	450-500	Stable, Hazy	180	0.15	280	4.1	~500	Elliptical hole, 400x700 ft. (SD)	.22	5 to 15	
29 Sept	0834-	2	W of Apt.	CH-46 &CH-47C	300-350	Conv.	180	0.09	330	2.9	~500 ~500	Circular hole, ~1600 ft. dia. (SD)	2.0		3 to 8
29 Sept	0911-0924	6a	SW	CH-46	300-350	Conv.	140	0.09	330	2.9	~500	Trail, 700x1300 ft. (SD)	.72		
29 Sept	0927-0935	6b	SW	CH-46	300-350	Conv.	140	0.18	330	2.9	~500	Trail, 800x1600 ft. (SD)	1.0		

Figure 9. Photographs Illustrating the Initial (Before Test) Appearance of the Fog on the Days of Operation. The dates and times of the aerial photographs are indicated. Each was taken looking westward from the vicinity of the Greenbrier Valley Airport and each shows a terrain prominence called "Weavers Knob," which has a peak elevation of 2920 ft. The approximate altitudes (msl) of the fog top of the different days are indicated by the numbers above the photographs at the right. The airport field elevation is 2301 ft.

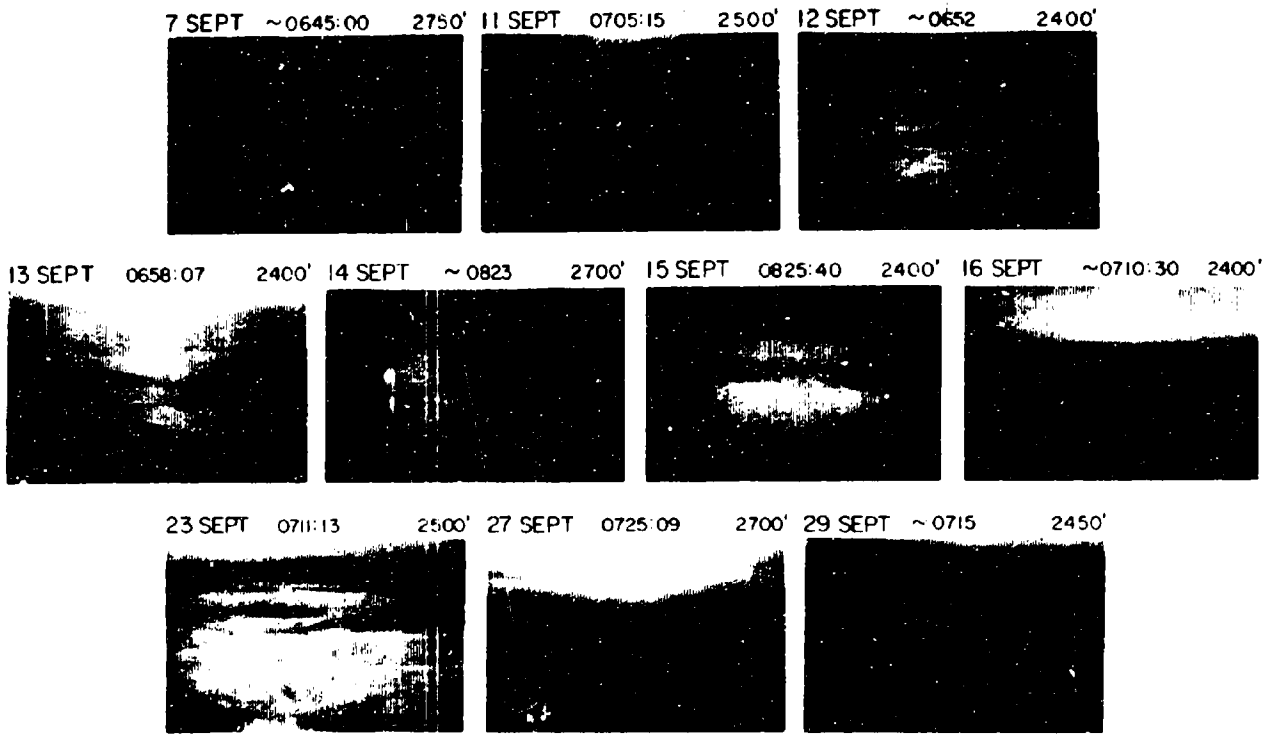
7 SEPT ~0645:00 2750'
11 SEPT 0705:15 2500'
12 SEPT ~0652 2400'
13 SEPT 0658:07 2400'
14 SEPT ~0823 2700'
15 SEPT 0825:40 2400'
16 SEPT ~0710:30 2400'
23 SEPT 0711:13 2500'
27 SEPT 0725:09 2700'
29 SEPT ~0715 2450'

Figure 10. Time Cross-Sections of Meteorological Conditions on Days of Tests. The shaded regions reveal how the fog depth and structure varied with time of day. The regions, where unbounded at the top, indicate that the fog depths were estimated from surface and upper-air information. Where bounded, they indicate that the depths were established from helicopter measurements. The "scalloping" of the upper boundary lines points out the observed nature of the fog-top surface. Profiles of temperature and dewpoint are shown which were obtained by wiresonde instruments (see text criticisms). The fine vertical lines demark the times and vertical extent of balloon ascents made with the U.S. Army "temperaturesonde" unit. Upper winds are shown that were measured in the manner described in the text. Each full barb on a wind arrow represents 2 mph of windspeed. Arrows without barbs signify that wind direction was determined but wind speed was not (the two were measured independently). The isotherms shown are drawn as solid lines, where data were plentiful, as dashed lines, where data were sparce, and as dotted lines, where a theoretical assumption of extrapolation was employed (refer to text). The relative humidities at flight altitude are noted and the black bars in the diagram regions above the fog-top, reveal the time periods and flight altitudes of the hover experiments. The numbers above the abscissa lines give the horizontal visibilities at the surface level (in yards, as observed at the NE site). The numbers above these, within the drafted squares, represent the fog LWC, in gm/m^3

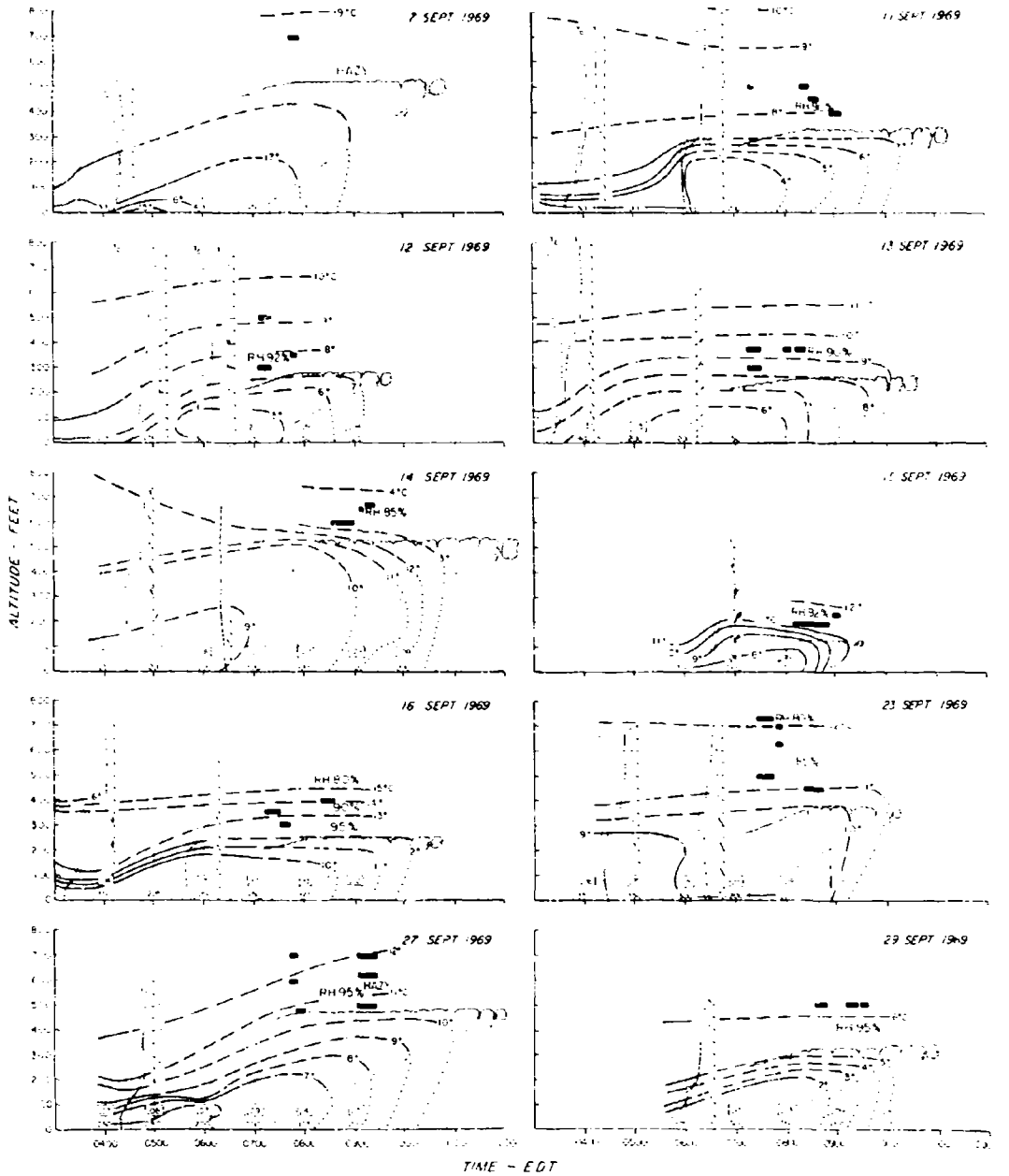
7 SEPT 1969
11 SEPT 1969
12 SEPT 1969
13 SEPT 1969
14 SEPT 1969
16 SEPT 1969
23 SEPT 1969
27 SEPT 1969
29 SEPT 1969
HAZY
RH 95%
ALTITUDE - FEET
TIME - EDT

soundings, since, in comparison with other temperature information, the values at most levels were anomalously small, by about 1 to 2°C. It should also be noted that three classes of "isotherm reliability" are indicated in the drafting by (a) the solid lines, which were drawn where data points were plentiful and considered accurate, (b) the dashed lines, which were drawn to conform to data considered accurate but where the data points were sparce in space and time, and (c) the dotted lines, which are extrapolation lines based on theoretical assumptions about how temperature should vary with altitude above the surface within fog layers heated from below by the sun.*

The isotherms of the cross-section diagrams, their accuracy qualified as discussed above, suggest that the fog layers over the Lewisburg Airport usually formed within or beneath a temperature inversion, which, together with the fog-top itself, progressively lifted in altitude with time until about 0800 EDT. Simultaneously, the entire lower atmosphere below an altitude of about 400 to 500 ft was continually cooled by the radiative heat-loss processes of the early morning period preceding sunrise and extending into the first hour following sunrise, except at the surface level.

Detailed knowledge of the temperature-humidity structure of the lower atmosphere at the particular times of the clearing experiments was unavailable, since measurements could not be made at these precise times. It can only be stated that the atmospheric stability within the fog layer on the different days, averaged vertically over the entire depth of the layer, that is, the values of fog-top temperature minus surface temperature divided by fog depth (from the sectional diagrams corresponding to the test times), ranged generally from about 0.5 to

---

*It was assumed that convection, resulting from surface heating, would progressively "build upward" in altitude, from sunrise time to the dissipation time of the fog, to the levels indicated by the upward-sloping fine-lines of the diagrams. It was assumed that the upward rising currents would ascend moist-adiabatically and that the downward currents would descend following a lapse rate of temperature intermediate between the moist and dry adiabatic rates, which would become closer and closer to the dry adiabatic rate as time approached the natural fog dissipation time. The mean lapse rate of temperature under such conditions, considering both upward and downward motions and time changes, would perhaps be something like 8°C/km, which was the value used to obtain the dotted isotherms of the Figure 10 diagrams. This assumption corresponds approximately to that of standard fog-dissipation forecasting, for example, refer to O'Connor (1945) and Kagawa (1967), but differs somewhat from the fog-temperature profiles of Fleagle, Parrot and Barad (1952), which would be anticipated under stable, non-dissipative conditions.

3.5°C/100 m and that the stability of the clear air layer above the fog-top, to 200 to 400 ft above the top, within the flight altitude region, varied from about 0.8 to 5.7°C/100 m.*

The relative humidity in the upper clear layer at flight altitude ranged from about 80 to 95 percent on the days of tests. On two days (7 and 27 Sept) haze layers existed above the fog-top which made clearing efforts especially difficult for the helicopter pilots because of severely curtailed visibility.

The surface visibility during the test periods ranged from about 90 m to 230 m on the different days. The fog LWC at the surface varied from 0.06 to 0.27 gm/m^3.

The before-test, vertically-averaged, wind speed within the fog layer (Tables 1 and 6) was less than 8.1 mph on all days. The speed was less than 4 mph on 4 days (7, 11, 12 and 29 Sept) and ranged from 4 to 8.1 mph on 6 days (13, 14, 15, 16, 23 and 27 Sept). The corresponding, vertically-averaged, wind directions are also indicated in Tables 1 and 6. The directions were mostly from the NW quadrant, with variation from 269° to 360°.

The surface winds during the test periods are listed in Table 2. The speeds were less than 7 mph and usually about 2 to 3 mph. Except for 7 Sept, the wind directions at the surface level were generally from the NE quadrant, from about 010° to 080°.

4.2 Three Stages of the Fog

The summaries of Tables 1 and 6 and the cross sections of Figure 10 do not reveal certain features of the fog situations that were pertinent to the helicopter clearing tests. Three developmental stages of the fog over the airport were recognizable on the majority of days during the period from sunrise to the natural dissipation time of the fog. We might call these (1) the initial stable stage, (2) the middle convective stage and (3) the final convective-dissipative stage. These stages, for two particular days of the project period, have been described and illustrated by Plank and Spatola in a report that will be submitted for publication.

The helicopter clearing results achieved on any given day during the Lewisburg Program were correlated with these stages of the fog. In general, unless the fog depth exceeded about 400 ft, the clearing results were relatively successful during the stable stage; they were generally unsuccessful during the middle convective stage (unless the fog was shallow, with depth less than about

---

*The rather large stability values within the fog layer result, in part, because the fog-top level sometimes occurred at an altitude higher than that of the base (or break point) of the temperature profile.

Table 2. Surface Winds During Test Periods

Date	Time EDT	Wind Dir. o	Wind Speed mph
7 Sept 1969	0700	200	3.0
7 Sept 1969	0730	305	2.5
7 Sept 1969	0800	135	2.0
11 Sept 1969	0700	Calm	
11 Sept 1969	0730	Calm	
11 Sept 1969	0800	Calm	
11 Sept 1969	0830	Calm	
11 Sept 1969	0900	090	1.0
12 Sept 1969	0700	035	3.0
12 Sept 1969	0730	045	2.0
13 Sept 1969	0700	065	3.5
13 Sept 1969	0730	045	3.0
13 Sept 1969	0800	030	2.5
13 Sept 1969	0830	040	3.5
14 Sept 1969	0800	045	4.5
14 Sept 1969	0830	060	2.5
14 Sept 1969	0900	040	2.5
14 Sept 1969	0930	315	2.0
14 Sept 1969	1000	095	3.0
14 Sept 1969	1030	180	2.0
15 Sept 1969	0800	025	3.0
15 Sept 1969	0830	360	6.0
15 Sept 1969	0900	055	3.5
16 Sept 1969	0700	035	3.0
16 Sept 1969	0730	050	2.0
16 Sept 1969	0800	035	2.5
16 Sept 1969	0830	360	2.5
23 Sept 1969	0700	045	2.5
23 Sept 1969	0730	015	6.5
23 Sept 1969	0800	025	2.0
23 Sept 1969	0830	060	5.0
27 Sept 1969	0700	015	5.5
27 Sept 1969	0730	105	3.5
27 Sept 1969	0800	360	2.5
27 Sept 1969	0830	055	2.0
27 Sept 1969	0900	360	5.0
27 Sept 1969	0930	160	3.5
29 Sept 1969	0700	010	6.0
29 Sept 1969	0730	100	1.5
29 Sept 1969	0800	070	2.5
29 Sept 1969	0830	050	1.5
29 Sept 1969	0900	360	2.5
29 Sept 1969	0930	075	1.5
29 Sept 1969	1000	040	7.0

250 ft); and they were successful once again during the convective-dissipative stage. Clearing during the latter stage was helped materially, of course, by the natural dissipative tendency of the fog.

5. EXPERIMENTAL RESULTS

5.1 Results of Hover Experiments

The qualitative results of the hover experiments are discussed in this section. Particular quantitative findings, concerning such things as the steady-state clearing times, the entrainment values and the clearing efficiencies (ratios), are discussed in Section 7.

Thirty-five hover tests were performed on nine different days. The experiment times, helicopters employed, hover altitudes, fog thickness dimensions, cloud physics conditions and general clearing results are summarized in Table 1.

With regard to certain of the terminology employed in the table, the words "hole" and "trail" are used when definite knowledge exists that downwash clearing extended completely through the fog layer to the surface level. The words "depression" and "trough" are used when such positive knowledge is lacking. Furthermore, the three categories of the visual appearance of the fog-top surface, that is, stable, mildly-convective and convective, merely span the convective-appearance range observed at this locale during this September period. The categories are relative and no absolute connotation is implied.

The clearing dimensions at the fog-top level (TD) were ascertained photogrammetrically, from knowledge of the camera viewing angles, of the helicopter dimensions and, in several cases, of the spacings of the marker balloons over the airfield, which provided photographic scaling measures.

The clearing dimensions at the surface level (SD) were determined in two ways. First, they were established from photographs taken from the observational aircraft, which flew in a continuous circling path about the scene of the operations. These photographs showed the clearings from different viewing angles; the boundaries of the cleared zones at the surface level could be seen, and their locations established and plotted on an aerial photo-map which was available for the Greenbrier Valley Airport. The dimensions were also determined in like manner from still and motion picture photographs acquired from the helicopter(s) doing the clearing.

The summaries of Table 1 reveal that single helicopters of the types employed were able, even in the least successful tests, to create clearings of 300 to 600 ft diameter. In the most successful tests, the clearing sizes were as large as 1000 by 2800 ft. Photographs illustrating the "most successful" hover experiments are shown in Figure 11. An experiment that was "moderately successful" is illustrated in Figure 12. Two of the "least successful" experiments are illustrated in Figures 13 and 14.

It should be emphasized that the dimensional information provided in Table 1 pertains strictly to the zones of total clearing, that is, to the zones wherein the fog droplets were completely eliminated by the downwash mixing. No information is provided concerning the visibility enhancement effects that customarily occurred at the surface level surrounding the zones of total clearing. These effects were important and they occurred over large-area regions bordering the cleared zones, over areas that were perhaps equal to the areas of the cleared zones themselves. The magnitude and extent of the effects could not be reliably determined, however, since the visibility data of the Lewisburg Program were too few and qualitative.

Photographic examples of visibility enhancement effects are provided in Figures 13 and 14. In the test of the first figure (Test 6a of 11 Sept 1969), the

Figure 11. Simultaneous-Hover Test of 12 Sept 1969, Test 1, CH-47A at NE Site, CH-54 at SW Site. The upper photographs show general, overall views of the clearings produced by the two helicopters. The cleared zones at the surface level at the time of the second photograph were about 800 to 1000 ft wide by 2800 to 3000 ft long (see Table I for particular dimensions). The middle photographs were taken from the CH-54 helicopter, and they show views of the airport runway as seen through the clearing being created by this helicopter. An appreciation of the clearing size may be gained by noting that the white centerline stripes of the runway are spaced 200 ft apart, from the beginning of one stripe to the beginning of the next. The lower photographs illustrate the clearing as it appeared from the ground

~0713
FROM OBSERVATION AIRCRAFT

0715:05
FROM OBSERVATION AIRCRAFT

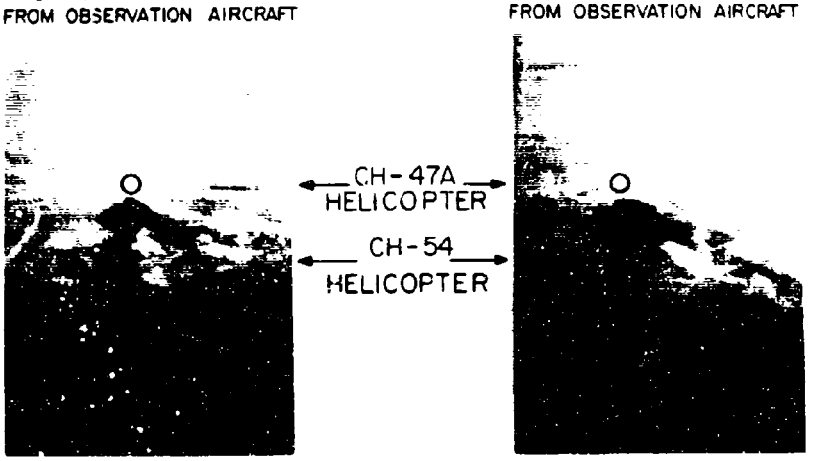

0708:25 FROM CH-54 HELICOPTER

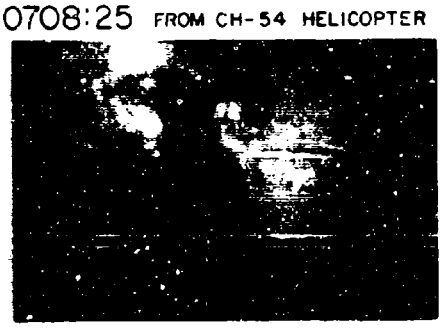

0714:56 FROM CH-54 HELICOPTER

SURFACE LEVEL - SHOWING CH-47A AT NE SITE

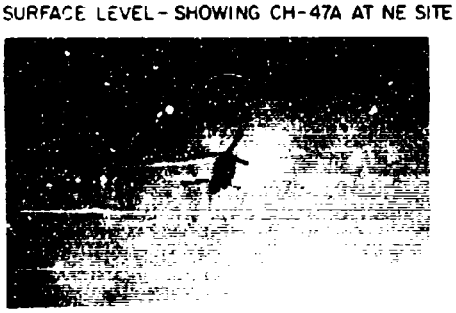

SURFACE LEVEL - SHOWING CH-47A AT NE SITE

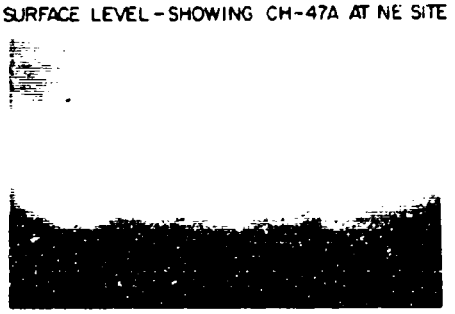

Figure 12. Hover Test of 16 Sept 1969, Test 2, CH-47A at SW Site. The time progression of clearing is illustrated in the upper photographs. The "ring clouds" surrounding the clearing can be seen. These clouds were commonly observed in the hover tests of the different days. Views from the clearing helicopter are displayed in the lower photographs. The picture at the lower right reveals the close-up appearance of one of the cumuliform elements of the cloud ring. The particular element is identified by the arrow shown in the upper middle photograph

FROM OBSERVATION AIRCRAFT

0731:20 LOOKING NE

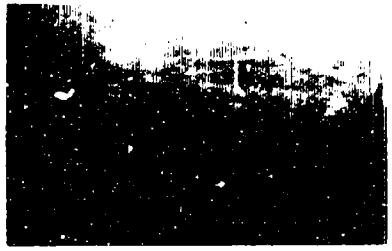

~0738 LOOKING SSE

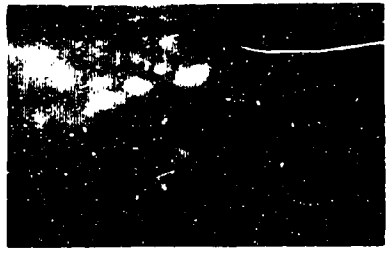

0742:30 LOOKING SW

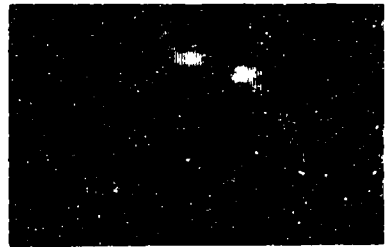

FROM TEST HELICOPTER

0733:28 LOOKING SW

FROM TEST HELICOPTER

0742:32 LOOKING SW

FROM TEST HELICOPTER

0735:48 LOOKING WSW

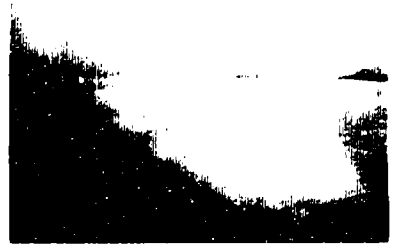

Figure 13. Hover Test of 11 Sept 1969, Test 6a, CH-47A at SW Site. The upper photographs show views of the clearing as seen from the C-119 observational aircraft. The lower photographs reveal the fog appearance before and during clearing. The visibility enhancement is apparent.

0819:10 FROM OBSERVATION AIRCRAFT

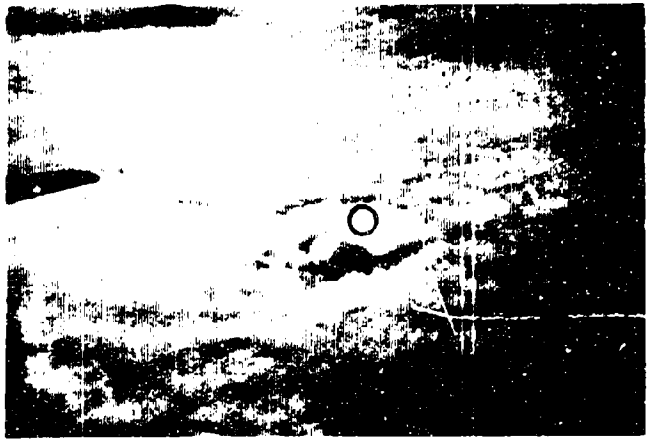

SURFACE LEVEL - BEFORE TEST

0826:00 FROM OBSERVATION AIRCRAFT

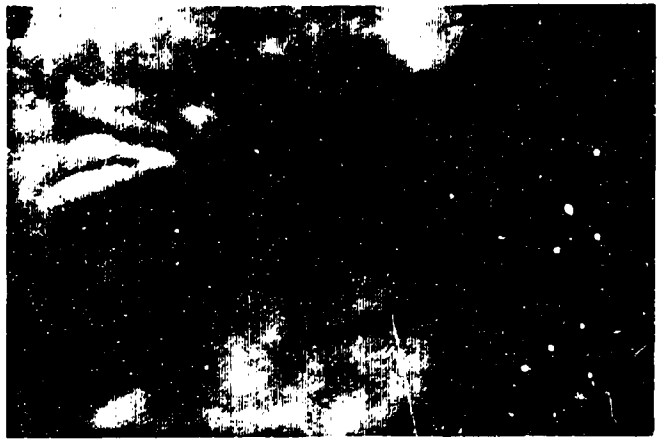

SURFACE LEVEL - DURING HOVER

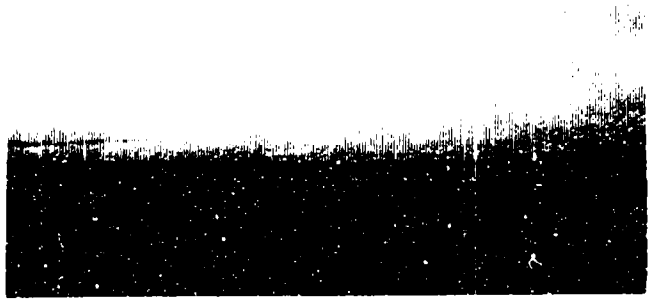

VISIBILITY ~100 METERS

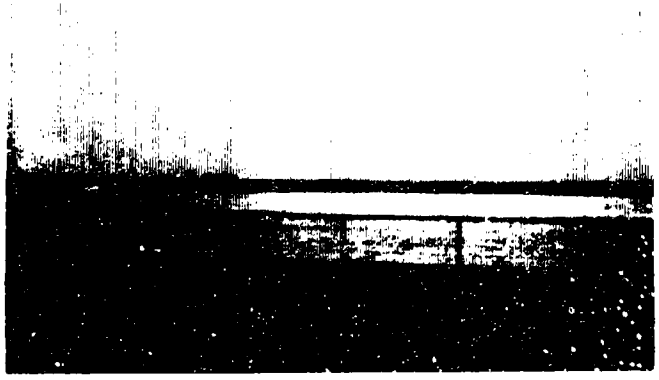

VISIBILITY ~400 METERS

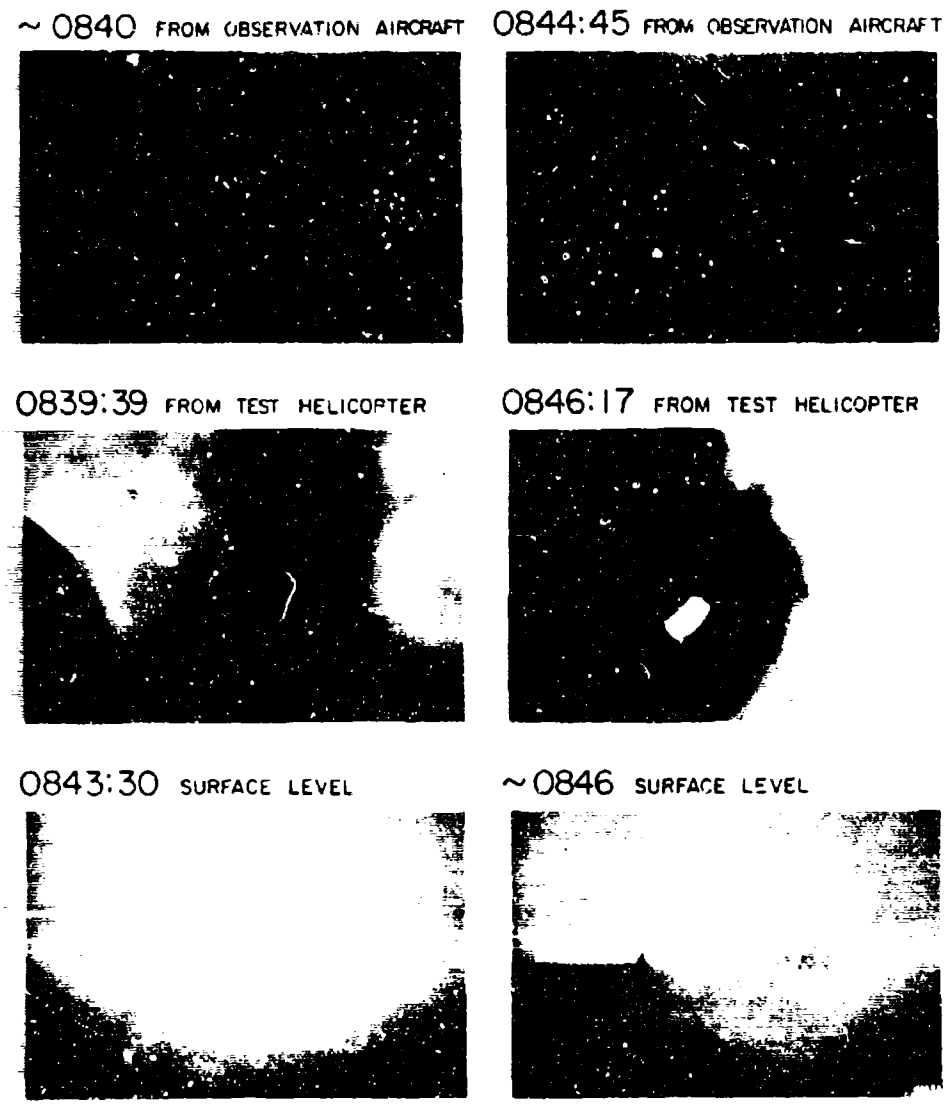

Figure 14. Hover Test of 14 Sept 1969, Test 1a, CH-47A at NE Site. These photographs illustrate a situation wherein the hovering helicopter produced little noticeable modification of the fog-top surface but caused substantial visibility enhancement effects at the ground. The visibility at the ground was improved from about 90 m to 400 to 500 m over a total distance extent of some 2000 ft

hovering helicopter created a relatively-small hole in the fog-top surface and the zone of total clearing at the surface was only about 700 ft wide by 800 ft long. But the surface-level photograph taken during the test clearly reveals ground objects located more than 1200 ft from the camera. Similarly, in the test illustrated in Figure 14 (Test 1a of 14 Sept 1969, a day when the fog layer was very deep and convective), the helicopter caused little noticeable modification of the fog-top surface. Yet surface observers reported a marked increase in the visibility from about 90 m before the test to about 400 to 500 m during the test.* The zone of improved visibility extended over a total distance of some 600 m.

The area extent of the cleared zones at the surface level was determined for each of the hover experiments for which sufficient data were available. The areas were computed under the assumption that the zones at the surface level had the shapes indicated in Table 1. For computational purposes, zones having a "trail shape" were presumed to be "long ellipses."

These area values, which are listed in Table 1, provide an approximate measure of the "clearing ability" of the helicopters in the particular tests. The values, thus regarded as indices of clearing ability, were used in various correlation efforts to determine the factors primarily responsible for the clearing differences of the different tests.

There were 27 hover tests involving single helicopters which permitted direct comparisons of clearing results. These tests are listed in Table 3 in order of increasing areal extent of the surface-level clearing. The test dates, times, and helicopters involved are identified, and the values of various parameters are tabulated which might conceivably account for the clearing diversities.

This table reveals that the areal extent of clearing ranged from 0.17×10^6 ft^2 (on 14 Sept) to 2.2×10^6 ft^2 (on 12 Sept). The two "worst days" of clearing were 14 and 27 Sept; the three "best days" were 12, 16 and 29 Sept.

It is reasonably apparent from the table that the fog depth was the principal factor that affected the clearing results. The cleared areas were small when the fog was deep; they were large when the fog was shallow. For example, for the 9 tests with fog depths exceeding 400 ft, the average size of the cleared areas was 0.23×10^6 ft^2; for the 9 tests with fog depths between 250 and 400 ft, it was 0.57×10^6 ft^2; for the 9 tests with depths of 250 ft or smaller, it was 0.89×10^6 ft^2. This negative correlation of cleared area with fog depth can also be demonstrated from the data by other statistical methods as well, for example, by simply cross-plotting the parameter values of the individual tests.

---

*Particular reference is made to the observations of Capt Vardiman, reported in Appendix A, which he made using an automobile to follow and determine the dimensions of the zone of improved visibility.

Table 3. Data for Single-Helicopter Hover-Tests Tabulated in the Order of Increasing Area Extent of Surface-Level Clearing. The values of parameters of known or suspected importance to the clearing results are listed

Date	Mid-Test Time EDT	Test No.	Area Extent of Clearing $ft^2 \times 10^6$	Heli-copter	Fog Depth	Test Time Before Natural Fog Dissipation Time min	Fog Top Appear-ance	Hover Altitude Above Fog Top ft	Stability, Surface to Fog Top Level ^oC/km	Surface Wind Dir. o	Surface Wind Speed mph	Relative Humidity at Flight Altitude %
14 Sept	0909	1b	.17	CH-47A	525	186	C	125	5.6	040	2.5	65
14 Sept	0842	1a	.19	CH-47A	525	213	C	75	9.4	060	2.5	65
27 Sept	0746	1a	.19	CH-54	475	254	S	225	25.6	360	2.5	95
27 Sept	0914	4	.19	CH-47A	475	166	S	225	13.8	360	5.0	95
27 Sept	0914	4	.19	CH-47C	475	166	S	150	13.8	360	5.0	95
27 Sept	0914	4	.22	CH-46	475	166	S	25	13.8	360	5.0	95
27 Sept	0746	1a	.25	CH-47A	475	254	S	125	25.6	360	2.5	95
27 Sept	0757	1b	.27	CH-54	475	243	S	0	25.6	360	2.5	95
13 Sept	0818	5	.28	CH-47A	250	142	M	125	12.6	040	3.5	90
11 Sept	0903	7	.33	CH-47A	325	132	M	75	23.2	090	1.0	90
23 Sept	0736	1	.35	CH-46	275	159	M	225	8.7	015	6.5	85
13 Sept	0759	4	.37	CH-47A	250	161	M	125	26.0	030	2.5	90
13 Sept	0723	1	.39	CH-54[X]	225	197	M	75	26.0	045	3.0	90
27 Sept	0757	1b	.39	CH-47A	475	243	S	125	25.6	360	2.5	95
23 Sept	0752	2	.42	CH-54	325	143	C	375	8.7	025	2.0	85
11 Sept	0829	6a	.44	CH-47A	325	166	M	175	23.2	Calm		90
13 Sept	0723	1	.45	CH-47A	225	197	M	150	26.0	045	3.0	90
23 Sept	0736	1	.57	CH-47C	275	159	M	325	8.7	015	6.5	85
11 Sept	0720	2	.61	CH-54[X]	275	235	S	225	31.7	Calm		90
23 Sept	0752	2	.66	CH-47C	325	143	C	300	8.7	025	2.0	85
16 Sept	0720	1	.71	CH-47A	200	205	S	150	26.2	050	2.0	90
29 Sept	0917	6a	.72	CH-46	325	103	C	175	14.1	075	1.5	95
16 Sept	0830	4	.79	CH-47A	250	135	M	150	23.6	360	2.5	90
16 Sept	0736	2	.92	CH-47A	225	189	S	75	26.2	050	2.0	90
29 Sept	0931	6b	1.0	CH-46	325	89	C	175	14.1	075	1.5	95
12 Sept	0713	1	1.9	CH-54[X]	225	152	S	300	28.9	035	3.0	85
12 Sept	0713	1	2.2	CH-47A	225	152	S	75	28.9	035	3.0	95

Note: The fog-top appearance symbols are, C - Convective, M - Mildly Convective, S - Stable
CH-54[X] is CH-54 helicopter with cargo pod

Another factor suggested to be of importance in the clearing was the "difference time" between the time that the tests were conducted and the natural dissipation time of the fog. These difference times are listed in Table 3 and they are employed in the "matrix diagram" of Table 4, which shows the average cleared areas (the values within the squares) corresponding to the three fog-depth categories cited above and also corresponding to the three time-difference categories covering (1) the nine particular tests conducted less than 155 min before the natural fog-dissipation time, (2) the nine tests conducted 155 to 190 min before natural dissipation, and (3) the nine tests conducted more than 190 min before natural dissipation. There is a suggestion of correlation in this table which indicates that the best clearing results occurred with shallow fog that was within one hour or so of natural dissipation. This is merely a suggestion, however, since the categorization parameters of the table may be interrelated to one another to a certain, unknown degree (because fog depth and fog dissipation time, in EDT, are normally correlated in positive fashion).

Other correlations were sought to explain other of the clearing differences, but without success. The secondary differences were apparently due to a multiplicity of causes involving such things as helicopter type, the hover altitude above the fog-top, the turbulent state of the fog, the wind drift situation, the thermal stability and moisture conditions within the fog layer and above, and the solar heating influence within the cleared zones (refer to Appendix D, Section D.4.2). Various of these factors were suspected to be important in particular tests but their possible influence simply could not be proved within the limited data sample of the project period.

"Wind trailing," that is, elongation, of the cleared zones in the downwind direction from the hover site was apparently an important factor on two of the days (12 and 23 Sept). But, as is demonstrated in Appendix D, Section D.4.2, wind trailing is not a simple function of the wind situation alone. It is also dependent on the turbulent state of the atmosphere, which will tend to "close in" the drift trails at different rates dependent on the intensity of the turbulence.

One of the original objectives of the Lewisburg Program was to compare the clearing abilities of different types of helicopters which were hovering under near-identical flight and cloud physics conditions. This was one of the purposes of the simultaneous hover tests of the program. Seven such tests were successfully performed with the CH-54, CH-47 and CH-46 helicopters. The comparison results are shown in Table 5. The helicopter weights at the test times are listed in the table.* Also given are the down-transport flux of air across the rotor

*The method of determining the weights of the helicopters during the individual tests is described in Section 7.2

Table 4. Average Area Extent of Clearing Observed in Hover Tests Classified (1) by Fog Depth and (2) by Test Occurrence Time Prior to the Natural Fog Dissipation Time. The area ($ft^2 \times 10^6$) is given by the first figure; the number of tests included in the sample is specified by the second figure

Fog Depth (ft) \ Occurrence time of test prior to the natural fog dissipation time (min)	>190	155-190	<155
>400	.258 5	.192 4	--- 0
250-400	.61 1	.454 3	.626 5
<250	.516 3	.645 2	1.29 4

plane (F_v) and the maximum velocity of the down-transport (W_m).* These are the parameters that should theoretically account for the clearing differences.

The table comparisons involving the CH-47 and CH-54 helicopters reveal that the lighter, tandem-rotor, CH-47 helicopter created larger cleared areas in all tests than did the single-rotor, CH-54 helicopter. There were some differences in hover altitudes but the overall results of the 5 tests strongly indicate that the clearing performance of the CH-47 was superior to that of the CH-54. This was apparently due to the large rotor-disk area of the CH-47 and to the associated large F_v value. The smaller downwash velocity of the wake air of the CH-47 was seemingly unimportant to the clearing results. The velocity was adequate to transport the wake air to the surface level, which evidently was all that mattered.

With regard to the two comparison tests involving the CH-46 and CH-47 helicopters (both tandem-rotor helicopters) the first test conformed to theoretical expectations, with the heavier CH-47 producing a larger cleared area than the CH-46, which was proportionally larger by the approximate F_v ratio of the two helicopters. In the second test, however, the CH-47 clearing was somewhat smaller than that of the CH-46. This possibly resulted from the different hover altitudes, although analysis uncertainties in measuring the cleared areas could equally well explain the anomaly.

5.2 Results of Hover-to-Land Experiments

Particular hover experiments were performed on four days during the project period (on 12, 13, 16 and 23 Sept; the specific tests are identified by asterisks in Table 1) for the purpose of creating cleared zones over the airport runway through which helicopters could be landed. Six landings were accomplished on these days through holes that either (a) were made by one or more helicopters to land another

*These F_v and W_m values were obtained from equations C7, C9, C10 and C13, of Appendix C.

Table 5. Comparison Results of Simultaneous Hover Experiments. F_v is the volume flux of air across the helicopter rotor(s). W_m is the maximum downwash velocity (see Appendix C for equations).

Date	Mid-Test Time EDT	Test No.	Ave. Fog Depth ft	CH-54 Helicopter					CH-47 Helicopter					CH-46 Helicopter				
				Ave Hover Alt ft	Helicopter Weight pounds	F_v ft^3/sec $x10^5$	W_m ft/sec	Cleared Area ft^2x10^6	Ave Hover Alt ft	Helicopter Weight pounds	F_v ft^3/sec $x10^5$	W_m ft/sec	Cleared Area ft^2x10^6	Ave Hover Alt ft	Helicopter Weight pounds	F_v ft^3/sec $x10^5$	W_m ft/sec	Cleared Area ft^2x10^6
12 Sept	0713	1	225	525	39,000	1.86	90.6	1.9	300	26,700	1.81	66.0	2.2					
13 Sept	0723	1	225	300	37,300	1.85	89.9	0.39	375	27,000	1.83	66.6	0.45					
23 Sept	0736	1	275						600	26,300	1.83	66.6	0.57	500	15,800	1.20	61.0	0.35
23 Sept	0752	2	325	700	30,300	1.69	82.0	0.42	625	25,600	1.80	65.6	0.66					
27 Sept	0746	1a	475	700	31,800	1.73	84.0	0.19	600	26,300	1.82	66.3	0.25					
27 Sept	0757	1b	475	475	31,300	1.70	83.0	0.27	600	25,800	1.80	65.6	0.39					
27 Sept	0914	4	475						700	22,500	1.69	61.4	0.19	500	15,300	1.17	59.4	0.22

or (b) were made by a single helicopter to land itself. Photographs showing aerial and ground views of each of these landing experiments are presented in Figures 15 to 19.

The photograph of Figure 16, which may have some historical significance, shows the CH-54 helicopter that was used to accomplish the first helicopter landing in fog through an artificially-created downwash-cleared zone. The helicopter, which was piloted by Major James H. Goodloe, 291st Aviation Company, Fort Sill, Oklahoma, is shown at the parking ramp of the Greenbrier Valley Airport, just after engine-shutdown following the landing.

5.3 Results of Runway-Clearing Experiments

Eighteen runway-clearing tests were conducted during the 10 mission-days of the program. The experiment times, helicopters utilized, flight altitudes, flight patterns and pattern extent, fog thickness dimensions, cloud physics conditions, and general clearing results are summarized in Table 6.

The clearing results achieved during the runway clearing experiments were found to be correlated, in general, with the results obtained during the hover experiments at comparable times. In other words, success in the hover mode was a good predictor of success in clearing the runway.

The runway clearing experiments were successful in clearing the full 6000 ft extent of the runway on two occasions, one on 15 Sept, 0810 to 0905 EDT, with shallow fog 100 to 150 ft thick (Figure 20), the other on 27 Sept, 1125 to 1140 EDT, during the dissipative stage of the fog about 40 min prior to natural dissipation.* A single helicopter was employed in each of these experiments.

Runway clearing was judged to be "partially successful" in four experiments on three other days, 12, 16 and 23 Sept. Partial success was defined as the ability, demonstrated or rationally arguable, of a single helicopter to maintain a cleared zone along the runway of at least 1500 ft extent (or of two helicopters to maintain 2500 ft of clearing, or of three to maintain 3500 ft, etc.) One of the experiments categorized as "partially successful" is illustrated in Figure 21.

Runway clearing was judged to be "unsuccessful" during 12 experiments on the remaining days with fog. Lack of success was defined as the inability, actual or probable, to maintain cleared zone dimensions as large as the minima cited above. One such experiment classified as "unsuccessful" is illustrated in Figure 22.

---

*Motion pictures exist showing the 27 Sept clearing but none are presented as illustrations since the photographer concentrated solely on documenting the clearing features and failed also to record the fog conditions of the surroundings.

Table 6. Runway Clearing Tests, Description and Summary of Results. (See symbols key of Table 1)

Date	Time Period EDT	Test No.	Helicopter(s)	Fog Characteristics: Depth ft	Top Appear.	Surface Vis. m	Surface LWC gm/m³	Wind in Fog Layer (Mean): Dir. θ	Speed mph	Flight Level ft	Airspeed mph	Type Flight Path	Runway Section for which Clearing Attempted	Results	Probable Reasons for Non-Successful Results
7 Sept	0710-0729	2	CH-54[X]	500-550	Stable, Hazy	150	---	300	3.1	600-700	~25	Racetrack	Full Runway	Unsuccessful	Fog too deep, airspeed too large, paths too long, successive trails non-overlapping
7 Sept	0730-0734	3	CH-54[X]	500-550	Stable, Hazy	160	---	300	3.1	600-700	~25	Racetrack	Full Runway	Unsuccessful	Same as above
11 Sept	0727-0802	3	CH-54[X]	250-300	Stable	130	---	342	3.0	300-450	~25	Back & Forth loop turns	Full Runway	Unsuccessful	Airspeed too large, paths too long, successive trails non-overlapping due to pilot inexperience
11 Sept	0802-0811	4	CH-54[X] & CH-47A	300-350	Mildly Conv.	110	---	342	3.0	400-500	~25	Back & Forth loop turns	Full Runway	Unsuccessful	Same as above
11 Sept	0811-0816	5	CH-47A	300-350	Mildly Conv.	110	---	342	3.0	~400	~25	Back & Forth loop turns	Full Runway	Unsuccessful	Same as above
12 Sept	0723-0742	2	CH-54[X] & CH-47A	250-300	Mildly Conv.	125	0.09	269	2.6	300-400	~25	Racetrack	SW Half of Runway	Partially Successful	
13 Sept	0734-0742	2	CH-54[X] & CH-47A	200-250	Mildly Conv.	140	0.11	341	5.4	300-450	~25	Racetrack	Full Runway	Unsuccessful	Airspeed too large, paths too long, successive trails non-overlapping due to pilot inexperience
14 Sept	0913-0926	2a	CH-47A	100-550	Conv.	90	0.21	343	5.7	600-700	~10	Back & Forth loop turns	SW Half of Runway	Unsuccessful	Fog too deep and turbulent
14 Sept	0929-1045	2b	CH-47A	500-550	Conv.	180	0.09	343	5.7	550-650	~10	Back & Forth loop turns	SW Half of Runway	Unsuccessful	Same as above
15 Sept	0820-0905	1	CH-47A	100-150	Stable	180	0.06	345	8.1	150-200	~15	Back & Forth Hover turns	Full Runway	Successful	
16 Sept	0745-0757	3a	CH-47A	200-250	Stable	115	0.13	345	4.5	200-350	~15	Back & Forth Hover turns	Full Runway	Partially Successful	
16 Sept	0757-0821	3b	CH-47A	200-300	Mildly Conv.	115	0.13	345	4.5	250-400	~15	Back & Forth Hover turns	SW Half of Runway	Partially Successful	
23 Sept	0806-0816	3	CH-54, CH-47A, CH-47C, & CH-46	350-400	Conv.	210	0.09	330	5.4	500-700	~20	Squadron Race track Passes	Full Runway	Partially Successful	
27 Sept	0825-0856	3	CH-54 CH-47A CH-47C, & CH-46	450-500	Stable, Hazy	165	0.15	280	4.1	600-700	~15	Squadron Race track Passes	Full Runway	Unsuccessful	Fog too deep, paths too long
27 Sept	1125-1145	II-1	CH-54	400-500	Conv.	---	---	280	4.1	~600	~20	Back & Forth loop turns	Full Runway	Successful	
29 Sept	0747-0831	1	CH-47C & CH-46	300-350	Conv.	230	0.03	330	2.9	300-400	~20	Racetrack	Full Runway	Unsuccessful	Fog too turbulent, paths too long, trails non-overlapping due to wind drift normal to runway
29 Sept	0854-0901	4	CH-47C & CH-46	300-350	Conv.	140	0.09	330	2.9	300-350	~20	Back & Forth Hover turns	Full Runway	Unsuccessful	Same as above
29 Sept	0901-0911	5	CH-46	300-350	Conv.	140	0.09	330	2.9	~350	~20	Back & Forth Hover turns	SW Half of Runway	Unsuccessful	Same as above

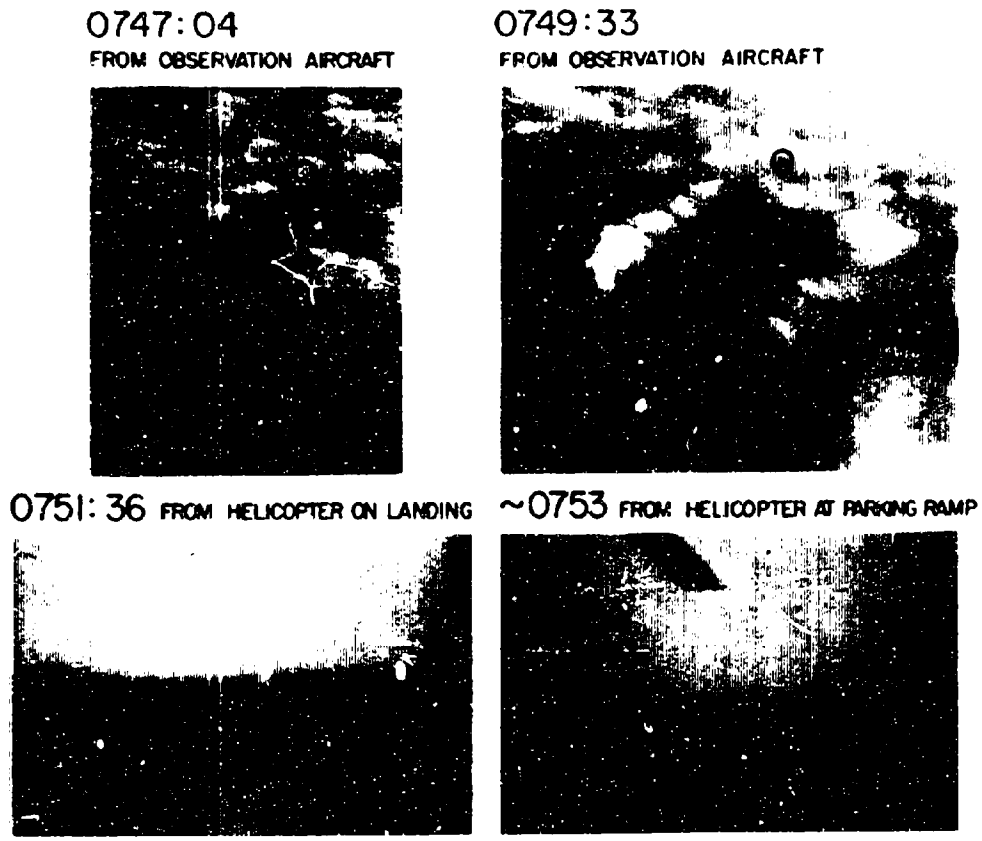

Figure 15. Hover-to-Land Test of 12 Sept 1969, Test 3, CH-47A Hovered to Create Hole to Land CH-54. The cleared zone at the landing approach time of the upper right hand photograph was about 700 ft wide by 2500 ft long. The lower photographs show the after-landing appearance of the fog as it began closing-in following hover termination

Figure 16. CH-54 Helicopter at Parking Ramp of the Greenbrier Valley Airport after Accomplishing First Landing in Fog Through an Artificially-Created, Cleared Zone, 12 Sept 1969, approximately 0755 EDT

Four helicopters, flying together in squadron formation, were employed for runway-clearing during experiments conducted on 23 Sept and 27 Sept. On the 23rd, the helicopters in these "squadron passes" made deep troughs in the fog top which extended to ground level (Figure 23). The experiment on this day might conceivably have been successful if more passes had been made. Only two passes were possible, though, due to fuel-time considerations. The squadron passes on 27 Sept were non-influential in modifying the fog for any sustained period. Ten passes were made but without appreciable effect. The fog layer was very deep on this day, about 475 ft, which probably exceeded the wake penetration limits of the helicopters. *

*An experiment was also conducted on 29 Sept 1969 to ascertain whether a C-130 aircraft could accomplish runway clearing by wake mixing. Ten runway passes were made with the C-130 at various airspeeds and flap settings. The aircraft wake created deep, well defined grooves in the fog top surface on various passes but clearing did not extend to the surface level. It was concluded that a heavy aircraft, such as the C-130, would probably be ineffective with fog of 300 ft depth but that it might be useful in certain clearing operations with fog of 50 to 100 ft depth.

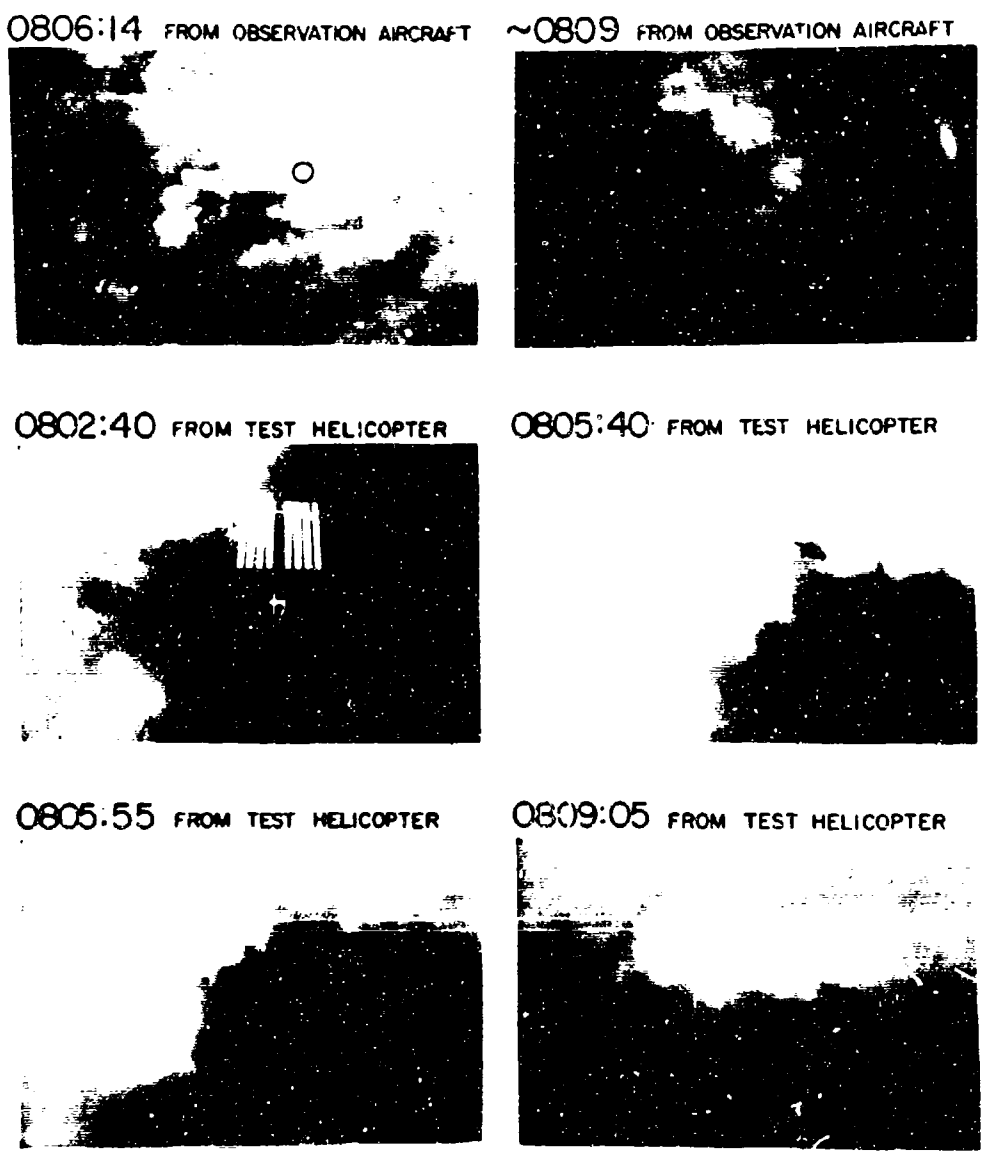

Figure 17. Hover-to-Land Test of 13 Sept 1969, Test 4, CH-47A Hovered to Create Hole to Land CH-54. The clearing situation of this day was more difficult than that of 12 Sept and the surface-cleared zone at landing time was only about 500 ft wide by 960 ft long. The landing was accomplished without difficulty, however

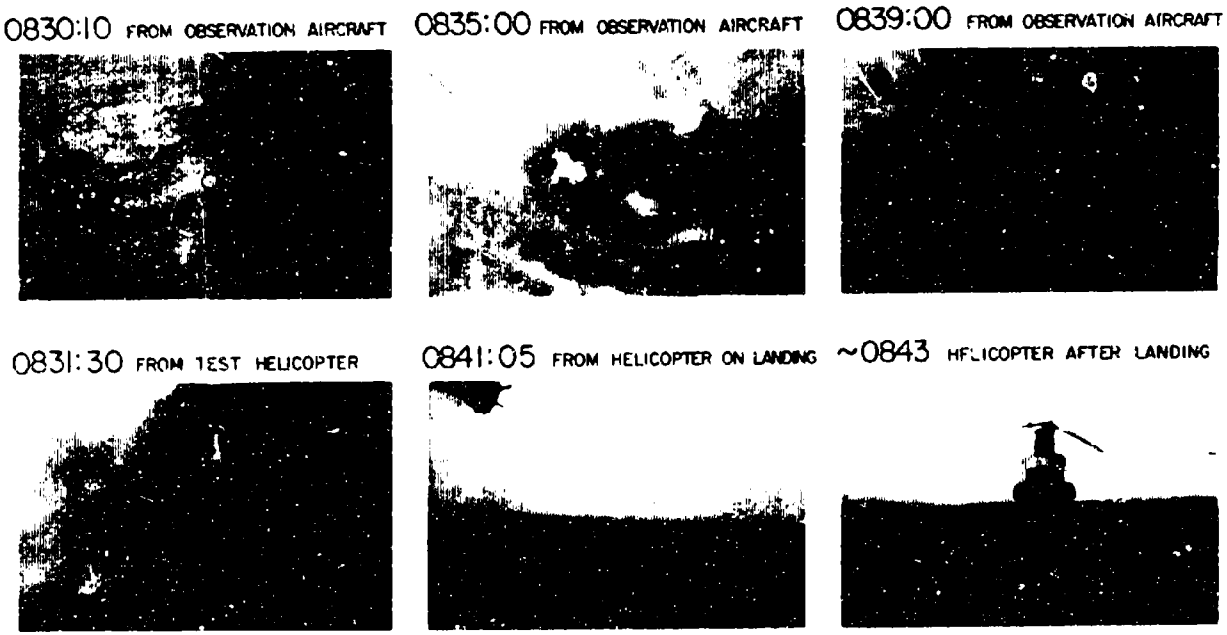

Figure 18. Hover-to-Land Test of 16 Sept 1969, Test 4, CH-47A Hovered to Create Hole to Land Itself. The upper photographs illustrate the time progression of clearing while the lower ones show views recorded during and after landing. The surface-cleared zone at landing time had a circular shape with a diameter of approximately 100 ft.

Figure 19. Hover-to-Land Test of 23 Sept 1969, Test 6, CH-46, CH-47A and CH-47C Hovered to Land CH-54, Then to Land CH-47C and CH-47A. The CH-46 remained hovering throughout to maintain clearing. The cleared-zone dimensions at the surface level varied somewhat at the different landing times but, on the average, were about 1000 ft by 2200 ft. Convective cells were present within the upper portion of the fog layer, as shown in the upper left-hand photograph. There were no natural breaks at test time, however, which extended completely through the fog

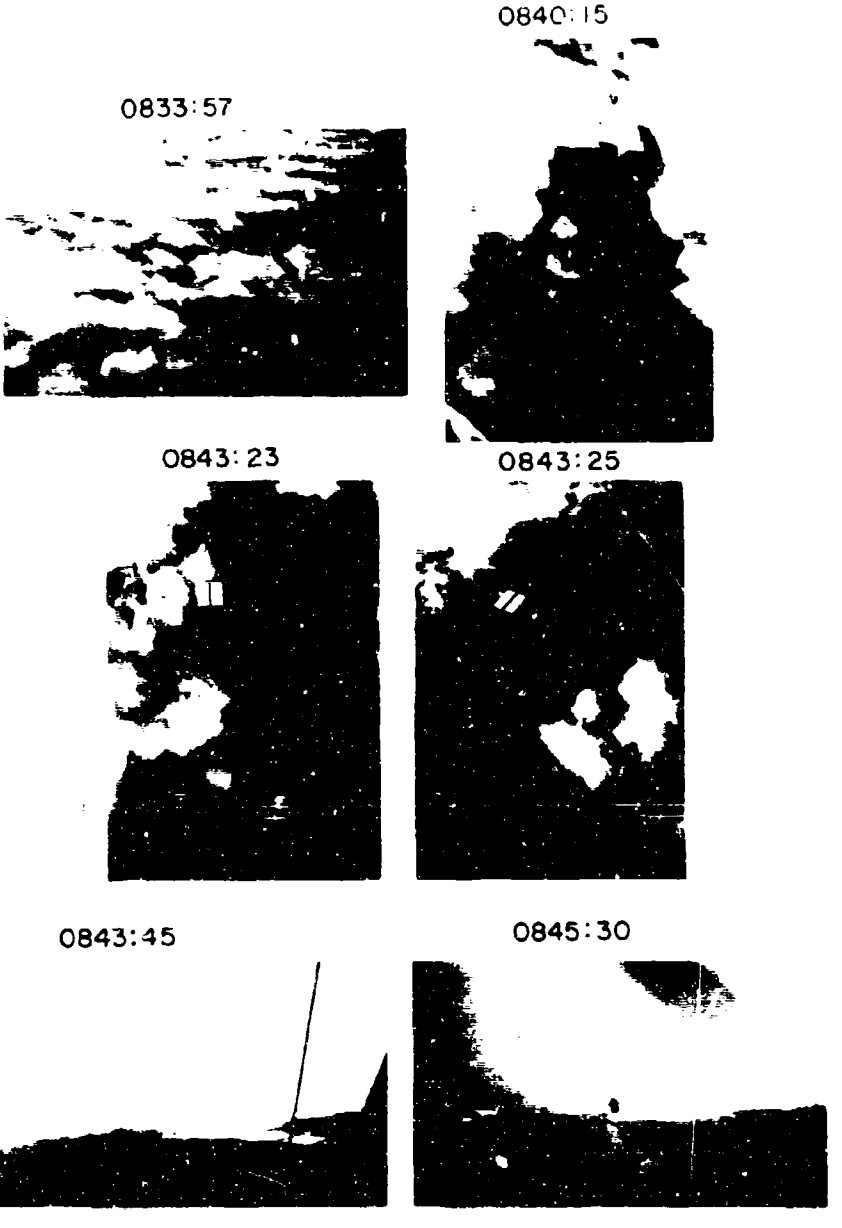
0840:15
0833:57
0843:23
0843:25
0843:45
0845:30

Figure 20. Runway-Clearing Test of 15 Sept 1969, Test 1, CH-47A, Full Runway Extent, Successful. The photographs show views looking toward the SW end of the runway which were recorded from the open back-ramp of the clearing helicopter. Clearing passes were made in both directions along the runway but only the 1st, 3rd and 5th alternate passes are illustrated here. The runway was completely and permanently cleared by 0843 EDT

It should be mentioned that substantial visibility enhancement frequently occurred along the runway, or portions thereof, during experiments that were categorized as unsuccessful. But no efforts were made to estimate the extent of such enhancement effects.

6. RECOMMENDED RUNWAY-CLEARING PROCEDURES

The simple categorization of the runway-clearing results into successful, partially-successful and unsuccessful does not tell the whole story about the experiments. The experiments, besides being tests of the helicopter-clearing technique, were also, in large measure, tests of flight-path design and of pilot-helicopter ability to fly the paths. Pilot proficiency in flying the paths at slow airspeed in close formation with other pilots was important too.

Flight-path-optimization and pilot-proficiency had necessarily to be acquired within the period of the Lewisburg Program, and many mistakes were made before the various problems were resolved. Most of the fog situations that "should have been clearable" occurred early in the program period, before path optimization and pilot proficiency had been achieved; the situations that occurred later, after path-skill acquisition, were mostly difficult ones that exceeded the helicopter capabilities for clearing.

The optimum type of flight path for runway clearing would appear to be a "back-and-forth type path with hovering turns." Such path can be flown either by a single helicopter or by two or more helicopters following each other. The path is begun in the hover mode and the pilots each fly slowly forward in the desired clearing direction at about 5 to 10 knots airspeed, an airspeed smaller than that of transitional lift. At the path terminus, a terminus dictated either by plan or by the clearing ability of the helicopter in the particular situation, the pilot slows to the hover state and makes a 180^{C}, hovering turn, revolving his helicopter about its own vertical axis. The pilot then proceeds forward once again, headed in the opposite direction.

The location and orientation of the flight path relative to the airport runway will be prescribed by the wind direction, wind speed, and turbulence conditions below flight altitude. The path should be flown upwind of the runway, so that the successive trails of clearing, on drifting downwind, will maintain continuous clearing over all, or some clearable part, of the runway. The lengths of cleared paths will be determined by the width of the trails being created, by the "closing-in-time" of the trails due to turbulent-diffusion, by the trail drift speed, and by the "circuit time" required to complete a back-and-forth path. The trail-widths and lengths of clearing that might reasonably be anticipated with a medium-size heli-

Figure 21. Runway-Clearing Test of 16 Sept 1969, Test 3b, CH-47A, SW Half of Runway, Partially Successful. Photographs are shown which were obtained from a Cessna aircraft, from the C-119 observational aircraft and from the CH-47A helicopter. The cleared zone behind the helicopter on most of the clearing passes had a length extent of about 800 to 2000 ft. This was insufficient to maintain complete clearing of the 3000 ft extent of the SW half of the runway. The path legs flown were too long. They should have been shortened to about 2000 ft

FROM CESSNA AIRCRAFT

~0758 LOOKING NE

~0800 LOOKING NE

FROM C-119 AIRCRAFT

0817:40 LOOKING NE

FROM CH-47A HELICOPTER

0800:43 LOOKING NE

0807:12 LOOKING SSW

0813:51 LOOKING ENE

Figure 22. Runway-Clearing Test of 11 Sept 1969, Test 4, CH-47A and CH-54, Full Runway Extent, Unsuccessful. Representative views of several of the clearing passes are shown which were recorded from the observational aircraft and CH-54 helicopter. The trails are relatively-narrow and lack penetration depth, which is characteristic of clearing passes performed at too large an airspeed (refer to Appendix D and Table 6)

FROM OBSERVATION AIRCRAFT

~ 0803

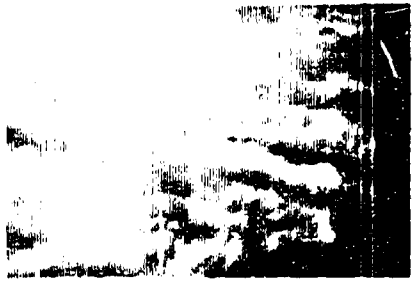

0804:53

0811:05

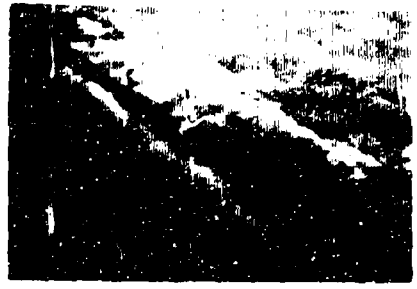

FROM CH-54 HELICOPTER

0803:17

0809:28

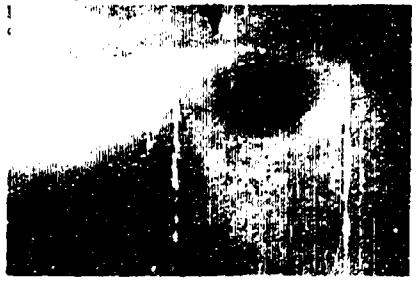

0810:12

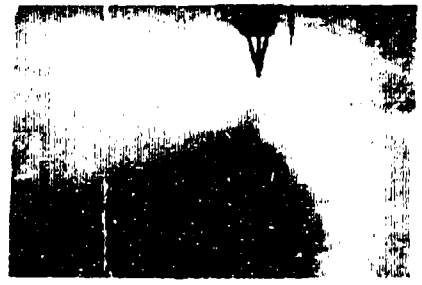

Figure 23. Runway-Clearing Test of 23 Sept 1969, Test 3, Squadron Passes with CH-46, CH-47A, CH-47C and CH-54, Full Runway Extent, Partially Successful. Photographs are shown which were obtained from the C-119 aircraft during the two clearing passes of the helicopters. Clearing was accomplished to the surface level on the second pass. Motion pictures acquired from the helicopters showing the form, extent and persistence of clearing strongly suggest that the fog along a major portion of the runway could have been eliminated with continued passes, but due to fuel-time considerations, the test had to be terminated after the second pass.

1st SQUADRON PASS

0807: 32

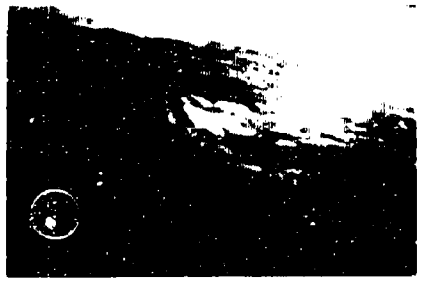

0807: 36

0809: 32

2nd SQUADRON PASS

0815: 36

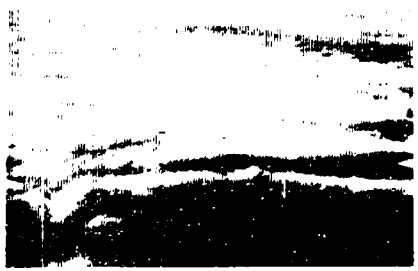

0816: 10

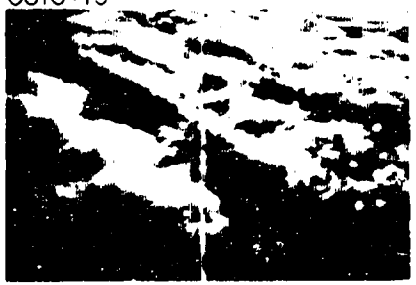

0816: 27

copter under different turbulent and cloud physics conditions are discussed and illustrated in Appendix D.

Optimum runway clearing in certain situations, primarily those where the wind is directed along the runway, might best be achieved in the hover mode. This mode of flight should not be discounted, since clearing can sometimes extend downwind of the hover site to distances of several thousand ft (refer to the hover tests of 12 Sept 1969, described in Table 1 and illustrated in Figure 11).

Certain problems of flight safety arise when helicopters are flown at slow airspeed in the ways required for fog-clearing. These problems are discussed in Appendix B. Recommended flight-control procedures for helicopter clearing programs are also discussed in this appendix and comments are made about the possibilities and difficulties of using GCA or ILS systems for such control.

Other comments, solicited from the helicopter pilots involved in the Lewisburg Program, concerning program evaluation and recommended procedures, are presented in Appendix A, Section A.3.

7. PARTICULAR ANALYSES AND RESULTS

For 16 of the hover experiments identified in Table 7, semi-quantitative information was obtainable concerning the wake penetration distances of the helicopters, the times required to attain steady-state conditions of clearing, the clearing ratios, the total entrainment values, and the persistence times of the clearings. This information is described here.

7.1 Wake Penetration Distances

In all of the hover tests, with one possible exception, the helicopter downwash always penetrated to the surface level from the hover altitudes.

The available analytical data, consisting of surface and aerial photographs of the clearings as well as photographs and notes concerning the downwash effects on the networks of balloons at the two target sites, indicate that the wake penetration distances of the different helicopters, under the stability conditions that prevailed during the test program, were approximately:

1000 ft, for the CH-54 helicopter,

800 ft, for the CH-47 helicopter (A and C models), and

700 ft, for the CH-46 helicopter

7.2 Helicopter Weights during Tests

The take-off weight of each helicopter was known for each sortie, as was the landing weight. In addition, information was available from Technical Manuals and

Table 7. Wake and Cleared Zone Parameters for 16 Hover Tests. See text for description of parameters

Date	Mid-Test Time EDT	Test No.	Site	Heli-copter	Average Fog Depth m	Average Hover Level m	1. Heli-copter Mass kg	2. Air Density at Flight Altitude kg/m^3	3. F_v m^3/sec	4. W_m m/sec	5. Δt sec	6. V_c $m^3 \times 10^6$	7. V_s $m^3 \times 10^6$	8. R	9. E
11 Sept	0903	7	SW	CH-47A	99	122	11,110	1.15	4915	19.3	250	2.2	6.0	1.8	3.9
12 Sept	0713	1	NE	CH-47A	69	92	12,120	1.15	5130	20.1	260	8.7	11.[illegible]	6.5	7.6
12 Sept	0713	1	SW	CH-54[X]	69	160	17,000	1.14	5275	27.6	240	11.0	14.6	8.7	10.5
13 Sept	0723	1	NE	CH-54[X]	69	92	16,920	1.15	5240	27.4	170	1.8	4.2	2.0	3.8
13 Sept	0723	1	SW	CH-47A	69	114	12,250	1.14	5180	20.3	150	1.9	4.6	2.4	4.8
13 Sept	0759	4	SW	CH-47A	76	114	11,430	1.14	5005	19.6	160	1.8	5.6	2.2	5.8
13 Sept	0818	5	NE	CH-47A	76	114	11,120	1.14	4940	23.0	170	1.8	3.9	2.0	3.5
14 Sept	0842	1a	NE	CH-47A	160	183	11,800	1.12	5130	20.1	150	1.9	5.5	2.5	6.1
14 Sept	0909	1b	SW	CH-47A	160	198	11,560	1.12	5080	19.9	150	1.8	5.8	2.3	6.7
16 Sept	0720	1	NE	CH-47A	61	107	12,070	1.13	5165	20.3	210	3.1	6.8	2.9	5.6
16 Sept	0736	2	SW	CH-47A	68	92	11,750	1.13	5100	20.0	200	4.2	9.8	4.1	8.0
23 Sept	0736	1	SW	CH-47C	84	183	11,930	1.11	5185	20.3	210	2.7	6.2	2.4	4.6
23 Sept	0752	2	SW	CH-47C	99	190	11,620	1.12	5090	20.0	225	4.1	8.8	3.5	6.7
27 Sept	0746	1a	NE	CH-54	145	213	14,420	1.12	4900	25.6	150	1.7	6.4	2.4	7.6
27 Sept	0746	1a	SW	CH-47A	145	183	11,930	1.12	5160	20.2	150	2.0	6.3	2.6	7.1
27 Sept	0757	1b	NE	CH-54	145	145	14,200	1.13	4840	25.3	150	2.0	5.9	2.6	6.7

CH-54[X] is CH-54 helicopter with cargo pod

cockpit gauge readings regarding the fuel consumption rate of each helicopter during the two conditions, namely (1) normal cruising flight, and (2) hover flight out of ground effect. These fuel consumption rates are listed in Table 8.

The particular weights of the helicopters during each of the hover experiments were determined by computing the fuel-weight-loss during the period prior to the experiments by pro-rating the fuel expenditure according to the previous total periods of normal-cruise flight and hover flight and by subtracting this weight-loss from the take-off weight. A consistency check on the calculations was provided by the helicopter landing-weight-figures recorded in the pilot logs.

These weights (converted to metric units of mass) are listed in Table 7, column 1.

7.3 Helicopter Down-Transport Flux and Velocity

Equations are developed in Appendix C which describe the down-transport flux (volume flux and mass flux) of air that is forced downward across the rotor plane of a helicopter (having either single or dual rotors) while it is hovering in the free air out of ground effect. Other equations are also developed describing the maximum velocity of the downwash, the maximum mean-sectional-velocity at a distance approximately one rotor-diameter beneath the helicopter.

The flux and velocity values which were determined from these equations for the particular helicopters used in the Lewisburg Program, and for the prevailing flight and environmental conditions, are listed in Table 7, columns 3 and 4.

7.4 Steady-State Clearing Times

The beginning times of the various hover experiments were recorded as accurately as possible, although there was considerable uncertainty, perhaps 30 sec to a min or so, as to just when the pilot, on slowly approaching the marker balloon over the target site, first attained a stable, hover condition.

The steady-state clearing time was defined as the time, subsequent to the beginning of hover, when steady-state conditions of clearing, and of visibility enhancement surrounding the clearing, first prevailed at the surface level, that is, it was the time when the dimensions of the helicopter-induced, fog-modification effects first reached their maximum size and when the "ring clouds" surrounding the clearings at the fog-top level (refer to the following section and to Figure 24) first attained their stable, continuing form. There is a proviso to this definition, however, which concerns situations in which the helicopter wake and cleared zones were being advected downwind of the hover sites. For such situations, the steady-state times were defined to be those times when the cross-trail dimension of the wake-modified zone, immediately downwind of the helicopter, within approximately 300 to 600 ft, first attained its maximum, stable width.

Table 8. Hover-State Parameters for Helicopters Employed in the Lewisburg Program and for Other Helicopters Referenced in the Text

PARAMETER	Symbol	Units	HELICOPTER TYPE						
			Single-Rotor Helicopters					Tandem-Rotor Helicopters	
			CH-54	CH-54[x]	CH-53B	CH-3E	UH-1F	CH-47	CH-46
Mass	M	Kg (pounds)	14,650 (31,000)	16,780 (37,000)	15,876 (35,000)	8,618 (19,000)	3,856 (8,500)	12,247 (27,000)	8,618 (19,000)
Rotor diameter	D	m	22.02	22.02	22.02	18.90	14.63	18.02	15.24
Mass flux of air across rotor(s) at standard gravity and air density (ref. Eqs. C8 and C12, Appendix C)	F_f	Kg/sec	5609	6130	5963	3771	1952	6060	4300
Maximum downwash velocity at standard gravity and air density (ref. Eqs. C7 and C11, Appendix C)	W_m	m/sec	24.5	26.7	26.0	22.4	19.3	19.8	19.6
Average fuel consumption rate and power setting		gm/sec %							
a. In normal cruise condition			345-25%	410-40%	290-50%	170-45%	60-45%	275-25%	150-50%
b. In free-air hover condition			425-45%	500-75%	375-80%	230-75%	90-70%	350-45%	205-75%
Assumed engine efficiency		%	30%	30%	30%	30%	30%	30%	30%
Wake warming immediately below helicopter due to engine exhaust heat	$\Delta\theta_e$	K°	2.3	2.4	1.7	1.5	1.4	1.7	1.4
Specific humidity addition to wake air immediately below helicopter resulting from water produced by fuel combustion	Δq_e	gm/kg	0.096	0.104	0.071	0.065	0.059	0.075	0.060

Notes: 1. CH-54[x] is CH-54 helicopter with cargo pod
2. With JP-4 fuel,
   a. heat of combustion is 10,220 cal/gm
   b. water produced by combustion is 1.27 gm/gm

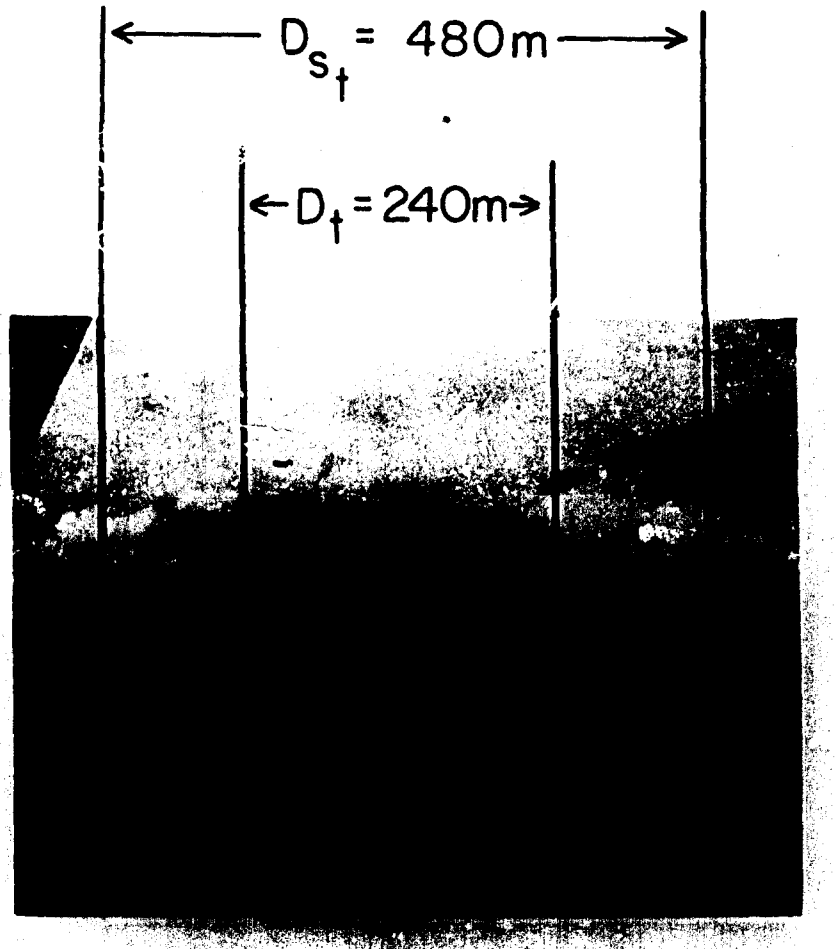

Figure 24. Wake Modified Region and Cleared Zone; a Case-Example Illustration, Test 2, 16 Sept 1969. The approximate mean-dimensions of the cleared zone and "ring clouds" at fog-top level are indicated. Refer to text discussion

The steady-state clearing times for the 16 hover tests previously mentioned are listed in Table 7, column 5.*

7.5 Methods of Specifying "Cleared Volume" and "Stirred Volume"

The definitions used to specify and methods used to determine the "cleared volumes" and "stirred volumes" pertaining to certain of the hover experiments will be described by reference to one particular experiment (Test 2 of 16 Sept 1969),

*These times are substantially shorter than the formation times listed in Table 1. The Table 1 times correspond to the occurrence times of the maximum clearing dimensions at the surface level, which included wind-trailing effects and other effects that were deliberately excluded in the above definitions of steady-state conditions and times.

which has been selected as an example. We will generalize our discussion by reference to this specific case.

Metric units of measurement are used throughout this section.

In a typical hover experiment performed under near-zero wind-speed conditions during the Lewisburg Program, the clearing situation, viewed from aloft, looked similar to that illustrated in Figure 24. A circular or elliptical zone of clearing occurred below the helicopter and, surrounding this, there was an annulus, or "ring," of cumuliform-type clouds, formed by the induced air-circulations of the helicopter wake.*

The fog layer in the illustrated situation was 68 m deep and the CH-47A helicopter used in the test was hovering at an altitude 24 m above the fog-top. Steady-state conditions of clearing were attained some 200 sec after the beginning of hover. The average diameter distance across the cleared zone at the fog-top level, measured as indicated in Figure 24, was approximately 240 m. The average diameter distance across the "cloud ring," surrounding the cleared zone at the fog-top, was approximately 480 m. The tops of the highest clouds of the ring extended some 15 to 30 m above the fog-top level.

The zone of clearing at the surface level in this experiment, during steady-state conditions, was about 320 m in diameter, this figure being a mean diameter, since the zone at the surface was elliptically-shaped, with axes 270 by 370 m.

The cross sections of Figure 25 illustrate the approximate geometry of this clearing situation and indicate how the "cleared volume" and "stirred volume" were defined and measured herein.

The "cleared volume," shown in cross section in the first diagram, had the approximate, three-dimensional shape of the frustum of a right elliptical cone, of volume

$$V_c = \frac{\pi H}{12} (D_s^2 + D_s D_t + D_t^2) \qquad (1)$$

where H is the depth of the fog layer, D_s is the mean diameter of the cleared zone at the surface level and D_t is the mean diameter of the cleared zone at

*Such "cloud rings" (or peripheral ridges of clouds, in cases of wind advection) usually occurred around the boundaries of the cleared zones in the Lewisburg hover tests, but not invariably. The presence or absence of these clouds was probably dependent on the thermal stability of the fog in the upper portion of the fog layer and on the water vapor content of the clear-air at flight altitude relative to the saturated vapor content of the air within the fog layer itself. Values of thermal stability smaller than a certain particular value combined with moist air aloft and large fog LWC would presumably produce the clouds whereas larger stabilities, drier air aloft and smaller fog LWC would not.

Figure 25. Cross Sections Illustrating Definitions of "Cleared Volume" and "Stirred Volume" for Case-Example. The cleared zone, or cleared volume, is indicated by the dotted section of the upper diagram. The helicopter wake circulation presumed responsible for the observed features of clearing is sketched in the second diagram (refer to Appendix D for complete discussion). The hatched section of the lower diagram illustrates the region defined to be the total wake zone, or "stirred volume"

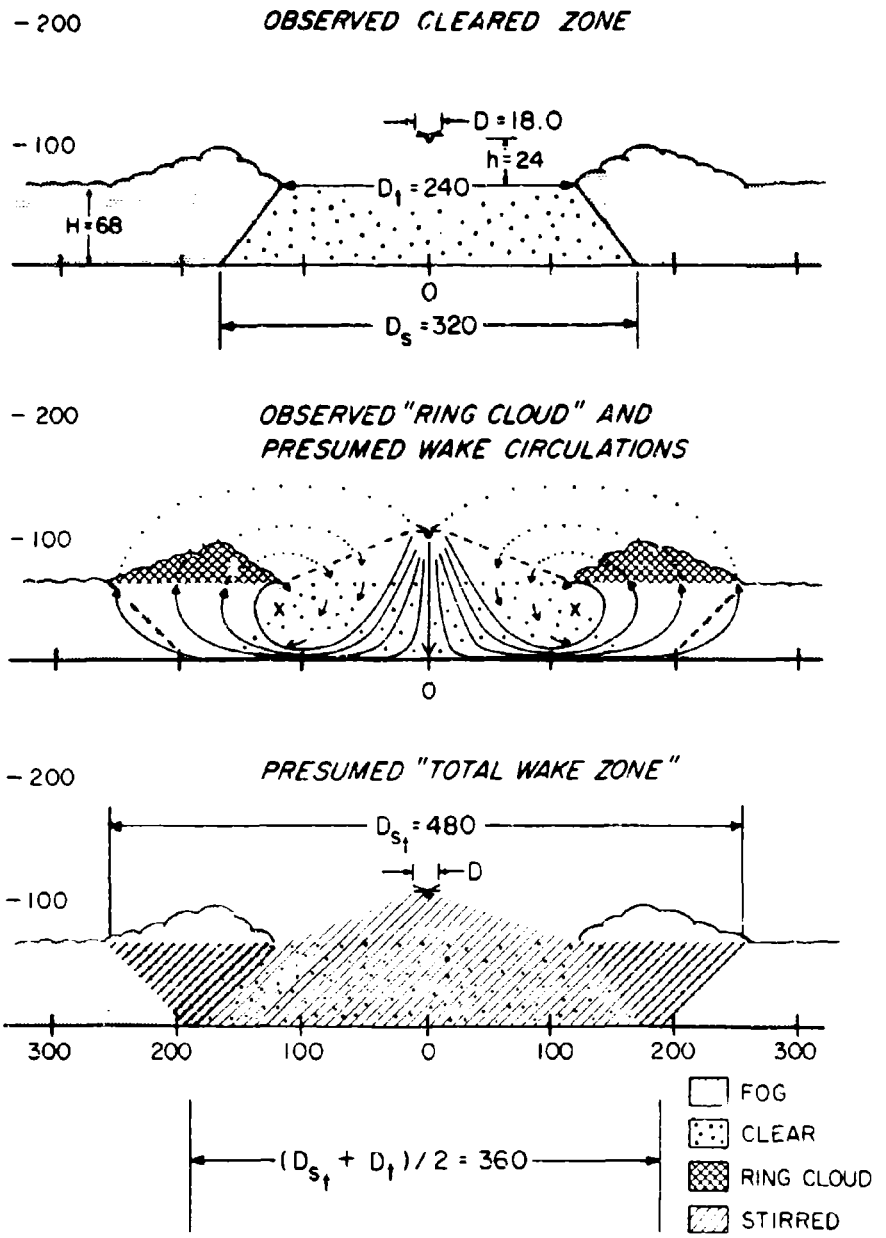
-200
OBSERVED CLEARED ZONE
-100
D = 18.0
h = 24
D_1 = 240
H = 68
0
D_s = 320
-200
OBSERVED "RING CLOUD" AND
PRESUMED WAKE CIRCULATIONS
-100
0
-200
PRESUMED "TOTAL WAKE ZONE"
D_{s_t} = 480
D
-100
300
200
100
0
100
200
300
$(D_{s_t} + D_1)/2 = 360$
FOG
CLEAR
RING CLOUD
STIRRED

the fog-top level.* For the particular dimensions of the example chosen, the value of V_c was 4.2×10^6 m^3.

The "stirred volume," illustrated in cross section in the lower diagram of Figure 25, requires some background discussion. The term "stirred volume" is intended to connote the total region of helicopter-induced air circulation and eddying which lies below the rotor plane. In other words, the stirred-volume is the volume of the total wake of the helicopter. This region has nebulous boundaries which can only be defined in terms of some "minimum circulation velocity," or "minimum eddy intensity," which has a value equal to that of the naturally-occurring turbulent motions of the atmospheric surroundings in the particular test situations.** Such definition implies that the size of the stirred volume will decrease with increased atmospheric turbulence. This implication is intended; and it is believed to be a valid physical relationship.

It is presumed that the ring clouds shown in Figure 24 were formed by a helicopter wake circulation of the type illustrated in the second diagram of Figure 25. The circulation depicted in this diagram is a type that would be theoretically expected when a downwash jet impinges normally on an underlying surface boundary (see Appendix D, where the theoretical and observed characteristics of helicopter wakes are discussed). The solid streamlines of the diagram show the flow direction in wake regions where the velocity is assumed to be larger than about 1 cm/sec; the dotted lines above the fog-top indicate the existence of a mean, continuity flow of air which has a velocity probably smaller than that of the normal turbulent motions of the atmospheric surroundings.

Assuming that the sketched circulation picture is correct, then the total wake volume of the helicopter at the steady-state time, that is, the total "stirred volume," will be given approximately by the 180°, azimuth rotation of the cross-hatched section shown in the lower diagram of Figure 25. Part of the wake region will be located in the clear-air layer above the fog, where the downwash air "fans out," from an initial diameter about equal to the rotor diameter, at the flight altitude,

---

*This Eq. also pertains to the frustum of a right circular cone or, with minor modification not described here, to the frustum of any elliptical cone, not necessarily a right elliptical cone. The dimensions D_s and D_t, which are referred to as "mean diameters," are actually the averages of the long and short axes of the horizontal sections of clearing that exist at the surface and fog-top levels, respectively. It is assumed in the Eq. that the mean sectional dimension of clearing within the fog layer, from surface level to top level, varies linearly with altitude. These comments apply analogously to Eqs. 2 and 3, which are presented later in the section.

**In the work reported by Plank and Spatola (1969), the wake was assumed to be bounded by the 1 ft/sec isotach surface of downwash velocity. The Lewisburg results suggest that a more-appropriate boundary value, which would better conform to the sizes and time scales of the clearings observed, would be about 1 cm/sec.

to a mean diameter, D_t, equal to that of the cleared zone, at the fog-top level. This part of the wake, again utilizing the frustum of an elliptical cone assumption, has the volume

$$V_1 = \frac{\pi h}{12} (D_t^2 + D_t D + D^2) \qquad (2)$$

where h is the helicopter hover altitude above the fog-top, D is the rotor diameter (the effective diameter with a tendem-rotor vehicle) and D_t is as defined previously. The footnote comments of p 62 also have application to this Eq.

The second part of the wake region lies below the altitude of the fog-top. It encompasses the entirety of the cleared zone and extends horizontally, at fog-top level, to the outer boundary of the cloud ring. It does not include the volume of that portion of the ring clouds which penetrates above the altitude of the fog-top, since the upward penetration of these clouds is probably caused by condensation and latent-heat effects, and is not the simple, direct product of rotor-driven air-motions.

The extent of the wake-stirred zone at the surface level could only be estimated. Efforts were made during the Lewisburg Program to determine the zone dimensions; this was one of the purposes of the tethered-balloon networks. The efforts were unsuccessful, primarily because the downwash zones, and cleared zones contained within the downwash zones, had dimensions larger than the network dimensions (refer to Figure 6, for example).

It was assumed that the wake-stirring influence at the surface level extended to the mid-diameter (mean diameter) of the ring cloud that could be seen from above the fog. This referenced diameter, projected to the surface level, is indicated in the bottom diagram of Figure 25. It is the dimension labeled $(D_{st} + D_t)/2$. This presumption about the stirred zone dimensions at the surface level is reasonably consistent with the circulation picture of the second diagram and it places the stirred zone boundaries beyond those of the cleared zone, which must be true, and which was observed.

With these postulates, the volume of the part of the wake region below fog-top level is given approximately by

$$V_2 = \frac{\pi H}{48} (7D_s^2 + 4D_s D_t + D_t^2) \qquad (3)$$

which is also the Eq. for the frustum of an elliptical cone, of an inverted cone (refer to footnote comments of p 62).

The total wake volume, or total stirred volume, at the steady-state time, will be composed of the two separate volumes, V_1 and V_2, that is,

$$V_s = V_1 + V_2 \tag{4}$$

The particular value of V_s for the case-example experiment, using the dimensions cited and illustrated, is 9.8×10^6 m^3.

The determinations of the "cleared volumes" and "stirred volumes" of the other hover experiments identified in Table 7 were made in a manner analogous to that of the case example just described. The cleared volumes were determined in a relatively straightforward manner, since the zone boundaries were visible interfaces separating clear air from cloudy air. Various difficulties were encountered in the determination of the stirred volumes, nevertheless, since the cloud boundary situations surrounding the cleared zones at the fog-top level sometimes differed from the simple "cloud ring picture" of the case-example illustration. It is beyond the scope of the report to describe each test on an individual basis. The stirred-volume values were established in a fashion similar to the examples described, following the same general definition scheme and measurement logic.

The particular V_c and V_s values for these tests are listed in Table 7, columns 6 and 7.

7.6 Clearing Ratio

A semi-quantitative measure of the effectiveness of helicopter clearing, which specifies the volume-clearing ability of the helicopter, is the "clearing ratio"

$$R = V_c/V_d \tag{5}$$

where V_c is the cleared volume as previously defined, where

$$V_d = F_v \Delta t \tag{6}$$

is the total down-transported volume across the rotor that occurs within the steady-state period Δt, and where F_v is the down-transport flux.

The values of this ratio can readily be determined for any particular hover experiment, from helicopter specifications and from easily-obtained clearing dimensions, and can be used to compare the clearing performance of different helicopters in different experiments and clearing programs.

The R values for the 16 tests of the Lewisburg Program are shown in Table 7, column 8. It is seen that the values ranged from 1.8 to 8.7, with the smallest values occurring on 13, 14 and 27 Sept and the largest values occurring on one particular day of 12 Sept. These days differ from the worst and best days of surface-level clearing which were noted in Section 5, paragraph 5.1. A comparison of Tables 4 and 7 also reveals that the best clearing, in volume-ratio terms, was not so obviously dependent on fog depth as was the area clearing at the surface level.

The tables demonstrate that the volumetric clearing abilities of the helicopters used during the Lewisburg tests were more nearly the same than were their surface clearing abilities.

Correlations were sought which would explain the clearing ratio differences appearing in Table 7. None were found. The test data were too few; the number of probably important variables was too large.

7.7 Total Entrainment

The total wake volume, or stirred volume, of a helicopter after hovering a time Δt, should be given approximately by

$$V_s = V_d + F_E \Delta t = V_d + V_E \tag{7}$$

where V_s is the stirred volume of previous discussion, F_E is the entrainment flux of surrounding air into the wake air and V_E is the total volume of air that mixes into the wake air during the steady-state period Δt.

Entrainment values are conventionally expressed in terms of the ratio of the amount of the entrained air to the amount of air originating from the motion source. In these terms,

$$E = V_E / V_d \tag{8}$$

or employing Eq. 7,

$$E = \frac{V_s - V_d}{V_d} \tag{9}$$

The E values for the 16 hover experiments of Table 7 were determined from this Eq. and Eq. 6, using the V_s, F_v and Δt values discussed earlier. The ratios are listed in the last column of the table.

The E values in the Lewisburg tests ranged from 3.5 to 10.5, which implies that, for every part of air that was originally down-transported across the rotor(s)

some 3 to 10 parts of air were entrained and mixed into the wake air from the environmental surroundings. These values are somewhat smaller, on the average, than the value of 9.0, which was cited by Plank (1969) as being typical of the AFCRL Smith Mountain program.

7.8 Persistence Times

Under the operational pressures of the Lewisburg Program, stemming from the use of several helicopters, their fuel-time limitations, the variety of experiments, the communication needs, etc., it was not always possible to continue to observe the natural filling in of the clearings produced in the hover tests. Hence, persistence times, that is, the time to closure of the clearing following helicopter departure from the test sites, were acquired for only certain tests. The times for these tests are shown in the last column of Table 1.

The helicopter clearings at Lewisburg generally persisted for about five min after hover termination. Persistence was as brief as 1 to 2 min on days when the fog layers exceeded 400 ft in depth. Persistence times with fog shallower than 400 ft typically ranged from 3 to 8 min, an example of which is shown in Figure 26. In one test, conducted with multiple helicopters on 23 Sept, in which a relatively-large clearing in fog was made within approximately 90 min. of natural dissipation, the persistence time was as long as 25 to 30 min (see Figure 27).

8. WAKE TEMPERATURES AND HUMIDITIES

The downwash air of a helicopter is warmed initially by the exhaust heat of the engines Plank and Spatola (1969), by about 1.4 to 2.4°C, (see the $\Delta\theta_e$ values of Table 8). This air, on descending through clear-air surrounding, follows a temperature lapse rate that departs from the dry adiabatic by an amount that is dependent on the atmospheric stability and on the entrainment rate at which environmental air is mixed into the downwash air, which is itself a function of atmospheric stability. Plank and Spatola have presented values of wake excess temperature (excess relative to ambient as a function of distance beneath the helicopter) for a particular HH-53B helicopter, for various stability conditions and for one assumed entrainment profile. This work indicates that wake temperatures a few hundred ft below a hovering helicopter might readily rise some 1 to 5 C° above ambient under normally observed stability conditions.

If the downwash air of a helicopter descends through a cloud or fog layer, however, that is, if it descends through a cloudy environment, the air entrained from the surroundings then contains liquid water in droplet form, which evaporates on mixing with the downwash air. The evaporation acts to cool the wake air, to a

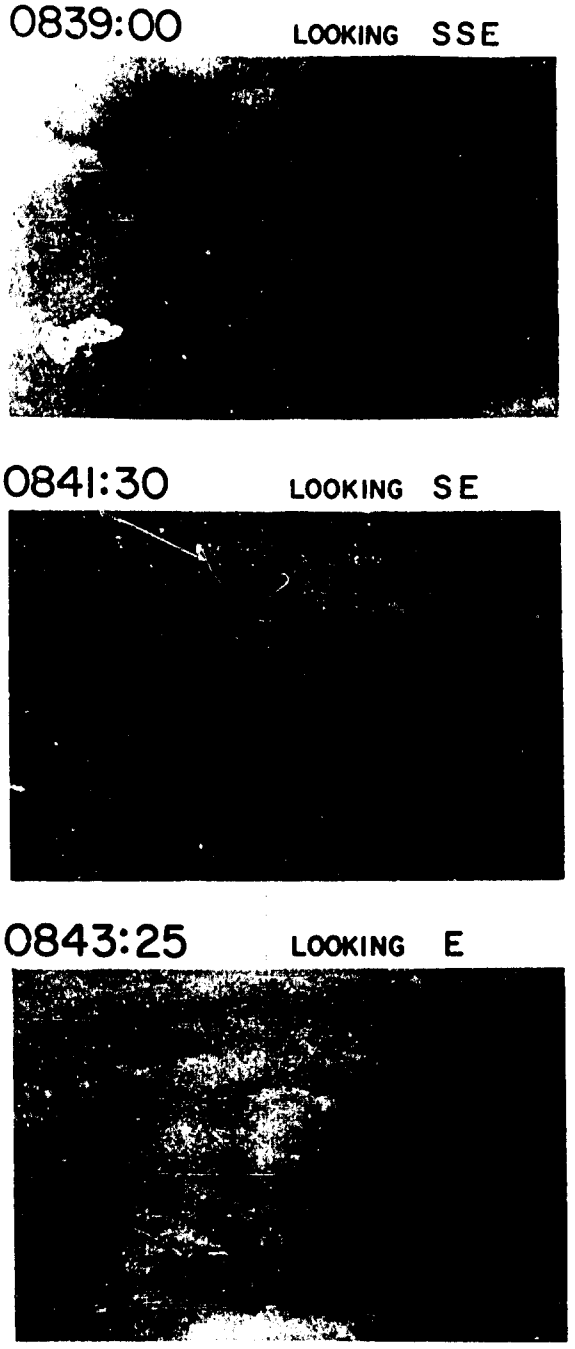

Figure 26. Photographs Illustrating Brief Persistence of Cleared Zone, Test 5, 16 Sept 1969. This clearing, which was about 1000 ft in diameter at the surface level at the time of the first photograph, was nearly closed by fog diffusion from the sides some 2 1/2 min later, and was definitely and completely closed after 4 min

degree that depends on the cloud LWC. Under certain conditions of cloudiness this evaporative cooling can offset adiabatic warming and the resultant wake temperatures can become colder than the surroundings, thereby producing an unstable wake wherein the air is accelerated downward.*

These comments point out the alternate possibilities that the wake air of a helicopter, as observed at the surface level in a fog situation during a hover experiment, might either be warmer or colder than the surroundings. They also suggest, by implication, the possibility that measurements of wake temperatures and humidities made during hover experiments might be employed in a reverse manner as a means for deducing the physical nature of the entrainment-mixing processes that occur within the wake.

These possibilities were known prior to the Lewisburg Program and provisions were made to acquire data of this type. Cambridge Systems dew-point recorders were mounted on jeep vehicles and the vehicles, during hover experiments, were driven across the helicopter

*The referenced conditions are primarily warm, tropical conditions with large cloud LWC, with relatively dry air above the cloud layer, and with comparatively small temperature inversion at the top of the cloud.

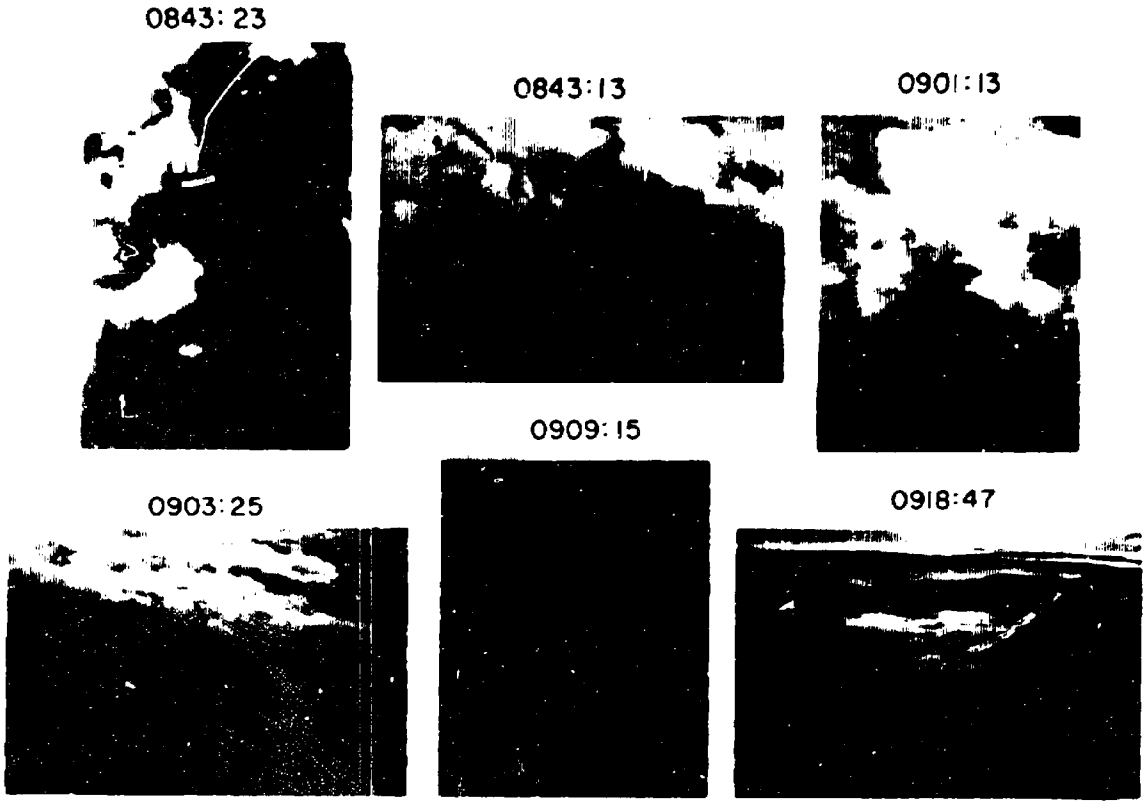

Figure 27. Photographs Illustrating Extended Persistence of Cleared Zone, Test 7, 23 Sept 1969. The helicopter-created clearing had dimensions at 0843 EDT which were about 1100 ft wide by 2400 ft long, which were larger than could be recorded in either of the first two photographs. Subsequent views of the clearing are shown for the times indicated. The clearing persisted and was a recognizable fog-top feature until some time after 0918 EDT, which was 31 min after the termination of hover

downwash zones. The jeeps were stopped periodically during their travel, to obtain stable instrument readings at particular points along approximate radial lines of the zones. The jeeps were backed into the wind at the stopping places, as nearly as possible in a variable downwash situation, and the engines were turned off, to avoid any possible exhaust-heating of the sensing elements. About 3 to 4 such stops and readings were made during each particular experiment. Some 5 to 7 min were required to complete the measurements.

Temperature and dew-point measurements of this type were acquired during 15 hover tests. In three tests, however, the location of the jeeps within the zones could not be established with sufficient surety to permit use of the data. Good measurements, made approximately as desired, were obtained in only 12 tests. The results of these measurements are presented in Figures 28 to 30. Profiles of wake excess temperature across the cleared zones are shown in Figure 28. Profiles of relative humidity are shown in Figure 29; profiles of excess specific humidity are shown in Figure 30. The particular dates and times of the tests are identified in the figures and the average diameter of each zone, that is, the average of the long and short dimensions of clearing that prevailed during the hover periods, is indicated. Data points (circled) are shown for only one radius half of the profiles. The other halves of the profiles were merely sketched-in on the basis of symmetry.

The values of the ambient temperatures and ambient specific humidities that existed within the fog at the surface level prior to the beginning of the tests are indicated in the Figure 28 and Figure 30 diagrams by the numbers which have been drafted to the left of the profiles, immediately above the abscissa lines. The fog depth at the time of the tests is specified by the first of the drafted numbers at the upper right; the flight altitude is specified by the second number. Both values are in meters.

The profiles of these figures reveal that the wake temperatures in the downwash zones were customarily some 0.3 to 3.0 C^{o} warmer than the surface surroundings and that the relative humidities ranged generally from 94 to 100 percent, that is, very near saturation. They also show that the specific humidity of the wake air, a measure of the water vapor content of the air, was larger, by some 0.1 to 1.2 gm/kg, than the saturation specific humidity of the undisturbed fog air of the surface surroundings.

This latter, seemingly paradoxical, result is explained by the fact that the clear air at the flight altitude, because of warmer temperatures aloft, was actually more moist, in terms of vapor content, than was the fog air itself. When this warm, moist air aloft was down-transported to the surface level by rotor action, it arrived at the surface with a larger specific humidity than the saturation humidity of the surface surroundings, even though the wake air was modified by entrainment-mixing during descent.

Figure 28. ΔT Values and Profiles Across Downwash-Cleared Zones. The profiles pertaining to tests performed by the CH-47 helicopter (A model) are presented above the horizontal dividing line. Those performed by the CH-54 helicopter are shown at the lower left; those by the CH-46 helicopter at the lower right. The mean dimensional extent of the cleared zones at the surface level at the test times, is indicated by the vertical lines. The ambient surface temperature within the fog surroundings is given (in ^{o}C) by the numbers above the abscissa lines at the left. The profiles show the temperature-excess values, relative to ambient, that were measured within the cleared zones. Measurements were made only along radial lines of the cleared zones, as indicated by the circled data points. The other halves of the profiles were merely drawn on the basis of symmetry. The fog depth at test time is given by the first of the drafted numbers at the upper right; the flight altitude is given by the second number. Both values are in meters

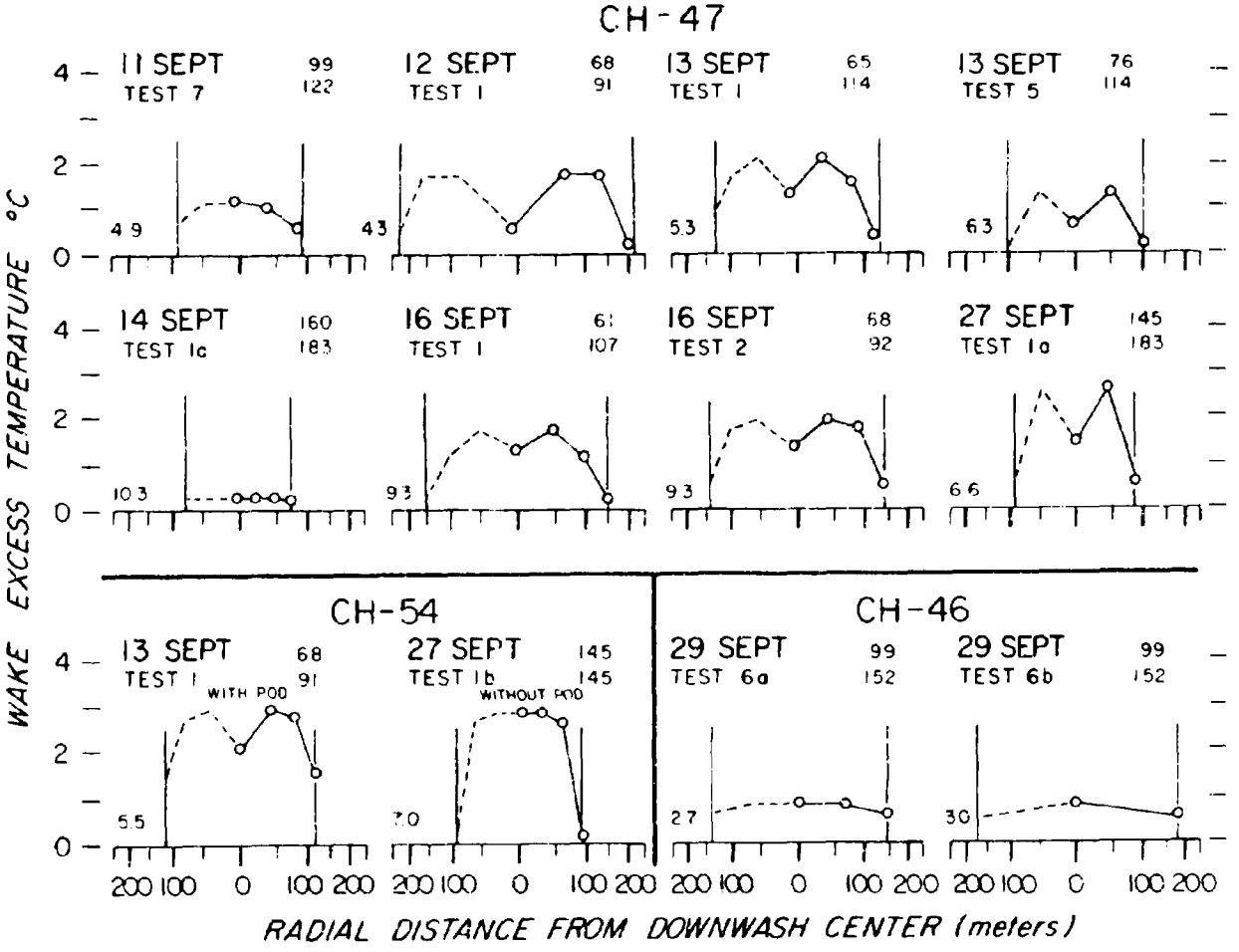
CH-47
11 SEPT
TEST 7
99
122
12 SEPT
TEST 1
68
91
13 SEPT
TEST 1
65
114
13 SEPT
TEST 5
76
114
14 SEPT
TEST 1c
160
183
16 SEPT
TEST 1
61
107
16 SEPT
TEST 2
68
92
27 SEPT
TEST 1a
145
183
CH-54
13 SEPT
TEST 1
68
91
WITH POD
27 SEPT
TEST 1b
145
145
WITHOUT POD
CH-46
29 SEPT
TEST 6a
99
152
29 SEPT
TEST 6b
99
152
WAKE EXCESS TEMPERATURE °C
RADIAL DISTANCE FROM DOWNWASH CENTER (meters)

Figure 29. Relative Humidity Values and Profiles Across Downwash Cleared Zones. The format of this figure is essentially as described in the Figure 28 caption except that the profiles show the relative humidity values across the cleared zones

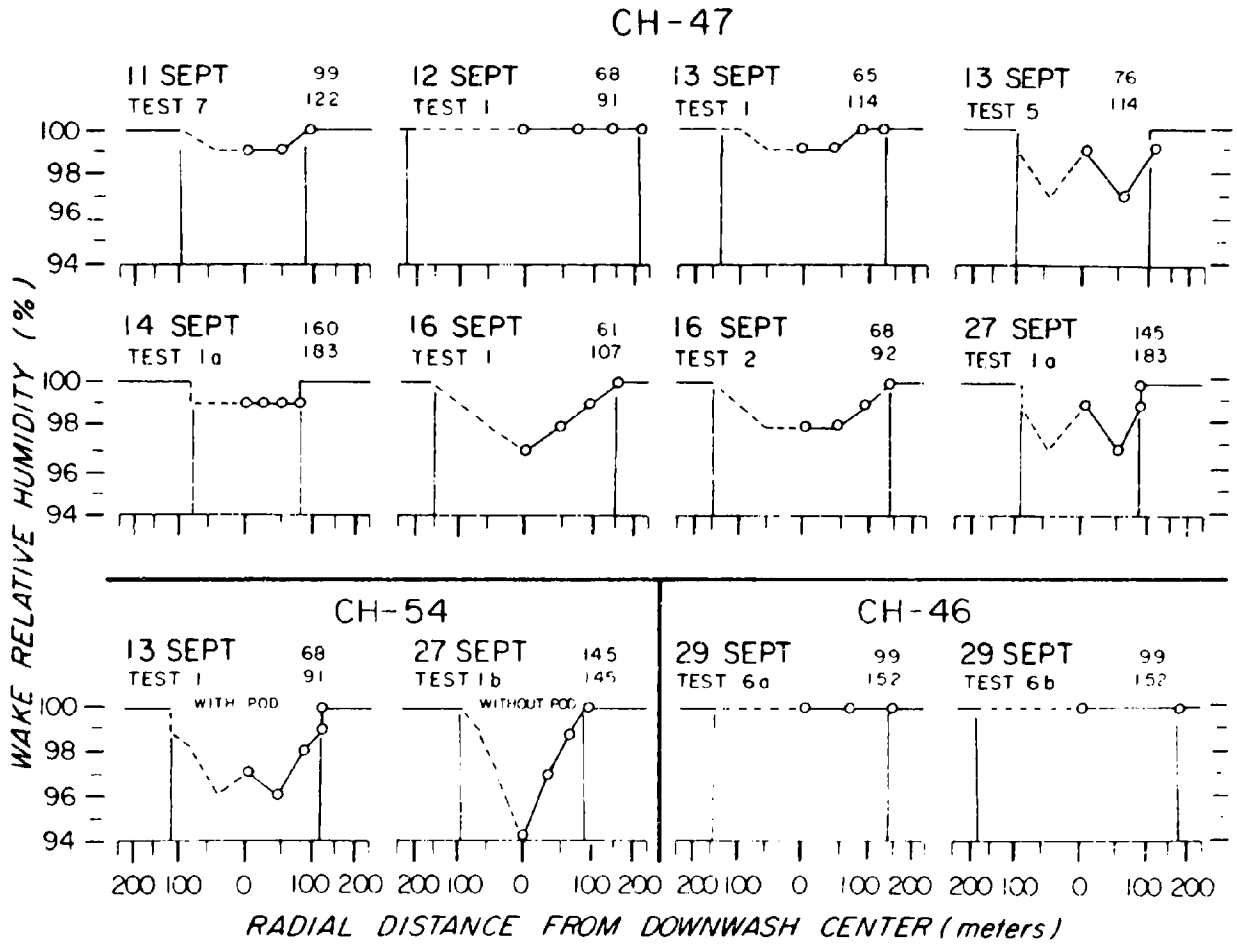
CH-47
11 SEPT
99
TEST 7
122
12 SEPT
68
TEST 1
91
13 SEPT
65
TEST 1
114
13 SEPT
76
TEST 5
114
14 SEPT
160
TEST 1a
183
16 SEPT
61
TEST 1
107
16 SEPT
68
TEST 2
92
27 SEPT
145
TEST 1a
183
CH-54
13 SEPT
68
TEST 1
91
WITH POD
27 SEPT
145
TEST 1b
145
WITHOUT POD
CH-46
29 SEPT
99
TEST 6a
152
29 SEPT
99
TEST 6b
152
WAKE RELATIVE HUMIDITY (%)
100
98
96
94
200 100 0 100 200
RADIAL DISTANCE FROM DOWNWASH CENTER (meters)

Figure 30. Δq Values and Profiles Across Downwash-Cleared Zones. The format of this figure is identical to that of Figure 28 except that the numbers above the abscissas at the left give the saturation specific-humidities within the fog surroundings and the profiles show the values of excess specific-humidity, relative to ambient. The units of both are in gm/kg

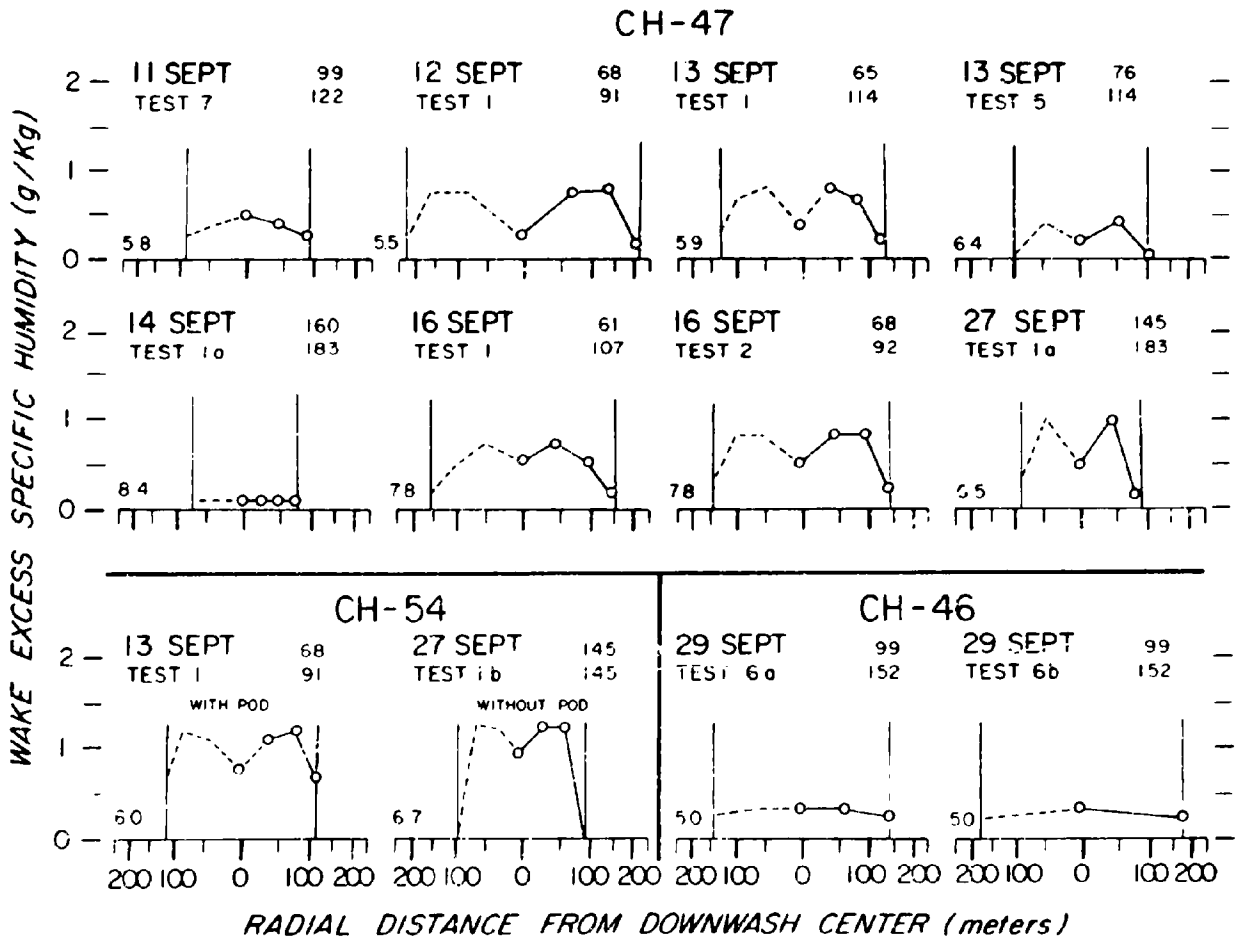
CH-47
11 SEPT
TEST 7
99
122
12 SEPT
TEST 1
68
91
13 SEPT
TEST 1
65
114
13 SEPT
TEST 5
76
114
14 SEPT
TEST 1a
160
183
16 SEPT
TEST 1
61
107
16 SEPT
TEST 2
68
92
27 SEPT
TEST 1a
145
183
CH-54
13 SEPT
TEST 1
68
91
27 SEPT
TEST 1b
145
145
WITH POD
WITHOUT POD
CH-46
29 SEPT
TEST 6a
99
152
29 SEPT
TEST 6b
99
152
WAKE EXCESS SPECIFIC HUMIDITY (g/Kg)
RADIAL DISTANCE FROM DOWNWASH CENTER (meters)

The evidence supporting this statement is contained in Table 9, wherein the temperature and specific humidity values pertaining to the 12 cited tests have been tabulated for (a) the flight altitude, (b) the surface level within the fog surroundings, and (c) the surface level within the central part of the helicopter-cleared zones. It is seen from the table that the largest values, in each and every test, occurred at the flight altitudes. The smallest values were the values observed at the surface level in the fog surroundings. The cleared zones had values intermediate between the two.

These tabulated values, when carefully inspected and compared with the profiles of Figure 30, indicate that the primary source of the humidity excess of the cleared zones was the large vapor content air aloft. A secondary source was the fog liquid water, which was evaporated into the wake air during descent mixing.*

This situation, wherein the vapor content of the air at flight altitude is larger than the saturated vapor content of the fog air, was specifically pointed out by Plank and Spatola (1969) as being one that is highly unfavorable for helicopter clearing, and one that might possibly result in the formation of new, even-denser clouds, rather than their elimination. This was the situation that generally prevailed during the Lewisburg Program. It is of interest to note that, except for the ring clouds mentioned earlier, the Plank-Spatola prediction of new cloud formation in such situations was not verified while the helicopter was hovering and clearing was being produced as a direct, dynamic consequence of rotor action. However, new clouds were created, which were thicker and more visually dense than before, after the helicopter(s) had departed the test sites and after the air of the former cleared zones had time to mix thoroughly and completely with the surrounding air. On various days of the Lewisburg Program, the general airport location of the testing operations could be recognized from the observational aircraft aloft, not because the airport vicinity was "clearer" than any place else in the fog surroundings, but because it was "more cloudy" than elsewhere in the surroundings.

9. WAKE GROUNDWASH VELOCITIES

On 16 Sept 1969, during two hover experiments, U.S. Army personnel carrying portable, cup-type, direct-reading anemometers were stationed within downwash zones at the surface level to measure the speed of the downwash-groundwash

---

*This source was of secondary importance because its contributions cannot exceed the values of fog LWC divided by air density, at the very most. For the 12 tests cited, this would account for some 10 to 30 percent of the observed excess humidity values of the Figure 30 profiles. The single exception to this statement is the particular test of 14 Sept 1969.

Table 9. Temperature, Specific Humidity and Fog LWC Values for 12 Particular Hover Tests

Date	Time Period	Test No.	Site	Heli-copter	At Flight Altitude		Within Cleared Zone at Surface Level		In Surface Surroundings		
					^{o}C T	q gm/kg	^{o}C T	q gm/kg	^{o}C T	q_s gm/kg	LWC gm/m^3
11 Sept	0858-0907	7	SW	CH-47	8.0	6.6	6.1	6.2	4.9	5.8	
12 Sept	0711-0717	1	NE	CH-47	7.7	6.6	6.0	6.2	4.3	5.5	0.20
13 Sept	0721-0730	1	SW	CH-47	9.5	7.2	7.3	6.8	5.3	5.9	0.11
13 Sept	0814-0819	5	NE	CH-47	9.5	7.2	7.5	6.8	6.3	6.4	0.08
14 Sept	0845-0855	1a	NE	CH-47	13.4	9.0	10.6	8.5	10.3	8.4	0.21
16 Sept	0717-0729	1	NE	CH-47	13.7	9.6	11.0	8.6	9.3	7.8	0.17
16 Sept	0734-0740	2	SW	CH-47	13.7	9.6	11.2	8.7	9.3	7.8	0.17
27 Sept	0749-0753	1a	SW	CH-47	11.9	9.0	9.2	7.6	6.6	6.5	0.14
13 Sept	0718-0729	1	NE	CH-54[X]	9.2	7.2	8.5	7.1	5.5	6.0	0.11
27 Sept	0758-0802	1b	NE	CH-54	11.9	9.0	9.9	7.8	7.0	6.7	0.14
29 Sept	0915-0920	6a	SW	CH-46	5.9	5.8	3.6	5.3	2.7	5.0	0.09
29 Sept	0925-0934	6b	SW	CH-46	5.9	5.8	3.9	5.4	3.0	5.0	0.18

CH-54[X] is CH-54 helicopter with cargo pod.

motions. Four persons were stationed 50 ft apart near the SW site along a line which was oriented normal to the runway. The anemometers were held in normal, horizontal position, just above head level, and the dial indications of wind speed were read and recorded periodically during the hover periods.

The experiments on this day were conducted with the CH-47A helicopter. In the first experiment, the helicopter hovered at an altitude 350 ft above the ground. In the second, it hovered 300 ft above the ground. The line of anemometers, in both experiments, was located near the upwind edge of the zone of clearing and was oriented in a direction approximately normal to the drift direction of the clearing. The wind speed values recorded during these experiments ranged typically from 5 to 20 mph, with gust speeds as large as 40 to 50 mph. It was difficult to establish the time-position relationships of helicopter, anemometer line and cleared zones with much certainty. It did appear, though, that the smallest wind speeds were generally observed near the drift axes of the cleared zones and that the largest speeds and gusts tended to occur toward the lateral edges of the clearings.

The helicopter downwash in several hover tests was sufficiently powerful to burst various of the tethered, 10 g balloons of the target networks by slamming them against the ground. The helicopters were apparently positioned over the networks in particular manner in these tests, since the effect was not observed universally in all tests. Balloon bursting was especially noticeable in one test (Test 6b of 11 Sept 1969) when the CH-47A helicopter involved was hovering and slowly circling at an altitude 500 ft above the ground. It is estimated that gust speeds in excess of 20 mph would have been required to rupture the balloons, considering their lift and the manner of tethering.

10. SUMMARY

Information concerning the results of a helicopter fog-clearing program conducted in September 1969 at Lewisburg, West Virginia, has been presented in this report. The program objectives, operational procedures, helicopters used, and measurements made were described and explained. The meteorological conditions on days of tests have been summarized and the results of the helicopter hover-experiments and runway-clearing experiments have been discussed.

The hover experiments revealed that the CH-46, CH-47 and CH-54 helicopters employed were capable of creating clearings of 400 to 2800 ft length extent within periods of 5 to 10 min. The largest clearings were generally observed in fogs shallower than 250 ft during tests that were conducted within 155 min or so of the natural dissipation time of the fog. The particularly large clearings of two of the

days were seemingly caused, in part, by "wind trailing", that is, elongation, of the clearings in the downwind direction from the hover site. This could not be proved, since wind trailing is a doubly dependent function of both wind speed and turbulence intensity (as described in Appendix D).

The best results during the runway-clearing experiments also occurred under these same conditions, but there were other factors, such as flight path design and pilot experience and proficiency, that materially affected the relative success of the experiments. Runway clearing was judged to be successful in clearing the full 6000 ft extent of the airport runway in two experiments, to be partially successful in four experiments and to be unsuccessful in 12 experiments. The categorization criteria were explained.

Particular hover experiments were performed on four days for the purpose of creating cleared zones through which helicopters could be landed on the airport runway. Six landings were accomplished, which would not have been possible otherwise.

Visibility enhancement effects which extended well beyond the boundaries of the fully-cleared zones were apparent in all experiments. But no attempts were made to determine the sizes of the affected regions or to assess the degree of the enhancement.

Semi-quantitative information of several types was obtained for particular hover experiments. It was ascertained, for example, that the wake penetration distance of the helicopters varied from about 700 to 1000 ft for the different helicopters employed, that the times required to attain steady-state conditions of clearing ranged from 150 to 260 sec, that the clearing ratios (the ratio of cleared volume to down-transported volume at the rotor level) had values of 1.8 to 8.7, and that the total entrainment of environmental air into the downwash air during the steady-state period was of the order of 3.5 to 10.5

Temperature-humidity data were acquired within downwash cleared zones during 12 experiments. The temperatures within the clearings were found to be some 0.3 to 3.0 C^{o} warmer than in the surrounding fog at the surface level; the relative humidities were 94 to 100 percent; the specific humidities were 0 1 to 1.2 gm/kg larger than in the surroundings. The excess specific humidity of the air within the cleared zones was explained as resulting primarily from the down-transport of large water-vapor-content air from aloft.

The unfavorable fog-clearing aspects of this down-transport situation were pointed out. It was noted that the situation, which was generally prevalent during the Lewisburg Program, had the theoretical potential for creating new fog, rather than eliminating fog. But it was also emphasized that no such fog-formation events of any consequence were observed experimentally, at least not while the helicopters were physically present performing the experiments. New fog of enhanced thick-

ness and visual density was seemingly created, though, after the experiments were terminated and after the air of the former cleared zones had had time to mix thoroughly with the surrounding air.

Anemometer measurements made during two experiments with a CH-47A helicopter hovering 300 to 350 ft above the ground surface revealed that the downwash-groundwash speeds within the cleared zones were typically about 5 to 20 mph with gusts to 40 to 50 mph.

The wake characteristics and fog-clearing capabilities of helicopters are described at some length in Appendix D. The descriptions are based on existing theory and on the totality of the findings of the Lewisburg Program, of the Thule AFB Program (conducted previously by CRREL) and of the Eglin AFB and Smith Mountain Programs (conducted previously by AFCRL). The wake characteristics are discussed and illustrated for the free-air situation and for the situation where the helicopter wake impinges on or trails across a surface boundary. The fog-clearing capabilities of medium-sized helicopters are estimated in terms of the trail widths, lengths, and plan-area extent of clearing that might be anticipated under meteorological conditions representative of the programs mentioned above. Comments are also made concerning the probable distribution patterns of seeding material dispensed within helicopter wakes.

II. CONCLUSIONS

It is concluded that cleared zones large enough to permit helicopter landings can be created by single helicopters (of the types used in the Lewisburg Program) in most naturally-occurring fog situations in which the fog depths are less than about 300 ft. If multiple helicopters are employed for such purpose, rather than single helicopters, this will (a) increase the size of the cleared landing zone in fog of 300 ft depth or (b) permit the creation of useable-size landing zones in fog of 400 ft depth, or possibly even fog of 500 to 600 ft depth, dependent on the particular situation and the number of helicopters employed.*

---

*The areal extent of surface-level clearing that can be accomplished by a helicopter, assuming that the wake penetration limits of the helicopter are not exceeded, is inversely dependent on the fog depth and on the airspeed employed in clearing. Hence, for a given fog depth and airspeed, multiple helicopters will provide larger areas of clearing than single helicopters approximately in proportion to the number of helicopters used. A helicopter can clear deep fog, compared to shallow fog, by flying at a slower airspeed. But the areal extent of the surface-level clearing with deep fog will be smaller than that with shallow fog. Reference is made to Appendix D and to Figures D10 and D11 where the areal clearing capabilities of helicopters are discussed and illustrated as functions of fog depth, flight altitude, airspeed and meteorological situation.

Single or multiple helicopters, with proper flight path design for the particular wind and turbulence conditions, should be able to clear and maintain clearing of most naturally-occurring fog, of depth 200 to 300 ft, over operationally-useful portions of airport runways which would permit aircraft take-offs and landings. This assumes that suitable flight coordination procedures between control tower, clearing helicopters and departing or landing aircraft could be devised.

It is manditory (refer to Appendix B), that helicopter pilots in clearing experiments or operations be provided some form of fixed ground references, such as marker balloons elevated above the fog-top. GCA or ILS systems will not provide the precision flight-path-control required. It is also deemed essential that the command-direction of the clearing operations be exercised from an observational aircraft aloft, where the full scene of the clearing operations can be continually observed. The pilots of the clearing helicopters require such direction from aloft, since they are flying so close to the fog-top that they cannot see the overall clearing results.

Under most fog conditions, except with deep fog where large wake penetration distance is needed, a tandem-rotor helicopter is concluded to be a more effective and versatile fog-clearing vehicle than is a single-rotor helicopter. Weight of weight, the tandem-rotor helicopter will produce larger cleared areas at the surface level than will the single-rotor machine. It is also more maneuverable and can better, and more safely, fly the slow-airspeed patterns required for fog clearing.

12. RECOMMENDATIONS

The following recommendations are made regarding research investigations that might profitably be conducted at the present point in time.

1. It is recommended that experiments be performed to ascertain whether dessicant-type seeding agents released into helicopter wakes would materially increase the size of the downwash clearings, would cause appreciable visibility-enhancement effects, and/or would substantially extend the persistence of the clearings.

2. It is suggested that means might also be considered for adding heat to the wake air of a helicopter. It might be noted in this regard that every 0.1 C^{o} of wake warming at the surface level (in the temperature range 5 to 20^{o}C) causes increased saturated-specific-humidity values of 0.05 to 0.1 gm/kg, which means that the air has an added absorption capacity for fog liquid water of about 0.05 to 0.1 gm/m^3.

3. An investigation is recommended to establish the optimum flight paths for single and multiple helicopters that would provide maximum, continuous clearing

of particular ground sites having specified dimensions and orientations, such as airport runways. Factors to be considered would be the wind-drift and turbulence conditions, the probable widths, lengths, and closing-in times of the helicopter trails, and the airspeeds and path circuit times of the helicopters. Certain of these factors are discussed in Appendix D.

4. Once these required flight paths are known, it is further recommended that a follow-up investigation involving the Federal Aviation Agency as participant or advisor be undertaken to determine the flight control procedures that would be needed to apply the downwash clearing technique to practical aviation problems involving the dispatching or landing of aircraft, particularly VERTOL and STOL aircraft, under restrictive visibility situations resulting from fog. Certain modifications or waivers of existing flight rules would seem to be required. Particular questions to be answered in such investigation would include:

a. Precisely how large a cleared zone along an airport runway is required to permit pilots of particular aircraft to take safe advantage of the clearings for take-off or landing purposes?

b. Will the downwash motion of the air within the clearings adversely affect the flight performance of aircraft attempting take-offs or landings through the zones?

c. If problems exist under b, can helicopter clearing be accomplished from particular (higher) flight altitudes that might alleviate or minimize the downwash effects?

d. If problems exist under b, and if c cannot be accomplished reliably, can flight procedures be designed whereby the clearing helicopters might be periodically diverted from active clearing just prior to the aircraft take-off or landing times?

e. Will the flight procedures under d also provide positive, fail-safe protection for all aircraft and helicopters in the event of a missed-landing-approach, or other such event necessitating emergency measures?

5. An investigation is recommended to determine the feasibility, problems, and cost benefits, of utilizing helicopters to clear shallow fog or smog from certain highway locations which are known places of large accident frequency caused by the fog situations of particular seasons and times of day.

6. It is suggested that experiments be performed to ascertain whether helicopters might be successfully employed to clear arctic ice-fog. The difficulties of flying helicopters under arctic conditions are recognized. It is also recognized that water produced by fuel combustion at temperatures below about $-30^{\circ}C$, under normally observed, arctic humidity conditions, is sufficient, in theory, to saturate the wake air of the helicopter just below the rotor level. Nevertheless, in view of our Lewisburg experience, where substantial clearing success was achieved under

moisture conditions which were also theoretically unfavorable, it is deemed worthwhile at least to attempt to clear ice fog with the helicopter technique. The resultant clearings might have rather transitory persistence but they might also be operationally useful, dependent on the particular problem at hand.

7. Because of the engine exhaust heat given to the wake air, and because of the normal "adiabatic warming" of this air during descent, a helicopter should be able, in theory, to create a cleared zone below its flight altitude while flying entirely within a fog layer, rather than above the layer. No recommendations are made regarding this clearing possibility, since the problems of flying helicopters at slow airspeed within fog layers under instrument flight rules are severely restrictive at present. The possibility is merely noted here in case there are unforseen or future clearing applications wherein these problems might be overcome. The pilots might fly at altitudes such that they never lose visual contact with the ground, for example. Or, a helicopter pilot, by hovering initially just above the ground, might be able progressively to increase his hover altitude, while maintaining continual visual contact with the ground, and thereby create a cleared zone within or through a fog layer "from the bottom up," so to speak. Such possibility has obvious civilian-military applications.

Acknowledgments

Particular acknowledgement is made of the extensive contributions of Dr. Emily M. Frisby to the Lewisburg Program. Dr. Frisby labored diligently during the planning phases to secure the helicopters and other logistic support that made the program possible. She also served as Co-Director of the joint program and as Manager of Field Operations for the U.S. Army. Particular acknowledgement is also made of the considerable assistance rendered by Mr. Americo S. Cerullo, who carried out much of the logistic planning and facility arrangements. Recognition is made of the supervisory and work efforts of Mrs. Elizabeth L. Kintigh, who directed the U.S. Air Force operations at the Greenbrier Valley Airport. Thanks is extended to Lt. Col Robert D. Leopold, Major Frank McCabe, and the other flight personnel of Marine Corps Squadron One who participated in several of the experiments. Thanks is likewise accorded to Major John A. McGraw and the other officers and enlisted men of the 103rd Special Operations Group, West Virginia Air National Guard, who flew the C-119 observational aircraft and who served as communications coordinators for the overall program.

Gratitude is expressed for the use of the facilities of the Greenbrier Valley Airport, Lewisburg, West Virginia which were made available to the Joint Services

Acknowledgments

by the Airport Association and the Airport Manager, Mr. John W. Gwinn. Mr. Gwinn and Mr. Paul Neal, the Assistant Airport Manager, were very cooperative and helpful throughout the course of the program.

The facilities of the Greenbrier Airport, White Sulphur Springs, West Virginia, were also made available to the Services by Mr. Charles Oscar Tate, Airport Owner and Manager. Although these facilities were not used during the program, because the fog layers were too deep over the White Sulphur Springs Valley to be cleared, their availability and the other aid given the program by Mr. Tate and his airport personnel, such as the provision of climatological data, are deeply appreciated.

The report manuscript was reviewed by Drs. Morton L. Barad and Robert M. Cunningham. Their constructive criticisms were most helpful.

A sincere debt of gratitude is expressed to each of the program contributors who are identified in the listing below.

LIST OF PROGRAM PARTICIPANTS

Logistic Planning and Support

Mr. Americo S. Cerullo, U.S. Air Force, AFCRL

Mr. Orville Snyder, U.S. Army Aviation Detachment, NAS, Lakehurst, N.J.

Flight and Support Personnel, Stationed at Roanoke, Virginia

Managerial

Mr. Vernon G. Plank, Program Co-Director and Flight Co-Director
U.S. Air Force, AFCRL

Mr. James R. Hicks, Flight Co-Director, U.S. Army, CRREL

Mr. Alfred A. Spatola, Flight Instrumentation, U.S. Air Force, AFCRL

Technical Assistance

Mr. Lacey Ransom, Electronics Specialist, University of Dayton, Dayton, Ohio

E-5 James F. Bush, Airborne Meteorological Equipment Technician, AFCRL

Pilots and Flight Crew, U.S. Army

291st Aviation Company, Fort Sill, Okla.

Major James H. Goodloe
CWO William Ruffin
SPEC 5 Miguel Muniz
SPEC 6 King Helton

177th Aviation Company, Fort Benning, Geo.

CWO William Stafford
CWO James Newhouse

Acknowledgments

SP6 Michael Hanes
SP6 B. Otis
Aviation Detachment, NAS, Lakehurst, N.J.
Mr. D.K. Mitchel
CWO John Brown
Mr. Louis Pelletier
Pilots and Flight Crew, U.S. Air Force
103rd SOG, W. Va. Air National Guard
Lt Col Guthre
Lt Col Carter
Lt Fleshman
Sgt Griffith
Sgt Abshire
Sgt Cunningham
Aerial Photography
Mr. Dave Atwood, U.S. Army, CRREL, Hanover, N.H.
Det. 5, AAVS, Andrews AFB, Virginia
TSgt McKenzie Wallace
SSgt Jerry Prestwood
Helicopter Fuel Provision, U.S. Army
Fort Lee, Virginia
SPEC 5, B. Goldsberry
PFC, R. Thomas
Field Personnel, Stationed at Lewisburg, West Virginia
Managerial
Dr. Emily M. Frisby, Program Co-Director and Field Director for the U.S. Army, ASL, Fort Monmouth, N.J.
Mrs. Elizabeth L. Kintigh, Field Director for the U.S. Air Force, AFCRL
Major F.W. Barry, Meteorological Measurements, U.S. Army Hq and Meteor. Support Co., Fort Huachuca, Arizona
Mr. Albert R. Tebo, Meteorological Instrumentation, U.S. Army, ASL, Fort Monmouth, N.J.
Anemometer Balloon Operations, U.S. Army
ASL, Fort Monmouth, N.J.
SPEC 5, R.A. Chisholm II
SPEC 4, N.A. Benson
SPEC 4, Jon Henry

Acknowledgments

Wiresonde Operations, U.S. Air Force
6th Wea. Sqdn. Mobile, Tinker AFB, Okla
TSgt Phillip Hess
SSgt Ken Barker
AIC Donald Gilbert
AIC Waine Walt
AIC Carl Detzold
Meteorological Observations, U.S. Army
USAECOM, ASL, White Sands Missile Range, N.M.
Hq and Meteor. Support Co., Ft. Huachuca, Ariz
Capt. M. McLaughlin
Sgt 1c W.B. Abbey
SSgt A. Escobar-Conde
SP4 J.R. Brown
RDT&E Support, Yuma Proving Ground, Ariz
SPEC 5 J.L. Shumaker
SPEC 4 R.J. Stroh
SPEC 4 R.L. Pszcola
SPEC 4 D.M. McCarthy
Fog Liquid Water Content Measurements, U.S. Army
SPEC 4 R.M. Backiel, CRREL, Hanover, N.H.
Motion Picture Photography, U.S. Air Force
Det. 5, AAVS, Andrews AFB, Virginia
SSgt Robbie Cameron
SSgt Laurence Miller

References

Fleagle, R.G., Parrott, W.H. and Barad, M.L. (1952) Theory and effects of vertical temperature distribution in turbid air, J. Meteor. 9:53-60.

Hicks, J.R. (1965) Experiments on the Dissipation of Warm Fog by Helicopter-Induced Air Exchange Over Thule AFB, Greenland, Special Rpt. 87, U.S. Army Material Command, Cold Regions Research and Engineering Laboratory, Hanover, N.H.

Kagawa, N.H. (1967) Modification to Kennington's Method for Predicting the Time of Radiation Fog Clearance, Dept of Transport, Meteor. Branch, Toronto, Canada.

O'Connor, J.F. (1945) Fog and fog forecasting, Handbook of Meteorology, McGraw-Hill, 727-736.

Plank, V.G. (1969) Clearing ground fog with helicopters, Weatherwise 22:91-98.

Plank, V.G. and Spatola, A.A. (1969) Cloud modification by helicopter wakes, J. Appl. Meteor. 8:566-578.

Plank, V.G. and Spatola, A.A. (1970) Observations of the Natural Dissipation of Appalachian Valley Fog, (Unpublished Manuscript submitted to Bulletin of the American Meteorological Society.)

Spatola, A.A. (1970) Climatology of Appalachian Valley Fog at White Sulphur Springs, West Virginia, During Peak Frequency of Occurrence Months (Unpublished manuscript, to be submitted for publication as an AFCRL Environmental Research Report).

Stone, R.G. (1936) Fog in the United States and adjacent regions, The Geographical Review 26:111-134.

Appendix A

Test Summaries, Notes of Surface Observers, and Pilot Comments

In this appendix, supplementary information is presented concerning the nature and time-extent of the individual tests (Section A1), concerning observations of clearing results made at the surface level (Section A2), and concerning pilot comments about their impressions of the clearing technique and results (Section A3).

A1. SUMMARY OF MISSIONS AND TESTS

The missions and tests performed during the Lewisburg Program are listed below in chronological order. The participating aircraft are identified by type-model number (see Section 2, Paragraph 2.4 for further description) and the nature of the tests is indicated.

Mission I, 7 Sept 1969

(Participating Aircraft - C-119, CH-54)

Test 1: Orbiting Lewisburg Airport, 0653 to 0709 EDT

Test 2: Runway clearing passes, without marker balloons, 0710 to 0729 EDT

Test 3: Runway clearing passes, with marker balloons, 0730 to 0734 EDT

Test 4: Circling NE balloon, 0735 to 0742 EDT

Test 5: Hover at NE Site, 0743 to 0757 EDT

Mission II, 11 Sept 1969

(Participating Aircraft - C-119, CH-54, CH-47A)

Test 1: CH-54 circling Lewisburg Airport across fog-top, 0711 to 0717 EDT

Test 2: CH-54 hover at NE site, 0717 to 0723 EDT

Test 3: Runway clearing with CH-54, back and forth, loop turns, full runway length, 0727 to 0802 EDT

Test 4: Runway clearing with CH-54 and CH-47A, back and forth, loop turns, full runway length, 0802 to 0811 EDT

Test 5: Runway clearing with CH-47A, back and forth, loop turns, full runway length, 0811 to 0816 EDT

Test 6: CH-47A circling and semi-hovering near SW balloon

a. 1st circling hover, 0817 to 0830 EDT

b. 2nd circling hover, 0830 to 0843 EDT

Test 7: CH-47A circling and then hovering near SW balloon, 0857 to 0910 EDT

Mission III, 12 Sept 1969

(Participating Aircraft - C-119, CH-54, CH-47A)

Test 1: Simultaneous hover, CH-54 over SW site, CH-47A over NE site, 0706 to 0720 EDT

Test 2: Runway clearing with CH-54 and CH-47A, racetrack pattern, SW half of runway, 0723 to 0742 EDT

Test 3: Hover to land, CH-47A hovering near SW site with some hovering assistance from CH-54, to create hole for CH-54 to land, 0743 to 0750 EDT

Mission IV, 13 Sept 1969

(Participating Aircraft - C-119, CH-54, CH-47A)

Test 1: Simultaneous hover, CH-54 over NE site, CH-47A over SW site, 0715 to 0732 EDT

Test 2: Runway clearing with CH-54 and CH-47A, racetrack pattern, full runway length, 0734 to 0742 EDT

Test 3: Circle pattern with CH-54 and CH-47A, between SW and middle (orange) balloon, to NW side of runway, 0744 to 0[illegible] EDT

Test 4: Hover to land, CH-47A hovering near SW site to create hole for CH-54 to land, 0757 to 0807 EDT

Test 5: Hover to open up hole over runway through which sun can heat runway area and possibly maintain hole, 0812 to 0824 EDT

Mission V, 14 Sept 1969

(Participating Aircraft - C-119, CH-47A)

Test 1: Hover at NE site

a. 1st hover, 0835 to 0900 EDT

b. 2nd hover, 0908 to 0910 EDT

Test 2: Runway clearing, back and forth, loop turns, SW half of runway

a. 1st back and forth, NW of runway, 0913 to 0926 EDT

b. 2nd back and forth, along (or close to) runway, 0929 to 1045 EDT

Mission VI, 15 Sept 1969

(Participating Aircraft - CH-47A)

Test 1: Runway clearing, back and forth, hovering turns, full runway extent, 0810 to 0905 EDT

Mission VII, 16 Sept 1969

(Participating Aircraft - C-119, CH-47A, Cessna 180)

Test 1: Hover at NE site, 0712 to 0729 EDT

Test 2: Hover at SW site, 0730 to 0743 EDT

Test 3: Runway clearing, back and forth, hovering turns

a. Full runway extent, 0745 to 0757 EDT

b. SW half of runway, 0757 to 0821 EDT

Test 4: Hover to land, SW end of runway, 0822 to 0840 EDT

Test 5: Observing hole-closing after landing, 0841 to 0843 EDT

Mission VIII, 23 Sept 1969

(Participating Aircraft - C-119, CH-54, CH-47A, CH-47C, CH-46)

Test 1: Simultaneous hover, CH-47C over SW site, CH-46 over NE site, 0726 to 0746 EDT

Test 2: Simultaneous hover, CH-47C over SW site, CH-54 over NE site, 0748 to 0756 EDT

Test 3: Squadron (4 helicopter) runway clearing passes, full runway extent

a. 1st squadron pass, 0806 to 0808 EDT

b. 2nd squadron pass, 0813 to 0816 EDT

Test 4: Trail width versus altitude test, CH-54 flying 500 ft above and ahead of CH-47C observes and photographs how CH-47C wake trail varies with CH-47A altitude above the fog-top, 0821 to 0829 EDT

Test 5: Joint CH-47A and CH-46 hover at SW site (test conducted at same time as test 4), 0822 to 0829 EDT

Test 6: Hover to land

a. 3 helicopters (CH-46, CH-47A and CH-54) hover to land CH-54, 0829 to 0840 EDT

b. 2 helicopters (CH-46, CH-47A) hover to land CH-47C, 0838 to 0843 EDT

c. CH-46 helicopter hovers to land CH-47A, 0843 to 0845 EDT

Test 7: Observing hole closing after landings, 0845 to 0903 EDT

Mission IX-1, 27 Sept 1969

(Participating Aircraft - C-119, CH-54, CH-47A, CH-47C, CH-46)

Test 1: Simultaneous hover, CH-54 over NE site, CH-47A over SW site,

a. 1st hover, 0741 to 0751 EDT

b. 2nd hover, 0751 to 0802 EDT

Test 2: Trail width vs altitude test, CH-54 flying 500 ft above and ahead of CH-47C observes wake trail variation of CH-47A with its altitude variation above the fog top, 0807 to 0815 EDT

Test 3: Squadron (4 helicopter) runway clearing passes, racetrack pattern, full runway extent

a. 1st pass, 0825 to 0829:30 EDT

b. 2nd pass, 0831 to 0834 EDT

c. 3rd pass, 0835 to 0836:30 EDT

d. 4th pass, 0838 to 0842 EDT

e. 5th pass, 0843 to 0847 EDT

f. 6th pass, 0848 to 0850 EDT

g. 7th pass, 0854 to 0856 EDT

Test 4: Simultaneous, 3-helicopter hover, CH-46 at SW site, CH-47C at middle (orange balloon) site, CH-47A at NE site, 0902 to 0927 EDT

Mission IX-2, 27 Sept 1969

(Participating Aircraft - CH-54)

Test 1: Runway clearing, back and forth, loop turns, full runway extent, 1125 to 1145 EDT

Mission X, 29 Sept 1969

(Participating Aircraft - C-119, CH-47C, CH-46, C-130)

Test 1: Comparison racetracks, CH-47C and CH-46 helicopters flying full-runway length racetrack over runway end to NW side vs C-130 aircraft flying larger racetrack on SE side of runway (off runway), 0747 to 0831 EDT

Test 2: Hover over farm west of Lewisburg Airport, joint hover with CH-47A and CH-46, 0834 to 0850 EDT

Test 3: Additional C-130 "long passes" across fog-top, 0850 to 0907 EDT

Test 4: Runway clearing, CH-47C and CH-46, back and forth, hovering turns, full runway extent (Test conducted concurrently with Test 3), 0854 to 0901 EDT

Test 5: Runway clearing, CH-46, back and forth, hovering turns, SW half of runway, 0903 to 0911 EDT

Test 6. CH-46 hover at SW site

a. 1st hover, 0911 to 0924 EDT

b. 2nd hover, 0927 to 0935 EDT

Test 7: Observing hover-hole closing, 0935 to 0947 EDT

Test 8: C-119 passes over fog-top along runway, 0946 to 1005 EDT

Test 9: Fog dissipation study, 1010 to 1058 EDT

A2. NOTES BY SURFACE OBSERVERS

Subject emphasis in the main text is primarily concerned with reporting the aerial observations of the clearing results of the Lewisburg Program. The surface observations, although not ignored, were not described in any systematic, chronological fashion.

Excellent observational notes were made at the surface level on all days of the Lewisburg Program by Mr. Albert R. Tebo, of the Atmospheric Sciences Laboratory, Fort Monmouth, New Jersey. These notes are presented below.

Particular notes, which were referenced in the main text, were made on 14 Sept 1969 by Captain Larry Vardiman, Headquarters Air Weather Service, Scott AFB, Illinois. These notes are also included, following the ones by Mr. Tebo.

A2.1 Notes by Mr. Albert R. Tebo

29 Aug, Fri:	Fog cleared by 1040 EDT
30 Aug, Sat:	Fog. Army tethered balloon set 1500 ft down runway from van site, which was near NE end of runway, site No. 1.
	Fog cleared by 1040 EDT.
31 Aug, Sun:	Fog. Fog already fairly heavy at 0210 EDT.
	Fog cleared by about 1030 EDT
1 Sept, Mon:	No fog.
2 Sept, Tue:	Fog, resulting from heavy rains the previous night.
	Fog cleared by 1040 EDT.

3 Sept, Wed:	No fog.
4 Sept, Thu:	No fog.
5 Sept, Fri:	No fog.
6 Sept, Sat:	No fog.
7 Sept, Sun:	Fog. CH-54 helicopter made passes along runway after sunrise, above fog, but no effect could be seen at surface. No hover over site No. 2, SW end of runway.
8 Sept, Mon:	No fog.
9 Sept, Tue:	No fog.
10 Sept, Wed:	No fog.
11 Sept, Thu:	Fog. Fog reported about 200 ft thick at sunrise. Passes along runway above fog by CH-54 and CH-47 did not clear hole. Hover over site No. 2 by CH-47 helicopter at about 0730 EDT cleared hole over parking ramp about 150 yd diameter. Helicopter could be seen patchily. Clearing at surface appeared to be larger than hole in fog-top. Fog-top reported about 500 ft high. Fog cleared from 1030 to 1050 EDT.
12 Sept, Fri:	Fog. Fog began at about 0300 EDT, fairly thick by 0400, thinning at 0500 EDT. Stars visible at zenith at 0600 EDT. C-119 aircraft overhead at 0634 EDT. CH-47 helicopter over at 0700 EDT. Hover over site No. 2 for approximately 2 min at 0705 EDT. CH-54 helicopter over site No. 2 at about 400 ft high at 0710 EDT, hover to 0715 EDT. Cleared area sufficient to see Army tethered balloon from terminal. CH-47 and CH-54 helicopters, resuming passes overhead along runway at 0718 EDT; cannot keep strip cleared more than 2 min. Wind too brisk.
13 Sept, Sat:	Fog. Helicopter over runway at 0703 EDT. Army tethered balloon set at 100 ft. 2nd helicopter over at 0709 EDT. 0718 EDT. CH-54 hovering at site No. 1. 0721 EDT. CH-54 hovering at about 200 ft. Good hole, 1/4 mile in diameter at surface. Hole drifts southward, even when helicopter holds steady. 0735 EDT, helicopter flies pattern along runway; cannot see any clearing effect at surface.

14 Sept, Sun: Fog. Fog already formed at 0300 EDT. Fog thick at 0600 EDT. Army balloon set at 700 ft. Fog-top supposedly at 600 ft. CH-47 over at 0827 EDT, hovers over site No. 1 at 0837 to 0900 EDT. Clearing on ground 800 ft in diameter, but could not see sky or helicopter at 0857.

0919 to 1030 EDT, repeated attempts to hover by helicopters over site No. 2 produced no apparent effect at surface; patchy intermittent holes could be seen at top of fog. Visibility only 200 yd. 1040 EDT, visibility improved on runway. 1100 EDT, fog turns into stratus.

15 Sept, Mon: Fog, Fog starts about 0545 EDT, only about 50 ft deep.

0815 EDT, CH-47 over. Balloons at 700 ft.

0823 EDT, 1st pass over runway, about 100 to 150 ft high, clears fog.

0825 EDT, and pass cleared runway to greater width.

0827 EDT, wind closed fog in, in less than 2 min.

0830 EDT, 3rd pass slowly. Strip is clear, and remains clear to 0845 EDT.

0845 EDT, sun takes over, keeps opening clear.

0855 EDT, fog clears through whole valley.

16 Sept, Tue: Fog. Fog developing well by 0300 EDT. Visibility 800 ft. 0707 EDT, CH-47 over. Fog thinning. Visibility 1800 ft. Army tethered ballon at 400 ft.

0712 EDT, CH-47 hovering over site No. 1.

0716 EDT, hover. Clearing on ground 200 yds diameter. Helicopter about 500 ft high. Clearing at fog-top not well defined.

0727 EDT, helicopter leaves.

0729 EDT, fog closed in.

0731 EDT, helicopter hovering over site No. 2

0735 EDT, clearing at surface 300 yd diameter.

0757 EDT, helicopter leaves.

0759 EDT, fog closed in.

0801 EDT, helicopter hovering over site No. 1.

0802 EDT, clearing at surface 250 yd diameter. Helicopter leaves.

0802 1/2 EDT, fog closes in.

0805 EDT and later, several other hovers clear openings, but passage by helicopter along runway does not.

17 Sept, Wed: No fog.

18 Sept, Thu: No fog.

19 Sept, Fri: No fog.

20 Sept, Sat: No fog.

21 Sept, Sun: No fog.

22 Sept, Mon: No fog.

23 Sept, Tue: Fog. Fog developing nicely by 0400 EDT.
0700 EDT, visibility 900 ft.
0711 EDT, one helicopter over; 0713 EDT, 2nd helicopter over; 0718 EDT, 3rd helicopter over; 0719 EDT, 4th helicopter over.
0729 to 0731 EDT, fog not too deep - 300 ft. Helicopter hoverings produce some top clearing, but cannot locate surface clearing at site No. 1. Surface winds increasing.
0736 EDT, clearing on ground near site No. 1, 300 yd long.
CH-46 hover.
0740 EDT, clearing at fog-top increases, clearing at surface lengthens
0745 EDT, clearing on top extends good portion of runway.
Wind brisk.
0747 EDT, CH-46 moves out.
0748 EDT, hole overhead closes in.
0748 1/2 clearing at surface closed.
0752 EDT, CH-54 hovers over site No. 1.
0753 EDT, clearing on ground 300 yd long.
0758 EDT, CH-54 moves out. Hole closes on top of fog.
0800 EDT, clearing on ground and hole on top closed.
0810 to 0834 EDT, helicopters begin single-file passes over runway. Clearings form in top of fog, but do not hold for more than a part of a minute. No clearing at surface.

24 Sept, Wed: No fog.

25 Sept, Thu: No fog.

26 Sept, Fri: Fog. Fog forming nicely at 0515 EDT.
0800 EDT, no flights. Aircraft fogged in at Roanoke.

27 Sept, Sat: Fog. Fog developing nicely at 0330 EDT.
0732 EDT, visibility 700 ft at site No. 2 (SW end of runway).
0741 EDT, visibility 300 ft at site No. 1.
0747 EDT, CH-54 hovering over site No. 1.
0748 EDT, clearing visible at top of fog.
0749 EDT, clearing at surface 200 yd diameter.
0750 EDT, helicopter moves out.
0751 EDT, hole at top closed.
0751 1/2 EDT, clearing at surface closed.
0756 1/2 EDT, helicopter CH-54 hovering over site No. 1.
0757 1/2 EDT, hole forming at top.
0758 EDT, clearing forming at surface.
0759 EDT, clearing at surface 300 yd long, 150 yd wide. Helicopter continuously partly obscured by fog, even though observer was looking along axis of hole.
0801 1/2 EDT, CH-54 moving out.
0802 1/2 EDT, hole and clearing closed.
0809 EDT, fog denser. Visibility 200 to 250 ft.
0812 to 0900 EDT, helicopters made 25 counted passes along runway, covering parallel strips not quite duplicating each previous coverage, at fast speeds, then slow speeds. Absolutely no effect was visible from the ground, either at fog top or at surface, except downwash was occasionally felt. Wind was light, at first, but picked up at end of period.
0800 EDT, fog still very dense.
0905 to 0925 EDT, helicopters hover in tandem. No effect.
Cannot land.
1045 EDT, fog lifting.

28 Sept, Sun: No fog.

29 Sept, Mon: Fog.
0735 EDT, visibility 800 ft. Can see Army tethered balloon through fog.
Fog looks shallow.
0737 to 0746 EDT, seven individual passes by helicopter along runway, south to north, produced swath in fog-top. Effect not discernible at surface.

29 Sept, Mon: 0749 to 0817 1/2 EDT, eight passes of the helicopters, two at a time, south to north, cleared swath at fog-top. No effect seen at surface. Wind was blowing east to west, so surface effect, if noticeable, would exist far west of runway.
0808 EDT, fog seems much thicker at surface. Swath at fog-top seems to close in variably after helicopter passes. 0822 1/2 to 0830 EDT, helicopters made two passes, two at a time, south to north, low. Clearing appears at surface for the first time, in swath pattern, 15 yd wide and length of runway. Surface swath drifted rapidly with wind, and diffused.
0746 to 0830 EDT, C-130 aircraft made twelve passes along runway, south to north, low. At 0757 1/2 EDT, it appeared that C-130 caused some breaking of fog. At other times, no discernible effect.

A2.2 Notes by Capt. Larry Vardiman

14 Sept, Sun: 0828 EDT, helicopter arrived at Greenbrier Valley Airport.
0837 EDT, small blue patch appeared south of helicopter.
0838 EDT, downdraft hit ground.
0839 EDT, can see helicopter, larger hole. Visibility on ground is about 1/4 mile, S, 300 ft N, 600 ft W, 450 ft E.
0840 EDT, visibility to S filled in.
0841 EDT, visibility to S back up to 1/4 mile, can't see helicopter.
0841:30 EDT, fog keeps drifting in from N at about 3 knots.
0842 EDT, visibility reduced toward S.
0848 EDT, can see helicopter with blue sky above. Wind about 10 to 15 knots within downwash area, with gusts to 30 knots. Maximum clearing 2000 ft long. Helicopter clearly visible. Blue hole from helicopter is long and narrow (and oriented) straight down runway.
0854 EDT, helicopter has been visible fairly-well, off-and-on for last 10 min.
0920 EDT, wind seems to have slowed considerably.

A3. PILOT COMMENTS ABOUT CLEARING PROGRAM

Written comments were solicited from the helicopter pilots involved in the Lewisburg Program concerning their impressions of the clearing technique and the results achieved. The comments received are presented verbatim; some are favorable, some unfavorable. No attempt is made to criticize or rebut any of the particular points raised.

A3.1 Comments by Major James H. Goodloe

Major James H. Goodloe, 291st Aviation Company, Fort Sill, Oklahoma, was the pilot of the CH-54A helicopter.

28 Sept 1969

"I feel that fog clearing by helicopter does have a limited value based on the experience gained during this exercise. It appears that helicopters could keep an airport open or clear that is "fogged in" under certain conditions. It was also proven that under certain conditions the helicopter can land in zero-zero conditions by making its own clearing. This could be of value under emergency conditions.

Some of the larger problems are navigation in "poor visibility" and control-of-the-operation. I do not feel that more than two helicopters should be utilized during a clearing operation due to time on target being lost in order to maintain separation, also the more helicopters involved, the more hazardous the operation becomes. I feel that the clearing operation could be much more effective at larger airports where navigation aids, such as ILS and GCA are available.

I feel that it would be worthwhile to continue the fog-clearing experimentation in major airports where helicopters are available. It would also be of much benefit if the pilots were very-familiar with the area and flew this mission on a continuing basis."

A3.2 Comments by CWO James P. Newhouse

CWO James P. Newhouse, 177th Aviation Company, Fort Benning, Georgia, was the pilot of the CH-47A helicopter.

26 Sept 1969

"Not knowing the technical objectives that were desired from the experiment as a whole, I can only comment from the point of view of a pilot flying in the right seat of a CH-47A helicopter.

If the desired objective of an operation is to clear an airfield, I think that a better method than what we tried is necessary. I feel certain that if the conditions are favorable an airfield could be cleared well enough for emergency operations; however, I don't think that the fog conditions can be predicted with much accuracy and the operation would become a "drill in trial and error."

Overall, I am certain that some of the techniques used to carry out the experiment could, with proper research and planning, be used in a tactical situation to land a helicopter through ground fog. The landing itself isn't actually a hard maneuver but the inexperienced pilot, or the average pilot without complete briefing on what to expect, would have a difficult time controlling the helicopter. Because the overall view from the helicopter is small while hovering near the fog top, the presence of a command and control aircraft at a higher altitude should be considered. Another important consideration in such a maneuver is the location of the exact point on the ground where the landing is desired. This would be extremely important in a tactical situation where the enemy controls the surrounding terrain."

A3.3 Flight Log Comments by Marine Corps Squadron No. 1, Marine Corps Air Station, Quantico Va., (Made on Days of Their Operations)

1. On 23, 27 and 29 Sept there was enough fog to run the experiments.

2. On 23 Sept the CH-46 took off from Quantico at 0530 EDT, arriving over Greenbrier Valley Airport at 0730 EDT. Contact was made with the command aircraft and at 0730 EDT the '46 started a hover on the south side of the northern balloon for 25 min at an altitude of 50 to 100 ft above the fog layer. The fog layer was 500 to 600 ft thick. After 5 min, an opening the size of the rotor diameter (about 40 ft) was formed. This hole could be maintained as long as the aircraft remained in the same location. An attempt to enlarge this opening failed.

3. Each helo hovered next to one of the balloons for 20 to 30 min. The flying crane was not carrying weight and in my estimation was not as effective as the Chinooks and the '46.

4. The next experiment conducted was to have the helos, in column, air taxi up the runway from south to north in a left hand race track pattern. The line up was as follows: the '46, flying crane, Chinook A and Chinook D. This experiment lasted 20 min. Air taxi speed on the first pass was 30 knots. This proved to be too fast to disperse the fog. The rest of the passes were flown at less than 20 knots. On each pass up the runway a trough completely through the fog was formed, but during the time (about 4 min) it took to get to the starting point the fog would move back in. This I think was due partly to the wind (NW at 3 to 5 knots on the ground).

5. In the last experiment for the day, the '46 and the Chinook A hovered over the south balloon for 5 min and created an opening big enough to let the flying crane and the Chinooks land at the airport. The '46 departed for Quantico. Total flight time for the day was 4.5 hr. Of this, 1.5 was spent in the project area.

6. On the 24th, 25th, and 26th there was a complete lack of fog in the project area.

7. The 27th there was fog in the project area. Due to weather at Quantico, and aircraft problems, take-off was not until 0645 EDT and the '46 arrived in the area at 0830 EDT. The fog layer was 800 to 900 ft thick, but a 500 ft thick haze layer was on top of the fog so only one helo hovered at a time. The results were the same as the previous experiment except it took 8 min to create the opening due to the thicker layer of fog.

8. An attempt to clear the fog off the runway was tried, but due to lack of visibility because of the haze this proved unsuccessful. The '46 returned to Quantico.

9. Total flight time for the day was 4.0 hr. Of this 1.0 hr was spent in the project area.

10. There was no fog on 28 Sept.

11. On 29 Sept take off was at 0600 EDT. The C-119 and the Chinook A were in operating area. The flying crane and Chinook D had left for another mission. The fog layer was 300 to 400 ft thick. The hover experiment results were the same as previous experiments. It took 5 min to create an opening. After about 10 min in a hover by the balloons the helos were moved off to allow aircraft to depart. The Chinook A and the '46 were moved over to a hill top where the fog was less than 100 ft thick. With the '46 flying wing on the Chinook an opening of 100 yd in diameter could be maintained. Air taxi speed of less than 20 knots was maintained and the time spent on this was 15 min. There was no wind at this time.

12. The two helos returned to the runway and air-taxied up and down the runway with a hover turn at each end using the 3 balloons as reference points. The fog was cleared from the runway and the opening could be maintained as long as the helos were air taxiing. The opening would close up in 3 to 5 min after the helos stopped.

13. Total flight time for the day was 5.1 hr with 3.5 hr spent in the project area.

Appendix B

Flight-Safety and Operational-Control Problems in Fog-Clearing

No major flight safety problems exist if a helicopter hovers or circles above a moving fog deck, following the motion of the deck. Problems can occur, however, if the helicopter hovers, or turns or circles slowly, over a fixed ground location above a moving fog deck in a situation where the wind and wind variability at flight altitude are unknown or not known in detail. The problems are mostly peculiar to single-rotor helicopters but can also occur, in degree, with tandem-rotor helicopters as well.

When hovering with respect to the ground, the nose of the helicopter, for aerodynamic reasons, should either be headed into the wind or some positive component of the wind should exist that is directed from nose to tail along the fuselage axis. If, for some accidental reason (to be explained), the helicopter should become rotated during hovering, such that the along-fuselage component of the wind assumed a negative sign, that is, became directed from tail to nose, the helicopter would then be flying backward, relative to its immediate surroundings, and it could conceivably (a) settle with power, if the backward speed exceeded a particular threshold value, or (b) fall-off backward, if the backward speed exceeded a certain larger value. In either case, the pilot, to recover from such stall situations, would require some 200 to 1000 ft of altitude, which is frequently not available in fog-clearing work.

If a helicopter is flown in a slow circular path around a fixed ground point, or flown in a slow 180° turn, as in terminating one leg of a clearing pass above

fog to begin a reciprocal pass, and if the wind speed at flight altitude has approximately the same value as the airspeed employed in the fog clearing (5 to 15 knots), potential stall situations of the types cited above could possibly occur when the helicopter was headed in the downwind turning direction, where the helicopter motion vector was essentially equal to, or smaller than, the wind vector. A particularly intense "wind gust," should it occur at such place in the turn, would increase the risk.

The stall situations cited above are not likely to occur if the pilot can see the ground clearly, or if he has a definite, fixed, visual reference. He would "sense" the situations by the "feel" of the controls. But, when visibility is reduced, when the horizon cannot be seen, and when there is a moving fog deck below, through which the ground may not be visible, or is only partially or occasionally visible, the relative-motion and changing visual-reference problems of the pilot may tend to destroy his anticipatory stall sense to a hazardous degree.

For these flight safety reasons, and for reasons of fog-clearing efficiency as well, no experiments or clearing operations with helicopters ought to be planned or conducted without the provision of some sort of ground-fixed, visual references for the pilot(s), such as marker balloons elevated above the fog top. In fact, it is the opinion of the authors that such visual references are mandatory, which opinion is also shared by certain of the pilots involved in the Lewisburg Program.

It is recommended that the operational control of a helicopter fog-clearing program should be exercised from an aircraft, or another helicopter, that flies at an altitude substantially higher than the fog-top or fog-clearing altitudes (some 500 to 1000 ft above) and keeps the overall scene of the clearing operations constantly in view by flying a circular or racetrack-type path about the scene. The desired clearing paths of the helicopters can be readily controlled by radio from such command aircraft, particularly if there are marker balloons above the fog which can be clearly seen from the command aircraft and which can be employed as position reference points in voice communications between command aircraft and clearing helicopters.

A question might be raised as to whether or not GCA or ILS guidance systems might be used to control helicopter fog-clearing operations (by themselves, in the absence of other control-marker aids as described above). The following comments reflect the lead authors' opinions, based on experience gained during helicopter experiments conducted at Travis AFB, California, in January 1969.

GCA systems, which usually operate on the doppler-radar principle, will not furnish reliable echo-position-information for helicopters moving at slow airspeeds and flying in close proximity to (or overflying) the GCA transmitting-receiving antenna. Moreover, guidance control in these systems is provided by means of voice command, which the helicopter pilot, in a fog-clearing situation with unknown

wind conditions and no fixed visual references, frequently finds difficult, or impossible, to respond to, for flight safety reasons, real or supposed. For example, the pilot, in a given situation, because of uncertainty about wind conditions, because of lack of knowledge of his precise location at the moment (relative to terrain obstacles, such as towers, etc., which might possibly be present nearby), and because of the non-presence of a well-defined, visual horizon (which forces him to fly partially on instruments and partially by his visual senses), may be unable, or reluctant, to respond to a GCA controller's request to execute a right-hand turn, or to perform some other type of maneuver. Such request-refusal situation, if it occurs several times, as is likely, rapidly destroys the controller's ability actually to control the clearing operations and results in radio communication confusion between controller and pilot which leads to mission failure.

With regard to ILS systems, it would seem that these are not sufficiently accurate to provide the precision path-control required in helicopter fog-clearing work, particularly in view of the fact that the optimum clearing paths, considering wind-drift problems, might be oriented at various angles to, and lateral distances from, the main ILS beam.

Appendix C

Development of Equations for Down-Transport Flux and Velocity

When a helicopter hovers in the free air out of ground effect within a stationary atmosphere, the gravitational force

$$G = M g \tag{C1}$$

where M is the mass of the helicopter and g is the gravity acceleration, is exactly balanced by the thrust force of the air that is transported downward by the rotor action. This thrust force is given by

$$T = F_f W_m \tag{C2}$$

where F_f is the mass transport (flux) of air across the rotor and W_m is the maximum induced-downwash-velocity, which occurs at a level about one rotor diameter below the helicopter. This is a basic, well-known, aerodynamic equation, [Dwinnel (1949), equation 13.1, or Eshbach (1952)].

The maximum induced-downwash-velocity of a hovering helicopter is also given by

$$W_m = \sqrt{\frac{2T}{\rho_f A}} \tag{C3}$$

Gessow and Myers (1952) where A is the rotor disk area and ρ_f is the air density at flight altitude.

Thus with T = G, as discussed above, this equation can also be written as

$$W_m = \sqrt{\frac{2Mg}{\rho_f A}} \tag{C4}$$

from which we obtain

$$F_f = \sqrt{\frac{Mg\rho_f A}{2}} \tag{C5}$$

In all of the above equations, it is implicitly assumed that the helicopter rotor is an ideal one, that is, that the rotor figure-of-merit is equal to unity. This assumption is justified here because, at the present stage of helicopter fog-clearing work, we are primarily concerned with the establishment of the orders of magnitude of the various clearing parameters. Moreover, our measurements of such things as clearing sizes, and the meteorological parameters, are not sufficiently accurate to warrant detailed aerodynamic analyses of the particular rotor and flight characteristics of each individual helicopter.

EQUATIONS FOR SINGLE ROTOR HELICOPTERS

The rotor disk area for a single-rotor helicopter is given simply by

$$A = \frac{\pi D^2}{4} \tag{C6}$$

where D is the rotor diameter.

When this equation is introduced into Eqs. (C4), and (C5), we obtain

$$W_m = \sqrt{\frac{8Mg}{\pi D^2 \rho_f}} \tag{C7}$$

for the maximum downwash velocity, and

$$F_f = \sqrt{\frac{\pi D^2 Mg\rho_f}{8}} \tag{C8}$$

for the down-transport flux, the mass flux. The volume flux is given by

$$F_{f_v} = \sqrt{\frac{\pi D^2 Mg}{8\rho_f}} \tag{C9}$$

EQUATIONS FOR TANDEM-ROTOR HELICOPTERS

The rotor disk area for a tandem-rotor helicopter is

$$A = \frac{\pi D^2}{2} \tag{C10}$$

which, introduced into Eqs. (4) and (C5), gives

$$W_m = \sqrt{\frac{4Mg}{\pi D^2 \rho_f}} \tag{C11}$$

for the maximum downwash velocity,

$$F_f = \sqrt{\frac{\pi D^2 Mg \rho_f}{4}} \tag{C12}$$

for the down-transport flux of mass and

$$F_{f_v} = \sqrt{\frac{\pi D^2 Mg}{4\rho_f}} \tag{C13}$$

for the down-transport flux of volume.

Appendix References

Dwinnel, J. H. (1949) Principles of Aerodynamics, Mc-Graw-Hill, First Edition.

Eshbach, O. W. (1952) Handbook of Engineering Fundamentals, John Wiley and Sons, London, Second Edition.

Gessow, A. and Myers, G. C. (1952) Aerodynamics of the Helicopter, The MacMillan Company.

Appendix D

Helicopter Wake Characteristics and Fog-Clearing Effects vs Airspeed and Flight Altitude

D1. INTRODUCTION

Knowledge of the wake characteristics of helicopters is of crucial importance to the intelligent design of fog clearing programs employing the downwash-mixing principle, or involving the release of dessicant-type seeding agents from helicopter vehicles.

The aerodynamic-hydrodynamic processes of wake formation below a helicopter (in the free air in the hover state) or behind a helicopter (in the free air in forward motion) are extremely complex and have not yet been described theoretically, at least in any satisfactory, comprehensive fashion. By the same token, few observational studies of the free-air characteristics of helicopter wakes have been published and these, where available, usually concern particular wake features near the helicopter, rather than considering the total wake, from formation zone to dissipation zone.

When helicopters are used in fog-clearing work, the helicopter wake is either "impinged on" a ground surface (during hover) or is "trailed across the ground" (during forward flight). In these cases, the wake circulations of the helicopter become doubly complicated, compared to the free-air situations, due to the presence of the surface boundary.

Additional complexities also occur in fog-clearing activities, because, with a fog layer present above the ground, the clearing of the fog does not occur through-

out the total wake region of the helicopter but only within certain portions of this region. The portions cleared, and the extent of clearing, are highly dependent on the flight conditions, on the physical characteristics of the fog and on the thermodynamic state of the atmosphere. Similarly, when seeding agent is dispensed from a helicopter, its distribution pattern following release is a complicated function of these same factors, and is also dependent on precisely where the agent release point is located within the helicopter, or relative to it, as with a sling-carried load.

The purpose of this appendix is to provide preliminary information about the helicopter wake situations cited above. The information presented, which can be called "experience information" guided by theoretical considerations," is based primarily on data acquired during the Lewisburg Program and during two prior cloud-clearing programs conducted by AFCRL. Other observational-theoretical work is also referenced and presented.

In the sections following, there is first described the wake characteristics of a helicopter flying in the free-air (in the hover mode and at different airspeeds) and next a consideration of situations where the wake impinges on, or trails across, a surface boundary. Finally, there is a discussion of the fog-clearing effects of the wakes and comment about seeding-agent distribution problems.

Considerable background analyses and computations were performed to obtain the diagrams and numerical values presented here. It is believed these results correctly depict the general, basic nature of the wake circulations and that the numerical values are in approximate, order-of-magnitude accord with reality. The reader should not attempt to use these values in any manner other than intended, as rough guidelines for general planning purposes.

The appendix diagrams were constructed to illustrate the general wake features of a helicopter of medium-size with a weight of about 25,000 lb, which was assumed to be flying in an atmospheric situation generally characteristic of what can be expected with radiation fog in temperate latitudes. The atmospheric stability below flight altitude was presumed to be uniform (devoid of sharp temperature-change layers) and to have values lying somewhere within the general range 0 to 2°C per 100 m.*

The appendix figures are designed to serve multiple purposes; consequently, frequent cross-references are made to the various figures.

---

*The atmospheric stability in most fog situations, as for example those illustrated in Figure 10, is actually quite variable with both altitude and time. It is necessary to assume a uniform stability situation, however, to permit generalized discussion of wake characteristics and to obviate any requirement for the specification of particular case-example conditions.

D2. WAKE CHARACTERISTICS IN THE FREE AIR

D2.1 Hover State; Free Air

The term "hover state" is used herein to denote the particular situation wherein the helicopter, while flying in a stationary atmosphere, maintains a fixed position relative to the ground. In other words, the ground speed of the helicopter is zero and the airspeed is also zero. The associated terms""hover" and "hovering" are likewise used primarily in this specific restrictive sense (whenever the reference is to theoretical work rather than to observational data).*

The jet-like characteristics of the wake of a helicopter hovering in the free air, and the variation of the wake velocities and temperatures with atmospheric stability and entrainment rate, have been described by Plank and Spatola (1969). These descriptions will not be repeated. Refer to Figure D1, upper diagram, wherein the general steamline-isotach picture of the wake of a medium-sized helicopter is illustrated for the free-air hover condition and for an assumed wake penetration distance of 800 ft. The entrainment rate of ambient air into the downwash jet of this diagram is somewhat larger than that of the Plank-Spatola paper and is more in accord with the observations of the Lewisburg Program, that is, the "outflair" of the wake with distance below the helicopter is greater in the diagram than in the cited paper.

D2.2 Forward Motion State; Free Air

The term "forward motion state" implies that the helicopter is moving forward relative to its air surroundings at the flight level, that is, it implies that the helicopter is moving through the air surroundings with the vector velocity

$$\vec{\Omega} = \vec{G} - \vec{V}_f \tag{D1}$$

where G is the helicopter motion vector across the ground, that is, it is the so-called "ground track vector," and $\vec{V}_f$ is the wind motion vector at the flight altitude. In the forward motion state, the vector $\vec{\Omega}$ is directed in the heading direction of the helicopter and the helicopter airspeed is given by

$$\omega = |\vec{\Omega}| = |\vec{G} - \vec{V}_f| \tag{D2}$$

---

*These terms are conventionally used to describe a situation wherein the helicopter merely maintains a fixed position aloft relative to the ground, irrespective of the motion state of the atmosphere. We require greater specificity of definition herein to permit theoretical discussion.

Figure D1. The Circulation Structure and Associated Fog-Clearing Effects of Helicopter Wakes in the Hover State at Different Flight Altitudes. The upper diagram illustrates a situation wherein the wake penetration distance of a helicopter hovering 800 ft above the ground is precisely equal to the hover altitude. The streamlines (solid) and isotachs of downwash velocity (dashed, in ft/sec) are shown. Fog clearing in such situations will be ineffective and will merely "dish in" the fog top. The second diagram illustrates how, at a lower hover altitude of 400 ft, where the downwash jet is "impinged" on the surface boundary, the wake air will spread radially across the ground surface and will eventually rise in the regions beyond the circulation centers of the spherical-type vortex. The associated, to be anticipated, fog-clearing situation is also indicated. The bottom diagram reveals how the wake air, at the yet smaller hover altitude of 200 ft, spreads farther across the ground at larger velocity, than at the 400 ft altitude. The volume extent of clearing at 200 ft in the illustrated situation is smaller, however, than at 400 ft; and it is seen that the cleared zone, which follows the course of the fastest-traveling air moving down from aloft, tends to "undercut" the fog layer. This type of clearing failure, that is, "undercutting", will occur mostly (a) under difficult meteorological conditions of clearing, with humid air aloft and large fog LWC, and (b) whenever the hover altitude of the helicopter is maintained too close to the fog-top level, which restricts entrainment within the upper clear layer and fails to maximize the down-transport of clear air into the fog layer, to the degree possible otherwise. See text for further description and discussion

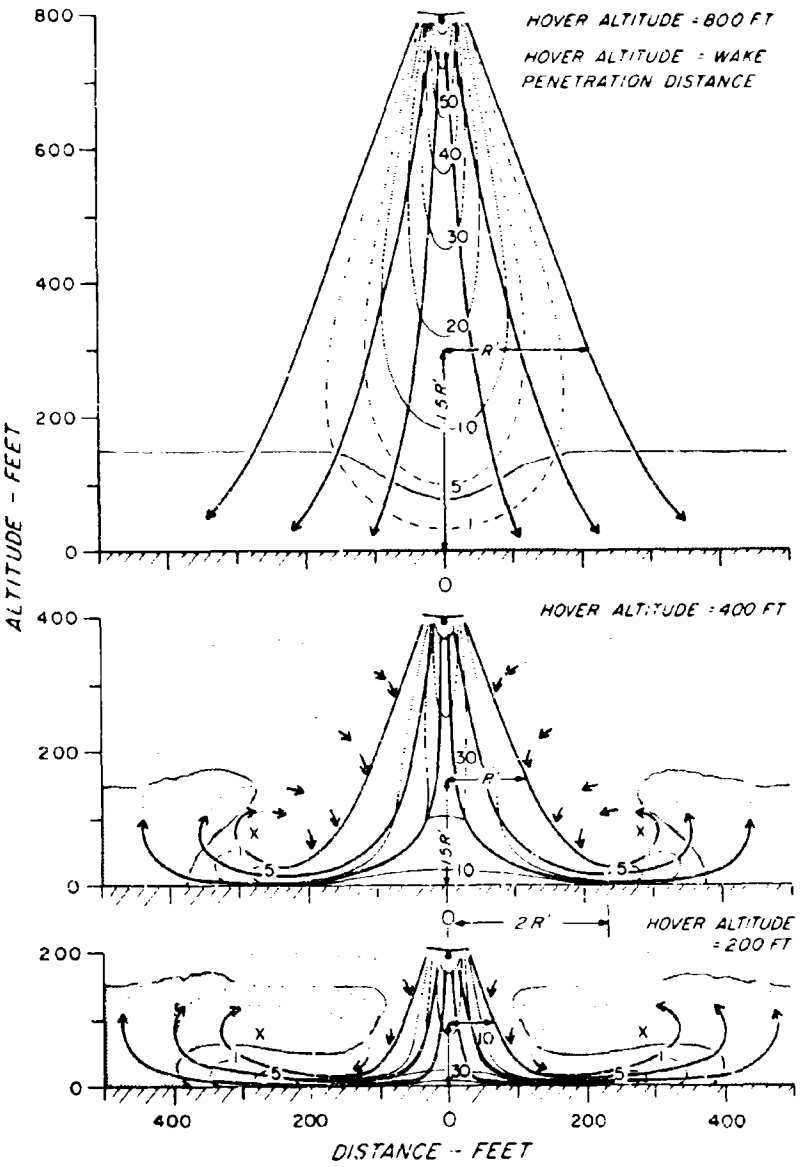
HOVER ALTITUDE = 800 FT
HOVER ALTITUDE = WAKE PENETRATION DISTANCE
HOVER ALTITUDE = 400 FT
HOVER ALTITUDE = 200 FT
ALTITUDE - FEET
DISTANCE - FEET
800
600
400
200
0
R'
1.5R'
2R'
50
40
30
20
10
5
1
X

It is important to note that the wake characteristics of a helicopter in the forward motion state are the same for any given airspeed, ω, providing that

$$\vec{V} = \vec{V}_f = \text{Constant} \qquad \text{(D3)}$$

within the wake region, which is to say that the wind is uniform within the altitude region encompassing both helicopter and wake.

The wake characteristics of helicopters in the forward motion state are discussed here in terms of airspeed. Hence, it should be clearly understood that the wake characteristics are identical irrespective of whether, for example (a) the helicopter is moving across the ground with the particular vector velocity $\vec{G}_1$ in a situation of zero wind, or (b) the helicopter is stationary above a fixed ground point in a situation where the wind, at flight altitude and within the wake region, has the uniform value $\vec{V}_f = -\vec{G}_1$. The vector $\vec{\Omega}$, from equation (D1) is positive in either case, indicating forward motion of the helicopter. Likewise, the airspeed from equation (D2), is the same in either case, having the particular value $\omega_1 = |\vec{G}_1|$. Similarly, there are other combinations of $\vec{G}$ and $\vec{V}_f$ which, from equations (D1) and (D2), will yield other cases of forward motion at this identical airspeed.

With these definitions of the "forward motion state," and "airspeed," a description of how the wake characteristics of helicopters vary with airspeed in the free air can be given. The nature and sources of the data are noted first, and then the analytical results are presented.

Motion picture photographs acquired during the AFCRL Eglin AFB Program Plank and Spatola (loc cit), recorded the releases of milled-salt tracing-agent from an HH-53B helicopter flying at speeds of 20, 40 and 60 knots (See Figure D2). Other motion picture photographs were loaned to the authors by Mr. William P. Neacy, of the AVCO Corporation, Wilmington, Massachusetts; they show releases of carbon-black agent, and plaster powder, from the rear ramp of a CH-46 helicopter which was hovering and moving forward at slow airspeed, for example, see Figure D3.

From photogrammetric analyses of these motion picture data, and from other "consistency type data," showing still and motion pictures of helicopter wake influences on clouds and on overflown water surfaces obtained during the AFCRL Smith Mountain Program, it was possible to construct the diagram of Figure D4, in which the "bottom-line profiles" of the wake of a medium-size helicopter are

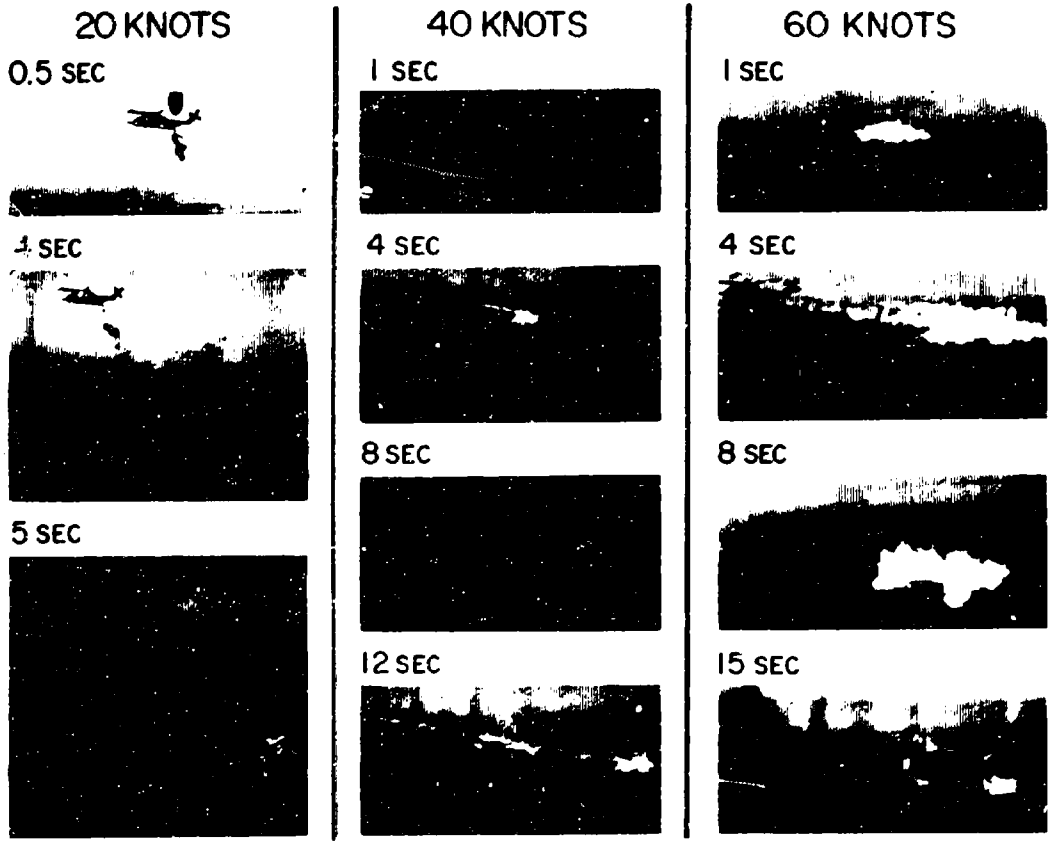

Figure D2. Time-Series of Photographs Illustrating the Release of Milled-Salt Powder from an HH-53B helicopter flying at 20, 40 and 60 Knots Airspeed. The streamers falling in the advancing direction of the helicopter, below the main trail, were caused by clumping of the salt

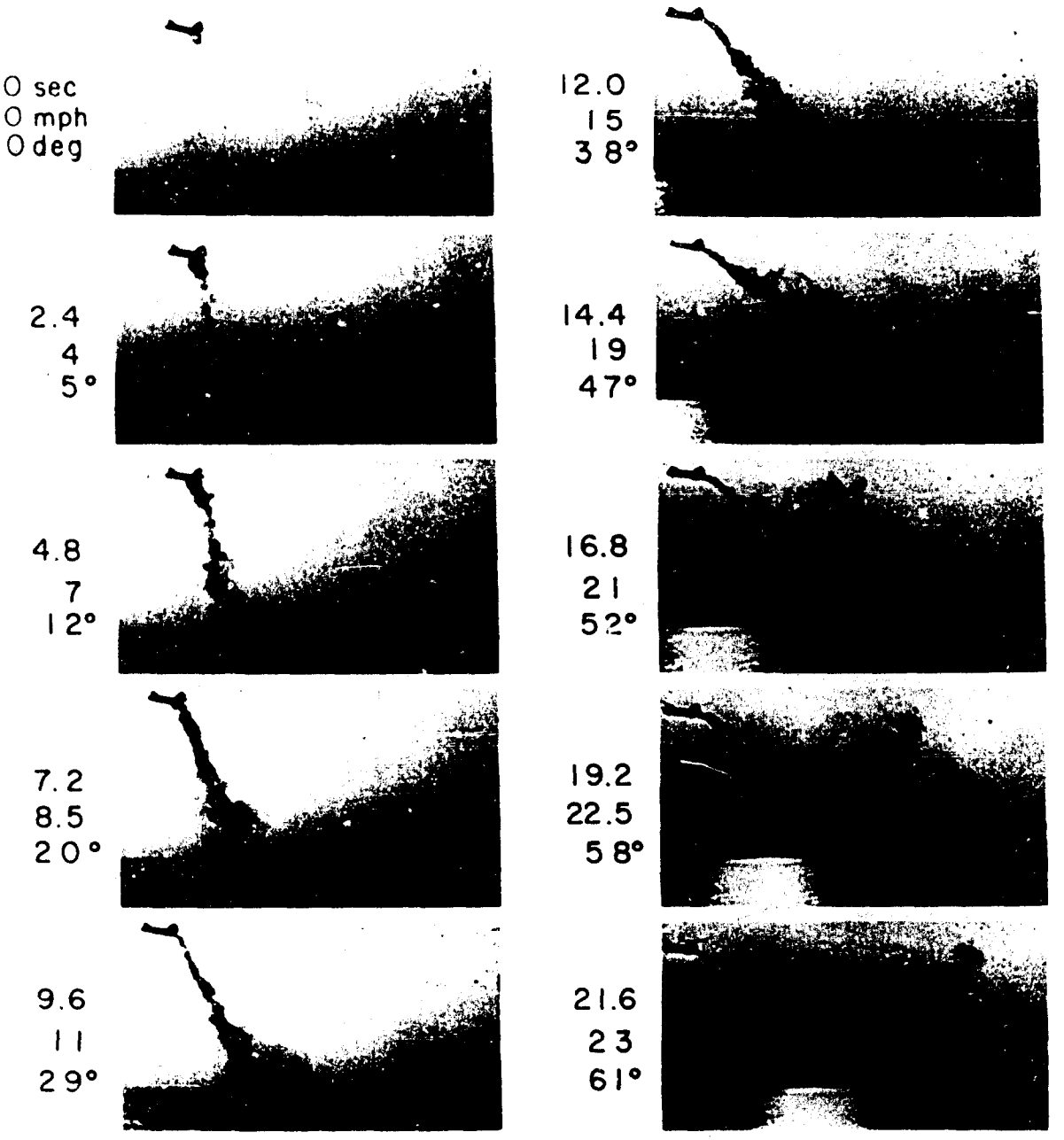

Figure D3. Time Series of Photographs Showing Release of Carbon-Black Agent from a Hovering-Accelerating CH-46 Helicopter. The flight altitude above the ocean surface was about 200 ft. The picture times, helicopter airspeeds and slope angles of the trail, from vertical, are indicated by the numbers at the left. The dimensional widening of the trail at airspeeds exceeding 19 mph is caused by the formation and subsequent presence of a trailing vortex sheet (refer to Section D2.2 and Figure D5)

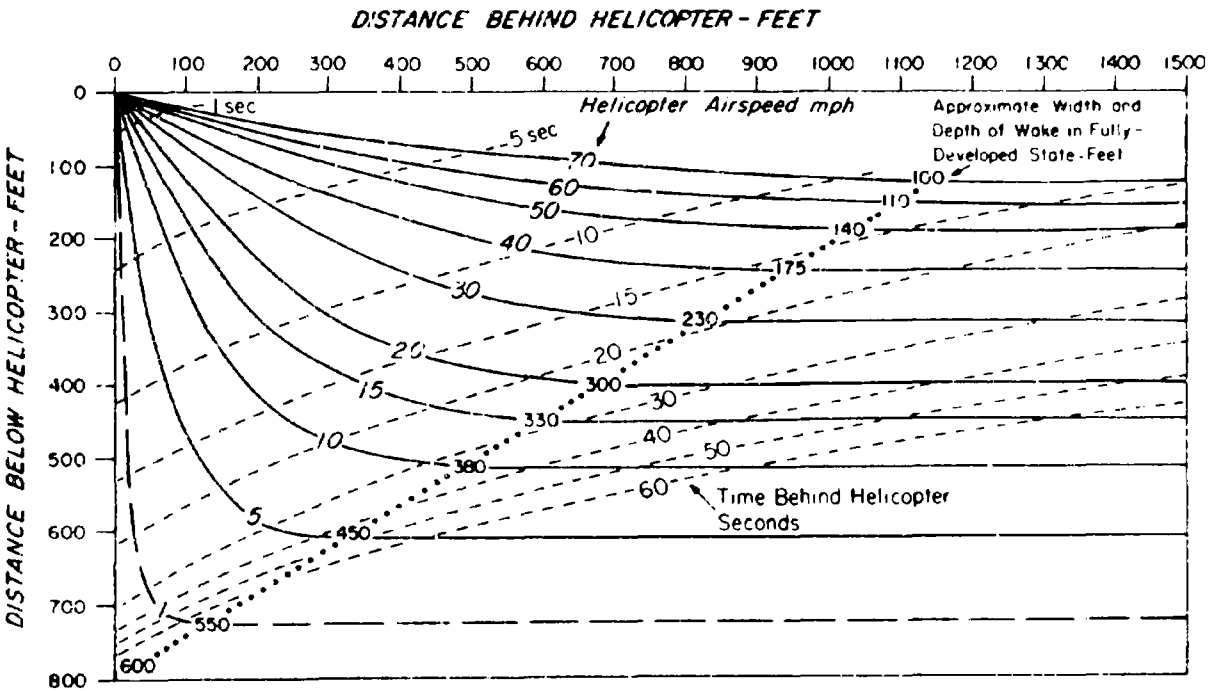

Figure D4. Profiles of the Advancing-Bottom Edge of Helicopter Wakes in the Free-Air at Different Airspeeds. The solid lines show the wake profiles that were empirically-deduced from tracing agent data (see text qualification of the particular profile for 1 mph airspeed). The dashed lines are isolines of elapsed time. The places where the wakes become fully-developed, that is, where the profiles asymptotically approach the horizontal, are indicated by the sloping dotted line. The approximate width or thickness dimensions of the wake, the two being the same in the fully-developed state, are specified by the numbers drafted along the dotted line

indicated for particular airspeed values within the range of 0 to 70 mph.* Isolines of elapsed time have been added to the diagram and the approximate width-height dimensions of the wakes, in their fully-developed states, where the trail bottoms become horizontal, have also been noted. Refer to Spreiter and Sacks (1951) for general background.

The so-called "bottom-line profiles" illustrated in this diagram are really isolines that demark the advancing-bottom edge of a wake surface that has some small threshold value of circulation velocity, something of the order of 1 ft/sec, perhaps.

It is seen from the diagram that the "profile angle" of the helicopter wake, the angle near the helicopter, between the profile lines and the vertical, increases rapidly with airspeed over the airspeed range 0 to 20 mph. The increase thereafter, with airspeeds exceeding 20 mph, is more gradual. It is also seen that the width-height dimensions of the fully-developed wake decrease with airspeed from about 500 ft, at near-zero speed, to about 100 ft, at 70 mph. Above 70 mph, the wake dimensions probably do not decrease appreciably from the 100 ft value.

The wake behind a helicopter at airspeeds exceeding 20 mph is observationally and qualitatively similar to that behind a moving aircraft, for example, refer to Gessow and Myers (1952). It is of the form of a trailing vortex sheet which emanates from the rotor blades.

The moving-wing theory of Spreiter and Sacks (p D7)would appear to have first-order, guideline-type application to the situation of a forward-moving rotor with cyclic-pitch variability.** If such anology is accepted, the two lower diagrams of Figure D5 illustrate the general form of the wake circulations that would be expected to occur behind a medium-size helicopter moving at 20 and 40 mph airspeeds. Rotated cross-sections are also shown, through the Section A A', at the 20 mph speed, and the Section B B', at the 40 mph speed. These sections have been drafted at twice the scale of the wake sketches. The section circulations are those of a "line vortex pair of opposed circulation type." The black central disks indicate the "core regions" of maximum circulation velocity, within which the air is assumed to be moving in a state of solid rotation.*** The solid lines are streamlines; the dashed lines are isotachs.

---

*The single exception to this statement concerns the isoline for 1 ft/sec airspeed and the implied isoline for zero airspeed. These show profiles of the central streamline of the wake and not the profiles of the advancing edges. The wake actually extends forward of the helicopter at very-small airspeed, due to the considerable width extent of the wake in the near-hover state, which is a fact not illustrated in the diagram.

**See Andrews (1954) and Smith (1966) for additional theoretical and observational information about vortex sheets.

***The flow field near the center of a rolled-up vortex sheet has been described by Hall (1961) and Manler and Weber (1967).

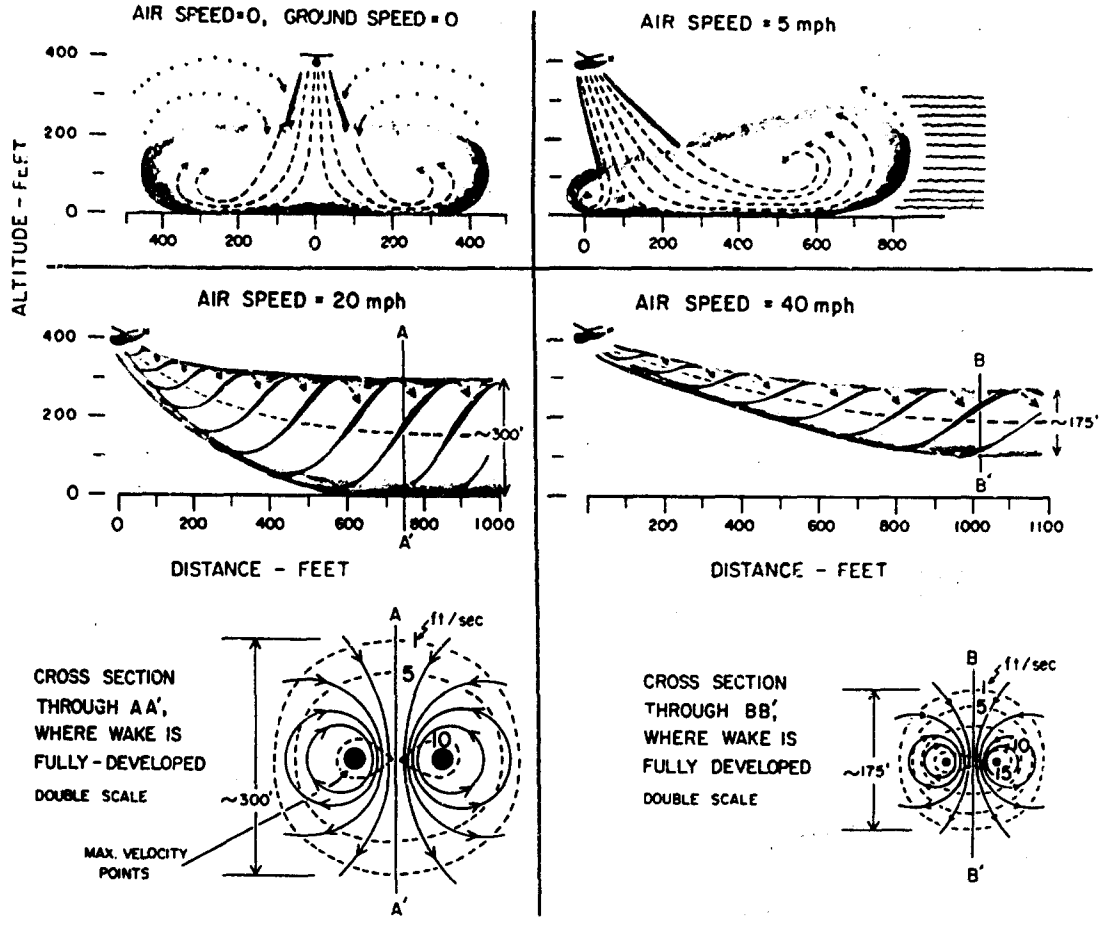

Figure D5. Appearance and Approximate Circulation Structure of Helicopter Wakes at Different Airspeeds. Diagrams are shown indicating the schematic nature of the wake circulations of a medium-sized helicopter flying at 400 ft altitude above the ground and at 0, 5, 20 and 40 mph airspeeds. The circulation at zero airspeed, in the hover state, resembles that of an inverted, spherical vortex. With airspeeds exceeding zero but smaller than that of transitional lift (which occurs at about 15 mph, refer to text definition and discussion), the circulation is like that of a "skewed" spherical vortex which is elongated in the flight path direction. For speeds exceeding the transitional lift speed, such as the illustrated 20 and 40 mph speeds, the helicopter wake has the form of a trailing vortex sheet. In the fully-developed state of the wake, indicated by the section lines A A' and B B', the circulations are those of a line-vortex pair of opposed circulation type. The nature of the circulations is shown in the expanded cross-section sketches of the bottom diagrams. The dimensional scale of the wake circulations decreases with airspeed, but the intensity of the circulations increases with airspeed. It should be emphasized that the streamlines shown in the upper diagrams, for the 20- and 40-mph wakes, are schematic only. The streamlines actually lie within sectional planes and there is little or no component of circulation in the flight path direction

There is little question, from the total observational evidence, but that the general form of the helicopter wakes of these diagrams is in first-order accord with reality. Moreover, there is little question but that the intensity of the wake circulations increases with airspeed, in accord with the Spreiter-Sacks theory, or that the width-depth dimensions of the wake, in the fully-developed state, decrease with airspeed. However, there are large, unresolved questions about the details of the streamline-isotach pictures presented, particularly regarding the spacing of the vortex centers and the numerical values of the isotachs. The sketch values are merely "best guess values" as deduced from motion picture observations of the rotation rates of tracing-agent and cloud streamers at particular radii from the vortex centers at particular distances behind the helicopters.

D3. WAKE CHARACTERISTICS IN THE PRESENCE OF A SURFACE BOUNDARY

D3.1 Hover State; Surface Boundary

When a helicopter hovers above a ground surface at a height smaller than the wake penetration distance of the helicopter, the lower part of the wake is "impinged" on the surface and the wake air is forced to spread radially outward from the nadir point. The theoretical nature of the three-dimensional spreading of a jet with uniform velocity profile, which is impinged on a boundary oriented normal to the jet axis, has been described in various aspects by Prandtl and Tietjens (1934), Pai (1954), Schlichting (1955), Poreh and Cermak (1959), Bradshaw and Love (1959), and various others. Hohler (1966) has summarized and used certain of this theoretical work with application to the helicopter-wake problem.

These theoretical results, particularly the results of Hohler, were employed here in guideline fashion to obtain first-estimate information about the probable nature of the air-flow fields beneath a helicopter hovering near a ground surface. The theoretical results, unfortunately, could not be applied directly, because (a) the downwash profile of a helicopter wake, that is, the incident profile, before boundary modification, is not uniform, as assumed in the theory; (b) the cross-sectional dimension of a helicopter wake increases with distance beneath the helicopter because of entrainment, and is not constant as is generally assumed with theoretical jets; and (c) the temperature of the downwash air of a helicopter is usually warmer, level for level beneath the helicopter, than the air of the surroundings; hence it is buoyant relative to the surroundings, which is an important factor neglected in the theory.

Reference is made to the three diagrams of Figure D1, which show sketches of the probable streamline-isotach situations of the wake of a medium-sized heli-

copter hovering at 800, 400 and 200 ft above a ground surface. The wake penetration distance of the helicopter was assumed to be 800 ft, corresponding to observations of the Lewisburg Program. This distance is precisely equal to the hover altitude of the first diagram. (The clouds and clearings also shown in the diagrams will be discussed later.)

In constructing these diagrams, reference was made to the work of Hohler (1966). It was assumed that the helicopter wake, on entering the "turning region" (Hohler's Zone II, see footnote*) from above, had the incident radius R' and that the region extended vertically above the ground a distance 1.5 R', where

$$R' = \frac{Am + D/2}{1 + 1.5\ m} \tag{D4}$$

where A is the helicopter altitude above the ground, D is the rotor diameter (a single-rotor helicopter is implied) and

$$m = \Delta R/\Delta Z \tag{D5}$$

where $\Delta R/\Delta Z$ is the mean, before incidence, radius increase of the wake per unit travel distance below the helicopter. $\Delta R/\Delta Z$, in other words, is a measure of the normal "downward-outward flair" of the wake from rotor level to the level at which boundary modification first commences.

The particular R' and 1.5 R' dimensions that define the "turning regions" in the three Figure D1 situations are indicated in the diagrams. These dimensions stem basically from the work of Hohler (1966), which is not theoretically rigorous. Although it is axiomatic that a turning region exists, we are actually uncertain whether its vertical dimension is 1.5 R' or perhaps some greater or smaller value.

In the theory of impinging-jets (refer to Hohler (1966) specifically), the air that moves radially outward from the nadir attains its maximum horizontal velocity at the radius 2 R' from the jet axis (see the middle diagram of Figure D1). The vertical depth of the layer is a minimum at this radius. The streamlines and isotachs of the Figure D1 diagrams have been drawn to conform with these maximum-minimum conditions, based on the presumptions that the vertical extent of the outflowing air at the 2 R' distance would be of the order of a few tens of ft and that this "boundary layer" would be shallower at the 200 ft hover altitude than at

*The turning region of a jet that is impinged normally on a flat surface is the region wherein the fluid motion is deviated and "turned" because of the presence of the surface. The fluid on entering the turning region has a flow direction that is normal to the flat surface whereas its direction on leaving is parallel to the surface.

the 400 ft altitude, which theory would suggest, and which hover tests performed over a water surface during the AFCRL Eglin AFB Program would appear to verify.

Continuity considerations were also employed to insure that the diagram sketches were reasonably indicative of reality. For example, if the radius of the incident jet entering the turning region from above is R', as previously defined; and if the mean sectional downwash velocity across the indident jet at the level 1.5 R', at the top of the turning region, is $\overline{W}$; then the mean outflow velocity in the horizontal at the radial distance 2 R' will be given by

$$\overline{V} = \frac{\pi R'^2 \overline{W} + E_t}{4\pi R' h} \qquad \text{(D6)}$$

where Δh is the vertical thickness of the outflow layer at the 2 R' radius and E_t is the "volume entrainment" of air into the jet from the surroundings that occurs within the turning region. It is assumed, in this equation, that the air density within the turning region is constant.

If we now postulate a situation, like that of the middle figure diagram for the 400 ft hover altitude, where R' = 120 ft, $\overline{W} \cong 4$ ft/sec, E = 0, by assumption, and h = 35 ft; also by assumption, then the value of V should, from the equation, be of the order of 3.4 ft/sec. This would be the expected value of the mean velocity of the outflow. Actually, again referencing Hohler (1966), and assuming that the form of the "groundwash profile" of his Figure 8 illustration is approximately valid at the 2 R' radius; the maximum outflow velocity, that is, the maximum horizontal wind at the peak of the velocity profile, should perhaps be about 3 times as large as the mean outflow velocity, or

$$V_m = 3\overline{V} \qquad \text{(D7)}$$

and this maximum wind should occur at the approximate level

$$\delta \cong \Delta h / 8 \qquad \text{(D8)}$$

above the ground surface.

Hence, the maximum outflow velocity in the case example might be anticipated to be about 10.2 ft/sec, occurring at a level some 4.4 ft above the ground.

These values, although obtained in a highly-speculative fashion from the theory, are roughly in accord with the groundwash velocities measured by anemometers during the AFCRL Smith Mountain Program and during the AFCRL-ASL Lewisburg Program (refer to Section 9 of the main text).

At radial distances beyond 2 R', the Hohler (1966) report describes a "wall jet region" [also refer to Galuert (1956) and Bakke (1957)] in which a turbulent boundary layer developes progressively within the outflowing air which results in an increased "layer depth" with travel distance associated with substantial decrease of the outflow velocities. This theoretical work cannot be applied to the helicopter wake problem, however, since the downwash-groundwash air of a helicopter is generally warmer than that of the surface surroundings (refer to Section 8 of the main text). The buoyancy of this air will logically modify the Hohler (1966) theoretical picture causing the streamlines in the region beyond the 2 R' distance to rapidly diverge, as the air begins moving upward, and the flow velocity to quickly decrease. The streamlines and isotachs of the second and third diagrams of Figure D1 have been sketched to illustrate this situation, which seems to be in general accord with observation.

The fine dotted lines of the two lower diagrams, which appear in the region above the fog-top, indicate the existence of a mean continuity-flow of air of very small velocity, which is probably smaller than the turbulent perturbation velocities of the atmospheric surroundings. This return continuity-flow must exist, of course, to close the circulation system.

The smallest hover altitude illustrated in the Figure D1 sketches is 200 ft. It may be logical to question what happens to the wake circulations as the hover altitude is decreased to zero. Will the wake widths increase as the lateral spreading of air increases? The answer is no, since, as the helicopter approaches the ground in a hover, the power required to suspend the helicopter decreases due to ground-lift effects, hence less energy is imparted to the wake circulations and the dimension-scale of the wake also decreases. With a helicopter hovering just above the ground surface, it is estimated that the wake-width is limited to above five rotor diameters.

D3.2 Forward Motion State; Surface Boundary

When a helicopter moves forward across an underlying surface boundary, the wake characteristics change with airspeed approximately as illustrated in Figure D5. The flight altitude assumed in these sketches is 400 ft above the ground.

At zero airspeed, the circulations of the impinging wake resemble those of the inverted spherical vortex described previously. The zero-air-speed wake is sketched three-dimensionally in the first diagram and the streamlines of the central (diameter-height) section are indicated. The upper boundary of the rising air is nebulous and indefinite. This boundary will vary considerably in altitude depending on the particular stability conditions of the atmosphere.

When airspeed is increased from zero to some slow speed, such as 5 mph, the spherical-type vortex of the hover state becomes elongated in the flight path

direction and the roll circulations of the vortex become smaller, scalewise, in the advancing direction of the wake than in the trailing direction. The approximate wake picture for the 5 mph speed is illustrated in the second figure diagram. The streamlines shown are the instantaneous streamlines of the flight path section. It is important to note that the particle trajectory lines in such wake, as would be made visible by appropriate tracing agent, would differ appreciably from these streamlines and that the form of the wake, as thus seen visually, would differ from the one illustrated. The wake, for one thing, would certainly extend downstream of the helicopter into the region of the sketch indicated by the horizontal wavy lines.

The data supporting this circulation picture at the 5 mph airspeed were obtained from photogrammetric analyses of motion pictures supplied by the AVCO Corporation, previously referenced, which showed tracing-agent releases from a CH-46 helicopter. One such release is illustrated in Figure D3.

When the helicopter airspeed exceeds the speed of transitional lift, the speed at which the cyclic-pitch rotor begins functioning like an airfoil, a speed of approximately 15 mph, the helicopter wake assumes the form of a trailing vortex sheet, as previously described in Section D2.2. This trailing sheet will intersect the ground surface, if the helicopter flight altitude above the ground is less than the vertical penetration distance of the wake. (These penetration distances for various airspeeds can be obtained from Figure D4. They are the distances from flight altitude to the "bottomline" of the wake in its fully-developed state.)

The third Figure D5 diagram illustrates a situation when the airspeed is 20 mph and the bottom part of the helicopter wake just intersects and trails across the ground surface. Reference is also made to the photographs of Figure D14, described later, which shows the results of smoke tests conducted by the Naval Rework Facility, San Diego, California, under conditions somewhat analogous to those of the sketch. The tremendous width-thickness extent of the wake is apparent in the photographs.

At an airspeed of 40 mph, as indicated in the last sketch of Figure D5, the helicopter wake does not intersect the ground surface at all. This illustrates a situation in which the wake penetration distance is smaller than the flight altitude.

The upper left-hand diagram of Figure D6 shows the wake width and wake thickness values which, total experience indicates, should reasonably be anticipated with a medium-size helicopter flying at various altitudes and airspeeds above a surface boundary. The width values are the horizontal, cross-trail, surface-level dimensions of the wake in its fully-developed state. The thickness values are the vertical wake dimensions, measured from the ground upward, which also pertain to the wake in its fully-developed state.

The upper solid line of this diagram, the one for zero wake width, is a plot of wake penetration distance versus airspeed. (These penetration values correspond to those of Figure D4.) The interior solid lines of the diagram indicate the wake-width dimensions that would be expected over the airspeed range 0 to 70 mph and the altitude range 0 to 800 ft above the ground. The dotted lines show the wake-thickness values corresponding to the various width values. The double fine line of the diagram, sloping downward, is the line of "maximum width" (versus airspeed and altitude). The dashed lines reveal the approximate times required for the first wake air (the fastest down-traveling air) to reach the surface level following helicopter passage over a particular ground point, or following the beginning of a hover, in the zero airspeed case.

Isolines of S/T (wake-width/wake-thickness) are shown in the diagram at the lower left in Figure D6. Five particular points are identified in the diagram, at the 20 mph airspeed, which are labeled A through E. The sketches at the lower right in the figure indicate how, in the fully-developed state of the wake, the cross-sectional appearance and circulation structure of the wake varies as the helicopter flight altitude is progressively lowered from 400 ft (at A) to 360 ft (at B) to 265 ft (at C) to 140 ft (at D) to 40 ft (at E). The bottom part of the wake is just tangent to the ground surface, at Point A, and the surface width of the wake, S, is zero, with S/T also being zero. Between Points A and D, as flight altitude is decreased, the wake-width increases and thickness decreases. The wake attains its maximum width at Point D, where S = 670 ft, with S/T = 6. Then, for flight altitudes below Point D, decreasing toward the ground, both the S and T dimensions of the wake begin to be limited and diminished by aerodynamic ground-effects, because less engine power is required for helicopter flight near a ground surface than in the free-air, hence less kinetic energy is transmitted to the wake.

The Figure D6 information discussed thus far was based on, and corresponds to, observational data which were acquired during the three experimental programs cited earlier. For example, hover experiments conducted at near zero airspeed during the Lewisburg Program revealed that the maximum wake-width of a medium-size helicopter ranged from about 1200 to 1800 ft and that this maximum width occurred generally at flight altitudes of about 250 to 350 ft. Likewise, data obtained from over-water tests during the Smith Mountain Program showed that the wake trails of helicopters flying at 20 to 30 mph airspeed attained their maximum widths, 500 to 700 ft, at a particular flight altitude (near 150 ft). Other observational data were also employed and various comparison checks made to insure that the form and values of the isolines of the upper left hand diagram of

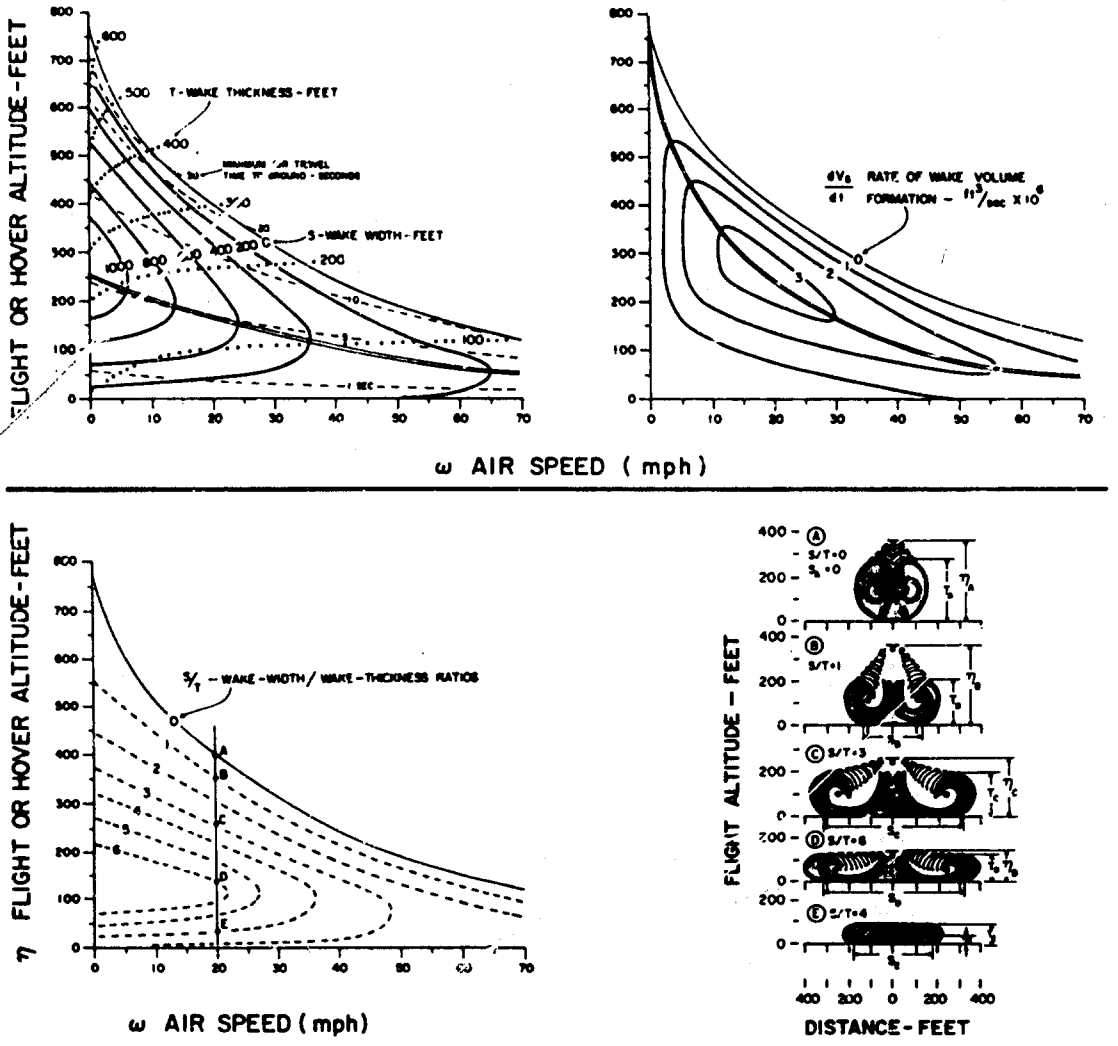

Figure D6. Dimensions, Cross-Sectional Appearance, and Volumetric Formation Rates of the Fully-Developed Wake of a Medium-Sized Helicopter. The diagram at the upper left shows the wake width (S), of the helicopter wake at the surface level (the solid lines), the wake thickness (T), of the vertical extent of the wake above the surface level (the dotted lines), and the minimum air travel time to ground (the dashed lines). The isoline of zero wake width is also an isoline of wake penetration distance (vs airspeed and flight altitude). The diagram at the lower left shows isolines of the ratio of wake width to wake thickness and the cross-sectional appearance of the wake, in its fully-developed state, corresponding to the particular indicated points, A through E, is shown at the lower right. The sectional diagrams also illustrate the definition and significance of the S and T dimensions. The diagram at the upper right shows the rates of wake volume formation (vs airspeed and flight altitude) which correspond to the S and T values just cited and explained. See text for further discussion

Figure D6 were rationally and numerically consistent with background theory and with the totality of previously acquired wake data.*

From the width thickness values of this cited diagram, we can readily determine the time rate of wake volume formation behind a medium-sized helicopter, that is, we can compute and plot, vs airspeed and flight altitude, the values of

$$\frac{dV_s}{dt} = \omega S T \qquad \text{(D9)}$$

where ω is airspeed, S is wake width, T is wake thickness, and where the subscript s on V is used to signify "wake-stirred volume." A rectangular wake-cross-section is assumed. These computations were made and the results are shown in the upper right hand diagram of Figure D6. The solid lines of this diagram are isolines of dV_s/dt; the double fine line indicates the line of the maximum values.

This diagram illustrates how, theoretically and experiencewise, a helicopter should be flown to maximize the volumetric amount of the wake stirring (wake mixing) of air along the flight path course. For example, with a helicopter flying 200 ft above the ground, dV_s/dt, according to the diagram, will be maximized at 25 mph airspeed. With a helicopter flying at 400 ft altitude, the maximum will occur at 8 mph, and so forth.

D4. FOG-CLEARING EFFECTS OF HELICOPTER WAKES

D4.1 Optimum Flight Conditions and Clearing Diagrams

In fog-clearing operations, the helicopter wake is trailed across the ground surface and the clear air, present above the overlying fog layer, is transported downwards into the fog layer by the wake. This air mixes with the fog and the cloud droplets are eliminated by evaporative processes.

To clear fog effectively, it is a prerequisite that the stirring-mixing influence of the helicopter wake should extend vertically throughout the entire layer depth of the fog, which is to say that the helicopter should be flown in a manner such that

$$T \geq H \ , \qquad \text{(D10)}$$

where T is the wake thickness and H is the fog depth.

---

*The values of greatest uncertainty and variability in this diagram are those for wake thickness at zero airspeed. There are questions of how wake thickness should be defined for the hover state. Additionally, and irrespective of precise definition, the values will vary considerably with atmospheric stability and wake buoyancy. The particular thickness values used in the diagram were assumed equal to the flight altitude, except near the ground in ground effect.

It is also desirable, to insure clearing effectiveness, that the rate of wake volume formation (dV_s/dt) be maintained as large as possible, which, other conditions being equal, will tend to maximize the fog-clearing rate as well.

If we assume that T = H, and at the same time perform a transformation of ordinate parameters, we can then convert the "wake diagram" of Figure D6 at the upper left into the "fog clearing diagram" shown at the top of Figure D7. By such conversion, we have implicitly assumed that a particular functional relationship exists among the three parameters, fog depth, flight altitude and airspeed. We cannot express this relationship mathematically but its empirical nature is indicated by the isolines of flight altitude that have been drafted on each diagram.

These isolines of flight altitude prescribe the particular helicopter altitudes that must be maintained to insure that the helicopter wake, for any given set of fog-depth and airspeed conditions, will have vertical thickness equaling the fog depth. For example, with a fog of 200 ft depth and with an airspeed of 15 mph, it is seen in Figure D7 (interpolating between isolines) that a flight altitude of 260 ft is required in order to accomplish the scale matching of wake thickness and fog depth. These diagram-prescribed altitudes correspond approximately to the optimum altitudes of our fog-clearing experience.

Under flight conditions cited, the diagrams of Figure D7 provide auxiliary information about the trail widths of clearing (first diagram), about the volume rates of clearing (second diagram), and about the plan-area rates of clearing (third diagram). These are the trail widths and clearing rates that would be anticipated when the clear-air above the fog is comparatively dry, that is, with relative humidity less than about 85 percent, and/or when the fog LWC is comparatively small, that is, of the order of 0.05 gm/m^3 or smaller.

More specifically, the first diagram of this figure shows the isoline values of

$$C = K S \tag{D11}$$

where C is the surface-level width of the cleared trail in the fog. This width is related to the wake-width, S, through the proportionality constant, K, which, in the diagrams of Figure D7, has been assumed equal to unity. The relationship between the C and S dimensions in a situation where $K < 1$ is illustrated later in Figure D12. The second Figure D7 diagram shows isoline values of

$$\frac{dV_r}{dt} = \omega C H \ , \tag{D12}$$

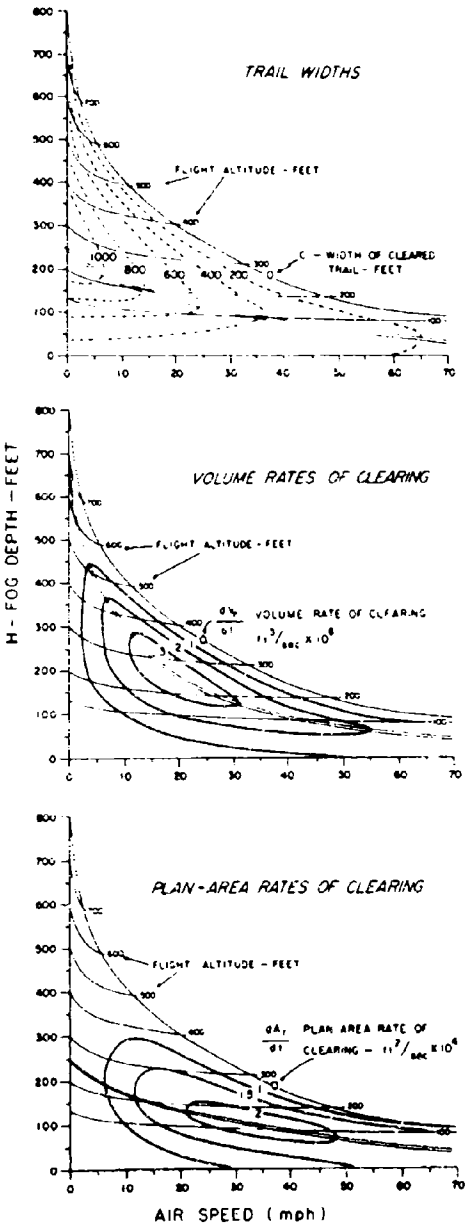

Figure D7. Trail Widths and Fog-Clearing Rates that Might Reasonably be Anticipated with a Medium-Sized Helicopter Flying in the Indicated Manner Under Optimum Cloud-Physics Conditions. The flight altitudes required to accomplish a "scale matching" of wake-thickness and fog-depth are shown by the fine solid lines that slope downward across each of the diagrams. The upper diagram (dashed isolines) reveals the widths of the cleared trails at the surface level that would be expected under the prescribed flight conditions. The second diagram shows the volume rates of clearing that would occur throughout the fog depth. The lower diagram indicates the rates at which plan-area clearing would occur at the surface level

where a rectangular-shaped cross-section of clearing is assumed, and the third diagram shows isoline values of

$$\frac{dA_r}{dt} = \omega C \quad . \tag{D13}$$

The subscript r applied to V and A denotes that these are the trail formation rates of the fully-developed helicopter wake which pertain to the removed zone of the trail which begins at the place of full-wake development. This zone is defined in Section D4.1.

It should be emphasized that these diagrams illustrate an idealized, optimum, clearing situation wherein the meteorological conditions permit clearing throughout the total wake volume. The clearing differences resulting from variations of the meteorological parameters are discussed in Section D4.3. It should also be noted that, although clearings of considerable area-volume extent can be created and maintained in the hover mode, the rates of formation of new cleared area or volume are actually zero in this mode.

The Figure D7 diagrams reveal that a medium-sized helicopter, under the flight and cloud physics conditions cited, and assumptions made, ought to be capable of creating trails of some 200 to 1000 ft width in fog layers 0 to 400 ft deep. The volume clearing rates should range from about 1×10^6 to 3×10^6 ft^3/sec, with the maximum occurring for fog of 200 ft depth at 20 mph airspeed. The plan-area rates of clearing should vary from approximately 1×10^4 to 2×10^4 ft^2/sec, with the maximum occurring with fog of 125 ft depth at 35 mph airspeed. A medium-sized helicopter cannot effectively clear fog of depth greater than about 400 ft. For fog deeper than this, a larger helicopter would be required.

The diagrams of Figure D7 are based on the assumption that the helicopter always flies in the optimum fashion described previously. A question arises as to what will happen if the helicopter flies at altitudes lower than optimum, or higher than optimum.

The helicopter, according to the flight-altitude isolines of the diagrams, cannot fly at altitudes much lower than optimum without descending into the top of the fog layer itself, which is patently undesirable. However, within the limits indicated, helicopter flight at altitudes lower than optimum, other things being equal, will tend to undercut the fog so that clearing occurs predominantly within a surface layer that does not extend completely throughout the entire vertical depth of the fog. At least this possibility exists. A situation of undercutting in the hover state is illustrated in the lower diagram of Figure D1. It can occur in the forward motion state as well.

Flight altitudes somewhat higher than optimum may be desirable if the air at such level has an appreciably smaller humidity than the air closer to the fog top. This is a meteorological factor not considered in the Figure D7 diagrams but one that should not be ignored. It might be better, for example, in a given situation, to sacrifice wake volume (volume formation rate) for the advantage of securing drier-air aloft, which would be transported downwards into the fog by the wake.

At flight altitudes much higher than optimum, which approach the wake penetration limits of the helicopter, the downward velocity components of the wake will be too small for effective fog clearing. The fog layer will only be modified in its upper portion. The helicopter wake will merely "dish in" the fog in the hover state, as illustrated in the upper diagram of Figure D1, or will merely create shallow top trails in the fog in the forward motion state, as shown in Figure 4 of the paper by Plank and Spatola (1969).

D4.2 Total Plan-Area Clearing Maintainable by a Medium-Size Helicopter

Consider how much total clearing, that is, plan-area clearing at the surface level, can be continuously maintained by a medium-sized helicopter in the presence of (a) turbulent-diffusion effects, which will usually tend to close in the cleared trails with time, and (b) solar-heating effects, which may, under certain circumstances to be defined later, tend to widen the trails with time.

It is essential for clarity to identify two kinds of cleared zones. The first is the "trail formation zone," which is located immediately below the helicopter in the hover state or immediately below and/or behind the helicopter, within the wake development region of previous mention, in the forward motion state. Clearing in the trail formation zone is produced dynamically as a direct consequence of the rotor action of the helicopter.

The second zone is the "removed zone." This zone exists only in the forward motion state and is located at distances behind the helicopter which lie beyond the place where the wake first becomes fully-developed. The wake circulations are decelerating and decaying with time within this zone.

A basic assumption at this point is that turbulent-diffusion and/or solar heating effects will not operate to modify clearing results in the "trail formation zone" but will only modify results in the "removed zone."

The procedure is as follows. First, will be given estimates of the area extent of the surface-level clearing that occurs within the "trail formation zone." Then there will be a description of the turbulent-diffusion and solar-heating effects that cause trail modification within the "removed zone," and also estimates of the total areas of clearing that should be maintainable with a medium-sized helicopter under particular conditions.

D4.2.1 Cleared Area within the Trail Formation Zone

Estimates of the length and area extent of the surface level clearing that occurs within the trail formation zone are provided in Figure D8. A sketch is shown which indicates the presumption about the shape of the cleared zone.

In making these estimates, it was assumed that the zone length in the hover state was simply equal to the diameter of the circular area of surface-level clearing. Thus,

$$L_F = C \quad , \tag{D14}$$

with the zone area being given by

$$A_F = \frac{\pi C^2}{4} \tag{D15}$$

It was further assumed that when the helicopter had the slightest forward motion, and for all airspeeds exceeding zero, the zone length at the surface level, from the place where the advancing edge of the wake first intersected the surface to the place of full wake development, would be given by

$$L_F = d - \Delta d + C \cos\alpha \tag{D16}$$

where d is the wake development distance, assumed to have the values indicated in Figure D4, Δd is the "lag distance," behind the helicopter, to the place that the central streamline of the wake first intersects the ground surface, C is the cleared width of the trail at the full development place, and α is the "slope angle" of the central streamline of the wake, that is, the average angle, from vertical, over the first two thirds of the penetration distance of the free-air wake.

The last term of (D16) details omitted, took empirical account of the fact that the helicopter wake, with air-speed increase from zero to approximately 15 to 20 mph, would swing progressively from a position of normal incidence on the ground surface to a position where the wake began trailing across the surface. The second term of the equation took into account the fact that the length extent of the surface clearing would increase with decreasing flight altitude, as the helicopter approached the surface boundary and the wake was "impinged" more forcibly on this boundary, and would also increase with airspeed.

It was assumed that the cleared area at the surface level in the wake formation zone would have the shape of a half ellipse, such as illustrated in the insert sketch of Figure D8. This "half ellipse" was presumed to have the width dimension

C, at its open, truncated, down-stream end, which corresponded to the surface-level width of the cleared helicopter trail at the place of full wake development. Hence, with this assumption, the surface area of clearing in the trail formation zone (in the forward motion state) is given approximately by

$$A_F = \frac{\pi C L_F}{4} \quad . \tag{D17}$$

The trail length and area values shown in Figure D8 were determined in this manner.

D4.2.2 Turbulent-Diffusion Effects in the Removed Zone

The magnitude of the turbulent-diffusion effects that would tend to close in the cleared trails in the removed zone, can be assessed as follows.*

First, let us specify a cross-boundary velocity vector, $\vec{B} = b\,\vec{n}$, where $\vec{n}$ is a unit normal vector pointing outward from the flight path line. In a turbulent situation, where diffusion is causing the trail boundaries to converge toward centerline, the coefficient b will have negative sign and the vector B (vectors actually, since there are two trail boundaries) will be directed orthogonally inward, toward the flight path line. In such situations, it follows that the trail will close completely at a given place in the time

$$t_c = \frac{C}{2|\vec{B}|} \quad , \tag{D18}$$

where C is the initial trail width at formation time, that is, at the wake development time.

During this trail closing interval, t_c, the helicopter creating the trail, if it is flying in a straight line fashion at constant airspeed, will have moved a length distance

$$L_R = \omega\, t_c \tag{D19}$$

*Turbulent diffusion, dependent on the exact properties and relative quantities of the air on either side of a cloud air-clear air interface, can also operate to advance the clear-air region into the cloudy region, rather than the reverse as assumed above. Such expansion in the helicopter clearing situation would only be a temporary one, however, since the total region of clear air is small compared to the total region of cloudy air. As mixing proceeded with time, the cloud air properties would eventually dominate. The role of turbulent-diffusion in closing artifically-produced holes in clouds has been discussed by Elliott (1970). The aerodynamic factors involved in the dissipation of a vortex sheet by turbulence have been described by Andrews (1954).

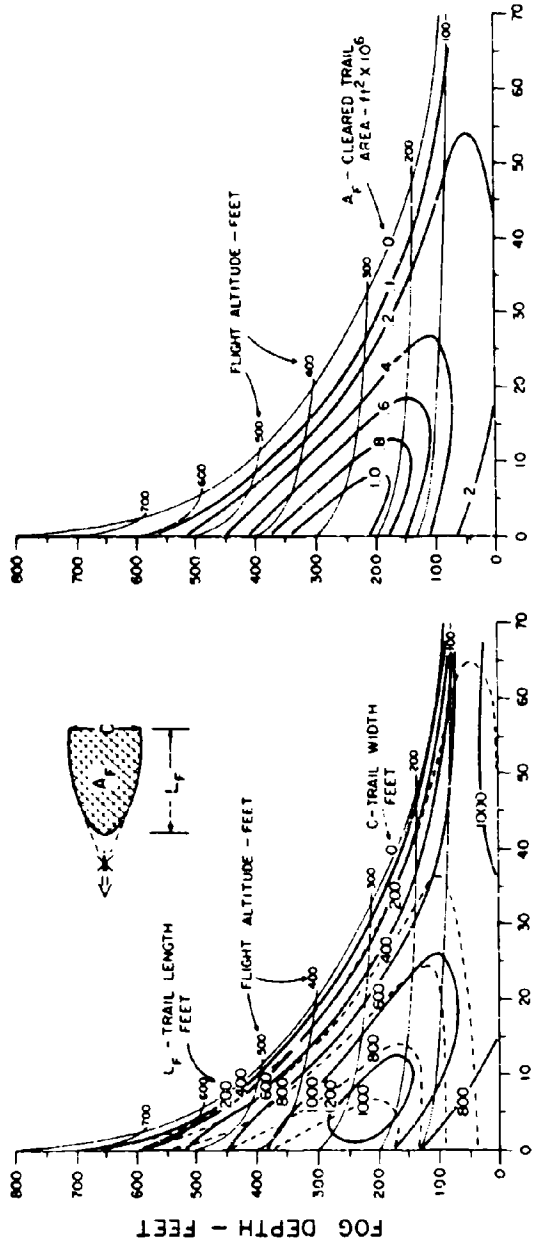

Figure D8. Length and Area Extent of Clearing in the Trail Formation Zone. See text for definition of zone and for description of how lengths and areas were determined

in the course direction. The trail behind the helicopter, behind the place of full wake development, will therefore taper backward to a closing point. Hence, in the plan view, the cleared trail behind the helicopter will have a triangular shape which has an area

$$A_R = \frac{L_R C}{2} \quad . \tag{D20}$$

This area A_R, plus the area A_F of the trail formation zone, is the largest area of clearing that the helicopter can continuously maintain. The clearing follows the motion of the helicopter in Lagrangian fashion. But, dependent on the particular conditions, clearing can also be maintained over a fixed ground location for substantial periods.

Equations (D18) to (D20) can be combined to obtain

$$A_R = \frac{\omega C^2}{4|\vec{B}|} \quad , \tag{D21}$$

which permits A_R to be determined in terms of airspeed, initial trail width and boundary velocity.

The cleared holes and trails created on certain days at certain times during the Lewisburg Program frequently closed-in within a matter of minutes after formation (refer to Table 1). It is estimated that the boundary closing velocity for these situations, called "turbulent situations," was about $-5\,\vec{n}$ ft/sec. On other occasions at Lewisburg, when clearing conditions were more favorable, the cleared holes and trails remained open for 5 to 10 min. It is estimated that the boundary closing velocity for these situations, referred to here as "slightly-turbulent situations," was about $-1\,\vec{n}$ ft/sec.

Computations were performed for these two types of situations, utilizing equations (D18) to (D21), the C values of Figure D7, and the cited $\vec{B}$ values. Information was obtained about the trail closing times (t_c) and about the trail lengths (L_R) and cleared areas (A_R) that could be maintained behind the helicopter. This information is presented in Figure D9. The two upper diagrams pertain to the "turbulent situation" while the lower diagrams pertain to the "slightly-turbulent situation." The first diagrams show the t_c and L_R values; the second show the A_R values.

The diagrams of Figure D10 indicate the total trail lengths,

$$L = L_F + L_R \quad , \tag{D22}$$

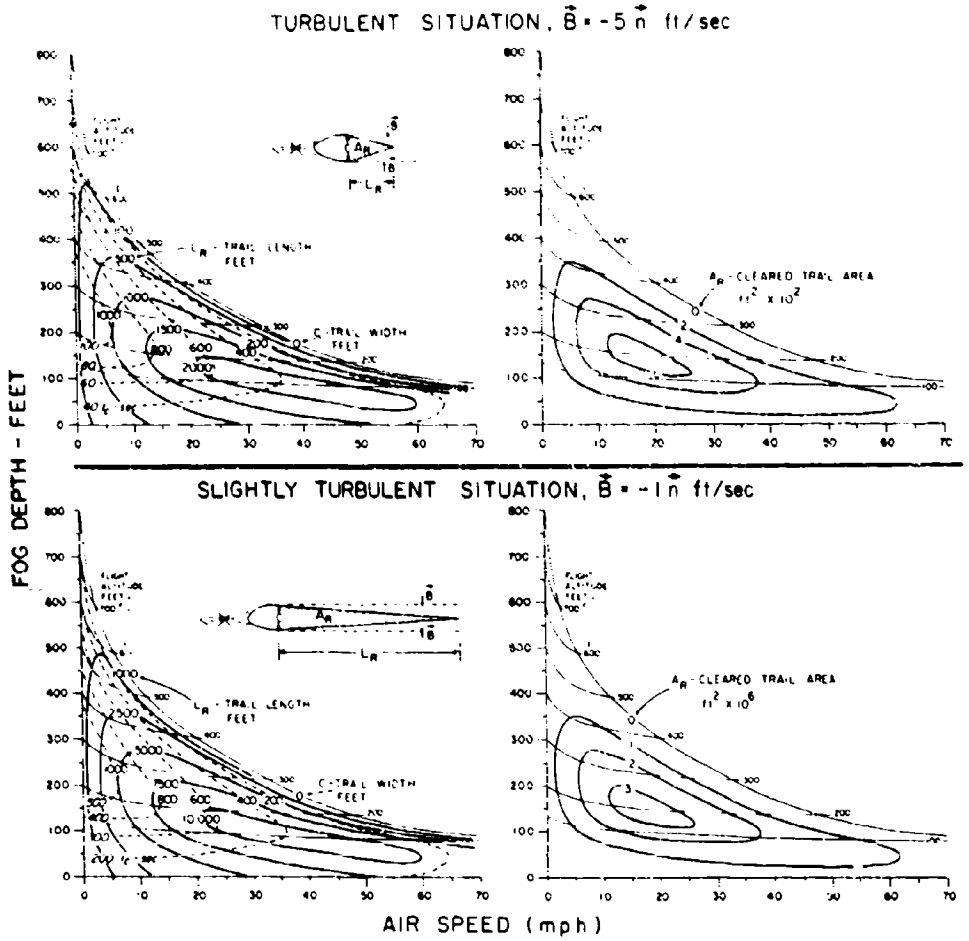

Figure D9. Length and Area Extent of Clearing in the Removed Zone, for Two Situations of Turbulent Diffusion. (See text for definition of zone and for discussion of diffusive, trail-closing effects.) The trail lengths (L_R) and cleared trail areas (A_R) within the removed zone pertaining to the text-described "turbulent situation" are shown in the upper diagrams. The lengths and areas pertaining to the "slightly turbulent situation" are shown in the lower diagrams

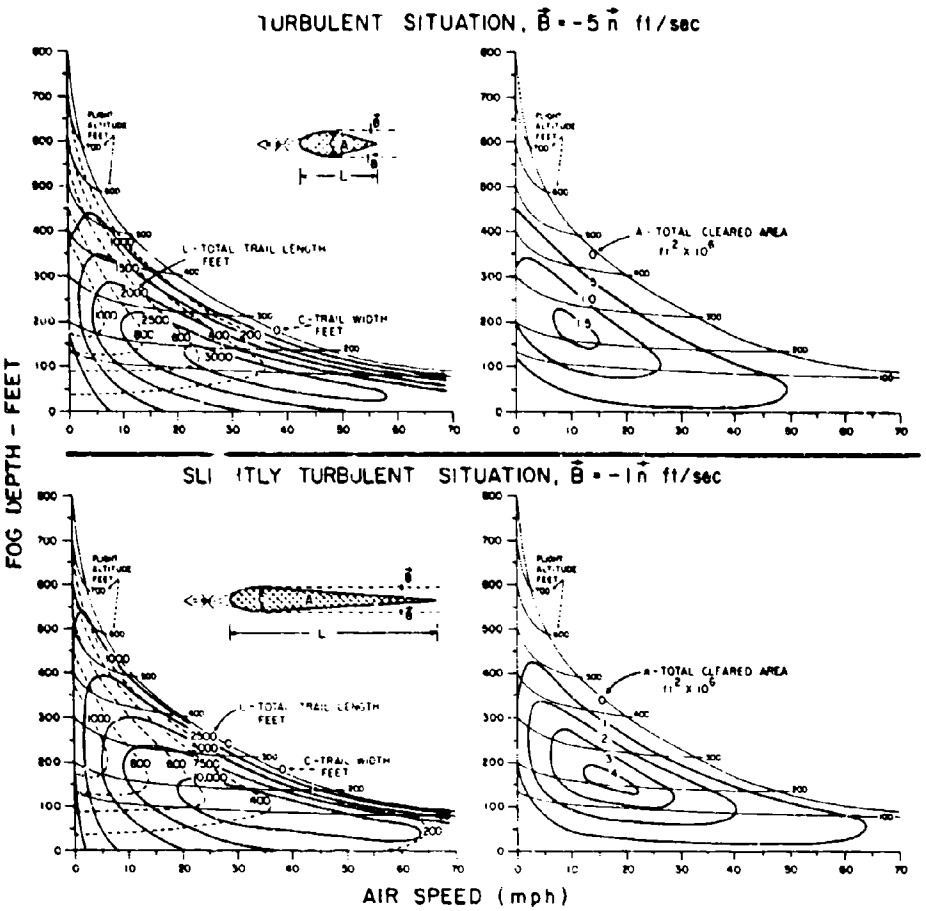

Figure D10. Total Length and Area Extent of Clearing, for Two Situations of Turbulent Diffusion. The trail lengths (L) and cleared trail areas (A) shown in the figure diagrams are the total values for both the trail formation zone and the removed zone. Those for the "turbulent situation" are shown at the top; those for the "slightly turbulent situation" at the bottom. These are the largest trail lengths and plan-areas of surface level clearing that can be continuously maintained by a medium-sized helicopter under the assumed turbulent conditions

and total cleared areas,

$$A = A_F + A_R \quad , \tag{D23}$$

which result from the contributions of both the "trail formation zone" and the "removed zone."

The Figure D10 diagrams, when compared, illustrate the large clearing differences that can occur due to differences in turbulent diffusion. The trail lengths and cleared areas are some 2.5 to 3.5 times larger in the slightly-turbulent situation than in the turbulent situation.

The trail lengths in the turbulent situation extend only about 3000 ft behind the helicopter, at maximum, which is a length substantially shorter than that of an airport runway. Likewise, the maximum area of clearing in the turbulent situation is only about 1.5×10^6 ft^2. This is slightly larger than the runway-area of a small airport, such as the Lewisburg Airport (area = 0.9×10^6 ft^2), but is much smaller than the runway-area of a major airport, such as Kennedy International or Travis AFB (areas $\cong 2.5 \times 10^6$ ft^2). Under very turbulent conditions, such as the illustrated, a single helicopter cannot clear the runway of even a small-size airport, much less that of a major airport. The helicopter can theoretically create a cleared zone of larger areal extent that the runway area; this is true. However, because of the trail length restriction, such cleared zone could never be created with dimensions equaling the runway dimensions, no matter how the helicopter is flown. Multiple helicopters would be required.

In the illustrated "slightly turbulent situation," on the other hand, the diagrams reveal that a single helicopter, if flown efficiently to minimize the turning times between successive clearing passes and to account properly for wind-drift problems, should be able to maintain continuous clearing of fog, having the assumed properties and depths indicated in the diagrams, over the runway of a small-size airport, or to create clearings of operationally-useful size over part of the runway at a major airport.

The diagrams of Figure D10, reflect and illustrate the general limits of clearing experience acquired during the Lewisburg Program (which can be ascribed to turbulent-diffusion effects).

D4.2.3 Solar-Heating Effects in the Removed Zone

Reference was made previously to certain solar heating effects that would tend to widen the cleared trails made by helicopters. These effects are now defined as those that result from the solar heating of the ground surface within the cleared zones, which effects give rise to convective circulations that operate

to expand the clearing boundaries. Such effects were noted by Plank (1969), in the Smith Mountain Program; they were also observed during the Lewisburg Program. They occurred primarily, it seemed, with fog of relatively-small LWC and/ or during the periods just prior to the natural dissipation stage of the fog.

The trail widening effects of solar heating operate to counter-balance the closing-in effects of turbulent diffusion. Hence, dependent on the particular situation, solar heating might operate either (a) to retard the turbulent rates of trail closure or (b) to so "dominate" the rate balance as to cause the trails to expand with time. In other words, the equation for plan-area clearing with solar heating influence included is given by

$$A_R = \left(\frac{dA_R}{dt} + \frac{dA_s}{dt} + \frac{dA_t}{dt} \right) t_f \quad , \tag{D24}$$

where dA_r/dt is the trail formation rate (refer to the values indicated in the lower diagram of Figure D7), dA_s/dt is the trail expansion rate due to solar heating, dA_t/dt is the trail closing-in rate due to turbulent-diffusion, and t_f is the total flight time. It would be correct to refer to dA_s/dt and dA_t/dt as being expansion and closing-in tendencies, rather than rates.

Two situations can be postulated, one in which the opposed widening-closing tendencies are in exact balance, that is $dA_s/dt = dA_t/dt$, and one in which the solar widening tendencies are predominant. In the first situation, the net boundary velocity, B', is zero, which means that the cleared trails in the removed-zone have constant width (equal to the width C of the fully-developed trail). The length of the cleared trails is given by

$$L_R = \omega t_f \quad , \tag{D25}$$

and the plan-area extent of the clearing, from (D24) is specified by

$$A_R = \frac{dA_r}{dt} t_f = \omega C t_f \quad . \tag{D26}$$

In the second situation, the helicopter trails in the removed zone will tend to "flair outward" with distance behind the helicopter. Assuming that the net boundary velocity in such situations has the value B' = + 1 n ft/ sec (a value that would reasonably account for the observations of the AFCRL Smith Mountain Program), the cleared trails will have the same length, given by (D25) above, and the cleared area A_R will be the sum of the two separate areas, A_{R_1}, as specified by (D26)

and $A_{R_2} = \omega|\vec{B}'|t_f^2$, which is the area of the "outflaring part" of the trail. In other words, the total cleared area in the removed zone will be given by

$$A_R = \omega t_f (C + |\vec{B}'| t_f) \quad , \tag{D27}$$

where $\vec{B}'$ is left unevaluated, that is, without the value $+ 1\ \vec{n}$ ft/sec inserted, to indicate clearly that the second equation term has area units.

Equations (D26) and (D27) were used to determine the cleared areas for these two situations which corresponded to the C values of Figure D7 and to the fog-depth and airspeed ranges of the figure. The total flight time of clearing, t_f, was assumed to be 300 sec (5 min) and the helicopter was presumed to be flying in a straight line fashion at constant airspeed. The isoline values of A_R for the two situations are shown in Figure D11, in the diagrams at the left. Those for the $\vec{B}' = 0$ situation, which is referred to as the "neutral situation," are shown in the upper diagram. Those for the $\vec{B}' = + 1\ \vec{n}$ ft/sec situation, which is labeled the "solar-expansion situation," are indicated in the lower diagram.

The two right hand diagrams of Figure D11 show the total areas of clearing, as specified by equations (D22) and (D23), which are the sum of the areas A_F, of the trail formation zone, and the areas A_R, just referenced, of the removed zone.

The cleared areas for the situations shown in Figure D11 may be compared with those for the turbulent situations shown in Figure D10. A common flight time, or total clearing time, of 300 sec is assumed for comparison purposes. The total cleared areas in the "solar-expansion situation," after 300 sec of flight, range up to about 30 times larger than the maintainable cleared areas of the "turbulent situation."

Whereas maximum area-clearing in turbulent situations is achieved at relatively small airspeeds, maximum clearing in situations of solar heating is achieved at larger airspeeds.

To summarize the work of this appendix, the important point illustrated is that the normal, to-be-expected variations of turbulent diffusion and solar-heating effects in the atmosphere can readily cause helicopter fog-clearing differences as large as a factor of approximately 30, depending on the particular circumstances.

D4.3 Dependence of Clearing Variations on Moisture Conditions

The discussions and illustrations to this point have been based on the assumption that fog-clearing would extend throughout the total wake volume. It was emphasized that this would occur only in conditions in which the fog LWC and/or

the relative humidity of the overlying clear air had comparatively small values, smaller than about 0.05 gm/m^3 and 85 percent, as stated before.

Under conditions of larger fog LWC and/or larger relative humidity aloft, helicopter clearing of the fog becomes more difficult. Clearing in such cases will extend not throughout the total wake volume but only within a portion of this volume. The width of the cleared trails will become smaller than the width of the helicopter wake and the vertical extent of the clearing will become smaller than the wake thickness. It is important to note that some degree of clearing should be anticipated even under the most unfavorable moisture conditions. This is the conclusion drawn from the results of the Lewisburg Program.

The problems of determining and describing the clearing differences arising from variations of the two cited moisture parameters are truly formidible ones. This is an area for future research. There is little specific information and the gross, general nature of the differences, can only be indicated.

With increased values of either or both of the referenced parameters, in a given situation where the flight conditions are assumed to be optimum as cited previously (refer to Figure D7), and all parameters other than moisture parameters are assumed constant, observational data suggest that helicopter clearing will tend to "undercut" and "create tunnels in" the fog. The vertical extent of the clearing above the ground, T_c, will be smaller than the wake thickness, T, by some proportionality constant, ν, such that

$$T_c = \nu T \ . \qquad \text{(D28)}$$

Likewise, the width of the cleared trails or tunnels, C, will be decreased relative to the wake width, S, in the manner stated previously in equation (D11) and illustrated in Figure D12.

Under the "worst" moisture conditions of the Lewisburg Program, that is, with fog LWC = 0.25 gm/m^3 and near-saturated relative humidities in the clear-air aloft, the K values of equation (D11) were determined to be about 0.5 to 0.7 and the ν values of the above equation were estimated to be about 0.12 to 0.35.* Thus, to a gross first approximation, the clearing situation under these conditions was generally analogous to that illustrated in the diagram of Figure D13, which has been drawn for an assumed K value of 0.6, with $\nu = 0.22$ (see footnote below).

---

*The ν values will decrease more rapidly than the K values, with increases of fog LWC and/or relative humidity aloft, since, as can be deduced from the lower diagrams of Figure D1 and from the lower right hand diagram of Figure D6, the clearing will tend to occur primarily along the course of the most-rapidly moving air of the downwash-groundwash circulations. Hence, clearing failure will happen first in the upward moving portions of the wake beyond the circulation centers and will severely curtail the vertical extent of the clearing while not decreasing the width extent to nearly the same proportional degree. It is suggested that ν and K might be interrelated, approximately as $\nu = K^3$.

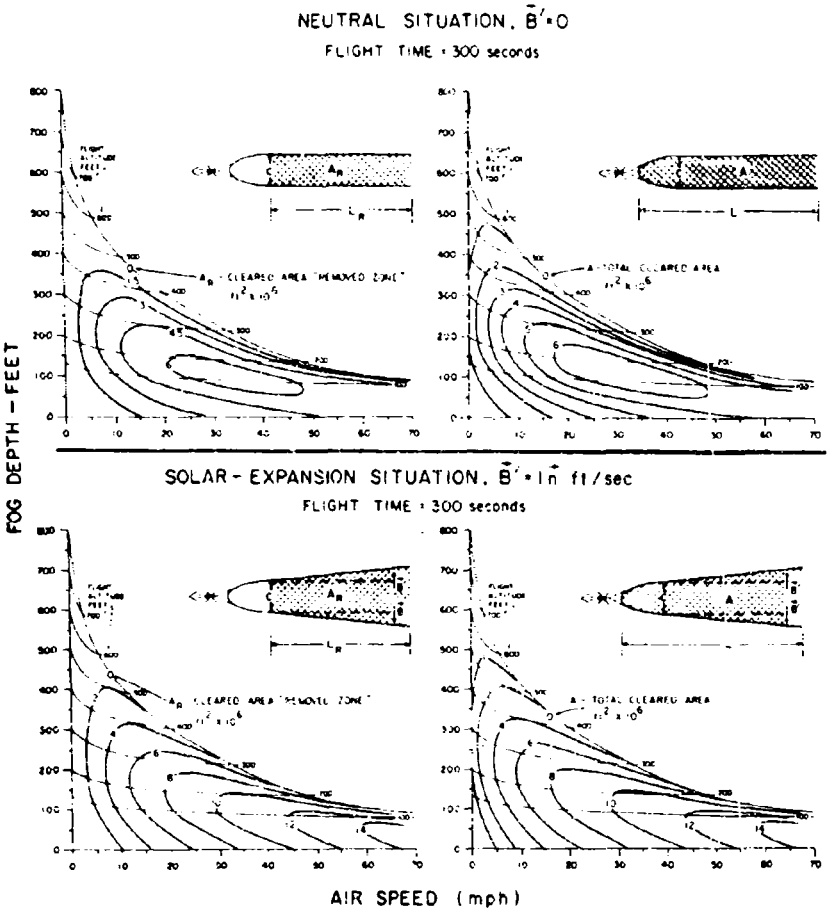

Figure D11. Cleared Areas for Two Situations of Solar-Heating. Solar-heating of the ground surface within helicopter cleared zones will, under conditions noted in the text, tend to widen the clearings. The cleared-trail areas in a "neutral situation" (where solar widening effects exactly counterbalance diffusive closing-in effects) are indicated in the upper diagram; the areas within the removed zone (A_R) are shown at the left; the total areas (A), of both the formation zone and removed zone, are shown at the right. Similarly, the lower diagrams illustrate the A_R and A values that would be expected in a particular, text-defined situation of clearing expansion

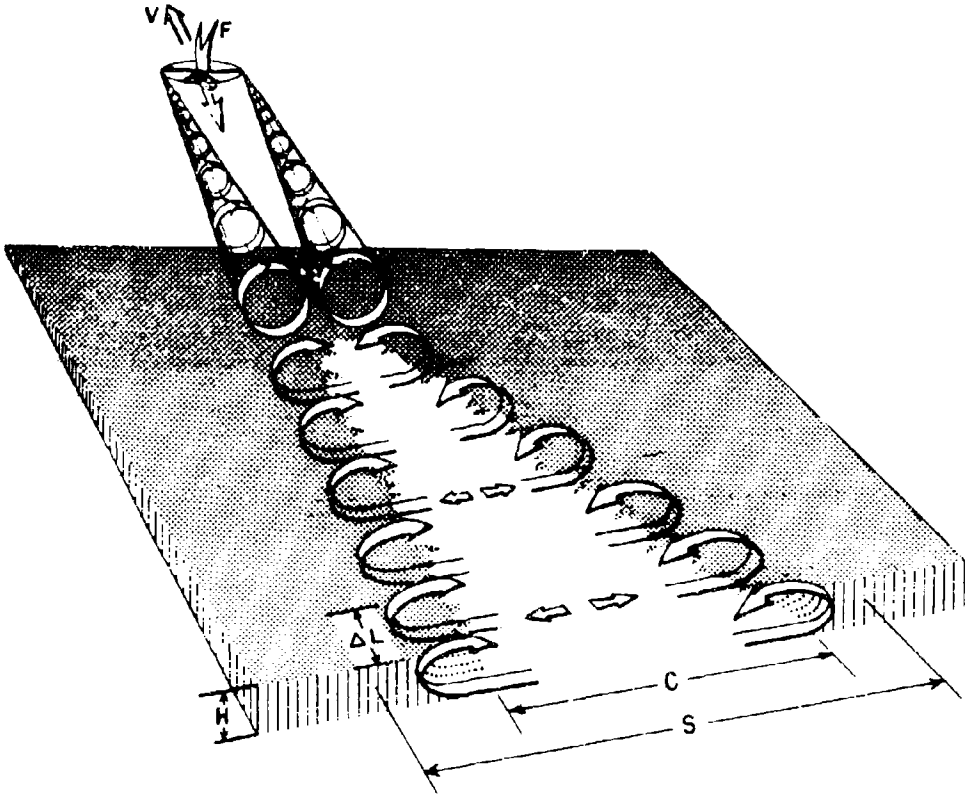

Figure D12. Schematic Drawing of the Vortex Circulations of a Helicopter Wake Which is "Trailed Across" the Ground Surface in the Manner Required for Fog-Clearing. The lateral spreading of the vortex centerlines when the wake is "impinged on" the surface boundary is indicated. The helicopter wake at the surface level will extend out to the approximate width dimension S, as shown. It is assumed here that the wake thickness exceeds the fog-depth H. The trail of clearing left by the helicopter will have a width C, which is some fractional part of the wake width S, dependent on the particular meteorological conditions

This diagram, when compared to the upper diagram of Figure D7, indicates the type of clearing differences that seemingly occur with variation of the moisture conditions. The range of difference, in terms of helicopter ability to accomplish plan-area clearing at the surface level, is about a factor of four.

This factor of four, when combined with the factor of 30, cited earlier as possibly arising from turbulent-diffusion and solar-heating effects, suggests that helicopter fog-clearing results in different atmospheric situations might vary totally by more than two orders of magnitude, dependent on the particular meteorological factors.

D5. DISTRIBUTION PATTERNS OF SEEDING AGENT

Droplet or particulate matter released from helicopters will not be distributed homogeneously throughout the total wake unless release is accomplished from all points of the rotor disk area (in the hover state) or from all points of a diameter line of the rotor, oriented normal to the fuselage axis (in the forward motion state). Release from other line or point sources will result in decreased distribution efficiency of variable degree.

Material released from a helicopter in the hover or forward motion states in situations where the wake intersects or trails across a surface boundary will tend to follow the streamlines indicated in Figures D1 and D6. The material, if the source is located along the rotor axis (in the hover state) or along the vertical centerline plane of the fuselage (in the forward motion state), will first be transported downward toward the surface, will then be spread laterally outward across the surface, just above the surface, and will finally be carried upward in the wake regions beyond the vortex centers. Terminal deposition of the material into the air or fog will occur within updraft regions of the wake in both motion states of the helicopter.

Efforts to obtain distribution enhancement in the hover state by the use of line or area sources, rather than point sources, would appear impractical. The material, almost irrespective of the design of the release device, unless it provides for release over an area nearly equal to the rotor disk area, will primarily follow the travel sequence cited above and will ultimately be deposited into the air or fog in the updraft portions of the wake.

If point-source release is employed in the forward motion state, and if the point is located along the vertical centerline plane of the fuselage, or close to this plane, the possibility exists that the material might sometimes be distributed preferentially into the trailing vortex of the "right hand side" of the helicopter, and sometimes into the vortex of the left side. This preferential, perhaps

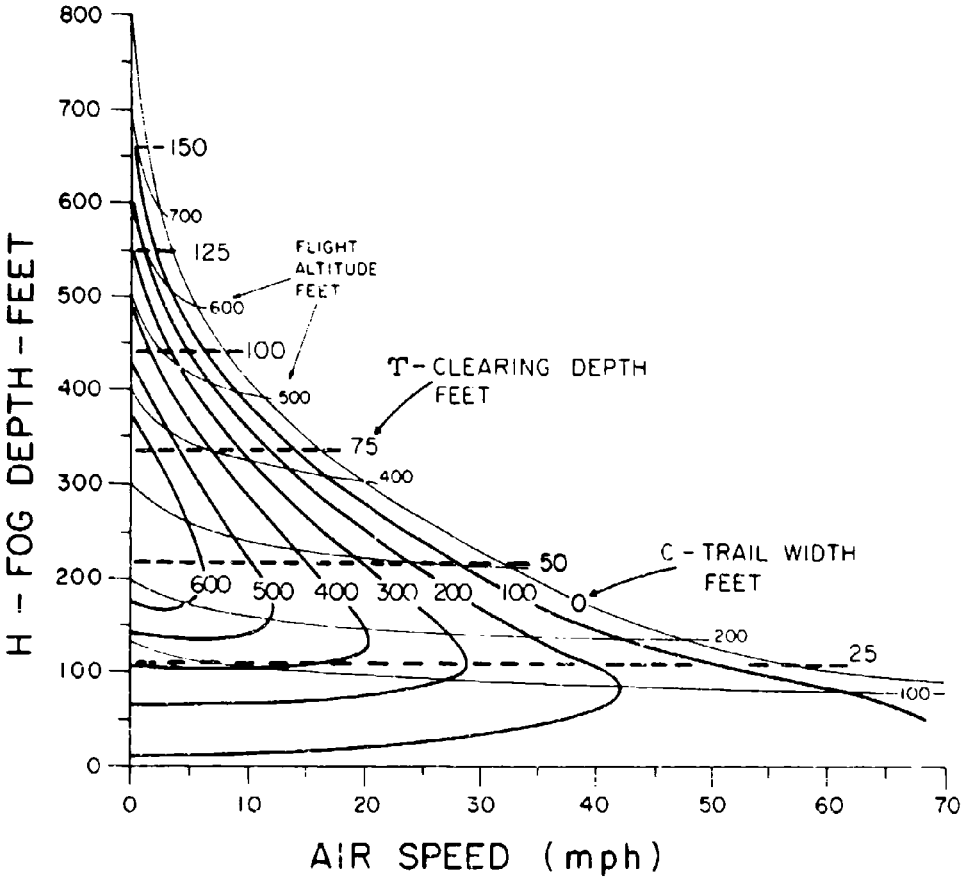

Figure D13. Approximate Width-Thickness Dimensions of Clearing Under Meteorological Conditions Representative of the "Worst" Encountered During the Lewisburg Program. The surface widths of the cleared trails shown in this diagram were reduced by about 40 percent relative to the widths that occurred under the optimum cloud-physics conditions illustrated in the upper left hand diagram of Figure D6. Moreover, the clearing did not extend vertically throughout the entire fog depth but only to distances above the surface that were about 20 percent of the fog depth, as indicated by the dashed, horizontal isolines of T, shown above. Hence, clearing, under the "worst" meteorological conditions, tended to "undercut" and create "tunnels" in the fog layers

alternating, distribution pattern can occur if the helicopter flight path is not maintained perfectly "straight and level" and in parallel alignment with the flight altitude wind. It is known that this sort of preferential distribution occurs with aircraft wakes. It is logical to anticipate that it can also occur with helicopter wakes.

At least two point sources, or a line source, are required to obtain a reasonably balanced and homogeneous distribution of material in the forward motion state. These sources should be located, or extend, a sufficient lateral distance on either side of the vertical centerline plane of the fuselage (some 2 to 6 ft would perhaps be sufficient) so that the material, on release, will be rapidly transported into the primary, central circulations of the trailing vortices, where it should become thoroughly distributed throughout most of the total wake within a relatively-short travel distance behind the helicopter. The necessity for lateral source displacement to achieve effective distribution of material into aircraft wakes has been discussed and demonstrated by Reed (1953).

An example of a near-optimum distribution of material into a helicopter wake is provided in the photographs of Figure D14. These photographs show the results of smoke tests conducted by the Naval Rework Facility, San Diego, California, with an H-3 helicopter flying at approximately 15 knots airspeed about 150 ft above the ocean surface. The smoke was produced by injecting some 1 to 2 gallons of oil per min into the last combustion stages of the engines. It is seen that the smoke has been well distributed into the wake from the exhaust port release places, which were located about four ft outboard from the fuselage centerline plane. The excellent distribution was due primarily to the off-axis location of the ports, to their close proximity to the rotor, and to the fact that the smoke was expelled laterally, with the exhaust gases, at large initial velocity. It also resulted, in part, because the smoke particles, being extremely small, followed the circulation streamlines with considerable fidelity.

The following conclusions are drawn from the work of this appendix which pertain to cloud seeding experiments that might be conducted employing helicopters as agent-release vehicles.

If seeding agents are to be released from helicopters in fog situations for purposes of extending the normal areas of downwash clearing, it is essential that the size-distribution properties of the agent be designed properly to account for the fact that terminal deposition of the agent into the fog will occur primarily within updraft regions of the wake which have been deflected by the surface boundary.

If the seeding objective is merely to distribute seeding agent as widely as possible along a trail crossing a fog-top surface (with the agent then falling gravitationally through the fog), the helicopter will have to be flown slowly across the top at flight altitudes appreciably higher than the altitudes discussed and illus-

trated herein. Flight altitudes will be required which insure that only the very bottom part of the trailing wake intersects the fog-top surface.*

Formidable verification problems are forseen for experiments having the first objective. It will be very difficult, without considerable, sophisticated instrumentation, to isolate and assess the normal clearing and visibility-enhancement effects of the helicopter from the added contributions of the seeding agent. Seeding with dissicant-type agents should improve visibility along the lateral boundaries of the wake trails and contribute to the persistence of the trails. But the degree of the improvement will be difficult to measure.

---

*These altitudes can be determined from Figure D4, by adding the wake penetration distances shown there to the anticipated fog-thickness values of the particular situations. The approximate distribution widths of the agent can also be assessed from the diagram, from the wake-width values of the fully-developed state.

Figure D14. Photographs of Smoke Tests Conducted by the U.S. Navy Which Reveal Nearly the Full Dimensional-Extent of the Wake of a Slow-Flying, H-3 Helicopter. The helicopter was flying above an ocean surface at an altitude of about 150 ft at approximately 15 knots airspeed. Smoke was produced as described in the text and was dispensed from the engine exhaust ports located on either side of the fuselage. Four views are shown which were recorded from an observational aircraft that was circling the helicopter. The distribution of the smoke into the wake from these release places was excellent, as can be seen

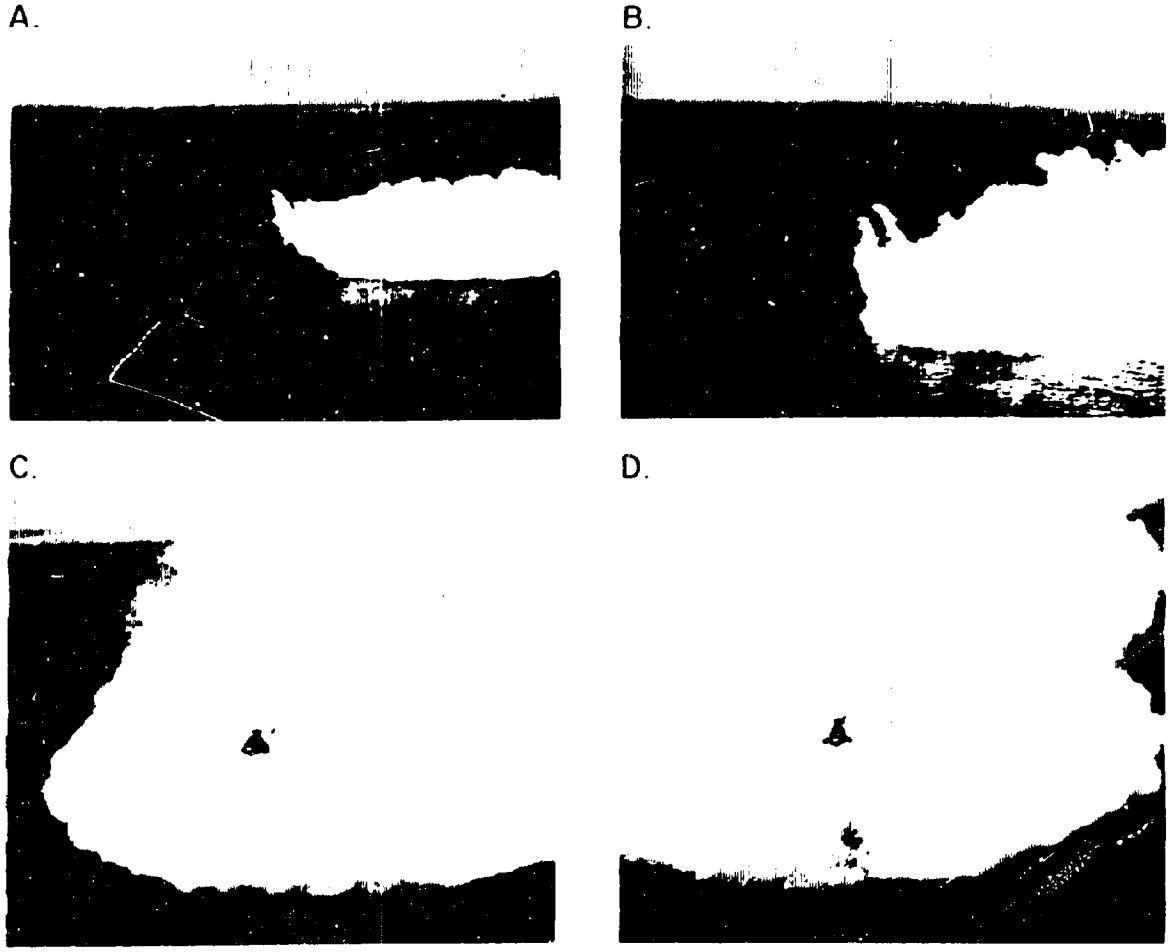
A.
B.
C.
D.

Appendix References

Andrews, D. R. (1954) A Flight Investigation of the Wake Behind a Meteor Aircraft, with Some Theoretical Analysis, Royal Aircraft Establishment Tech. Note AERO 2283, Ministry of Supply, London, England.

Bakke, P. (1957) An experimental investigation of a wall jet, J. Fluid Mech. 2 (Part 5):467-472.

Bradshaw, P. and Love, E. M. (1959) The Normal Impingement of a Circular Air Jet on a Flat Surface, Aeronautical Research Council, A. R. C., 21, 268, Fluid. Mech. Sub-Committee No. 2856, P. L. 20, 18 September 1959 (CVA Lib. No. 45, 884).

Elliott, W. P. (1970) The Role of Diffusion in Closing Artificially Produced Holes in Clouds. Unpublished manuscript, Dept. of Oceanography, Oregon State Univ., Submitted to J. Appl. Meteor.

Galuert, M. B. (1956) The wall jet, J. Fluid Mech., 1 (Part 6):625-643.

Gessow, A. and Meyers, G. C. (1952) Aerodynamics of the Helicopter, The MacMillan Company.

Hall, M. G. (1961) A theory for the core of a leading-edge vortex, J. Fluid Mech. 11:209-228.

Hohler, D. J. (1966) An Analytical Method of Determining General Downwash Flow Field Parameters for V/STOL Aircraft, Tech. AFAPL-TR-66-90, Air Force Systems Command, Wright Patterson AFB, Ohio.

Mangler, K. W. and Weber, J. (1967) The flow field near the centre of a rolled-up vortex sheet, J. Fluid Mech. 30:177-196.

Pai, S. K. (1954) Fluid Dynamics of Jets, D. Van Nostrand Co. pps 7-9, 78-79.

Plank, V. G. (1969) Clearing ground fog with helicopters, Weatherwise 22:91-98.

Plank, V. G. and Spatola, A. A. (1969) Cloud modification by helicopter wakes, J. Appl. Meteor. 8:566-578.

Poreh, M. and Cermak, J. E. (1959) Flow Characteristics of a Circular Submerged Jet Impinging Normally on a Smooth Boundary, 6th Conf. on Fluid Mech., The University of Texas, pp 198-207.

Appendix References

Prandtl, L. and Tietjens, O.G. (1934) Fundamentals of Hydro and Aeromechanics, United Engineering Trustees, Inc., Dover Publication Co. (1967).

Reed, W.H. III (1953) An Analytical Study of the Effect of Airplane Wake on the Lateral Dispersion of Aerial Sprays, NACA Tech. Note 3032, Langley Aeronautical Laboratory, Virginia.

Schlichting, H. (1955) Boundary Layer Theory, McGraw-Hill, New York.

Smith, J.H.B. (1966) Theoretical work on the formation of vortex sheets, Prog. in Aeron. Sci. (Edited by Kuchemann, et al) Pergamon Press, Oxford, 7.

Spreiter, J.R. and Sacks, A.H. (1951) Rolling up of the trailing vortex sheet and its effect on the downwash behind wings, J. Aero. Sci. 18:21-32.

DOCUMENT CONTROL DATA - R&D

(Security classification of title, body of abstract and indexing annotation must be entered when the overall report is classified)

1. ORIGINATING ACTIVITY (Corporate author)
Air Force Cambridge Research Laboratories (CRH)
L. G. Hanscom Field
Bedford, Massachusetts 01730

2a. REPORT SECURITY CLASSIFICATION
Unclassified

2b. GROUP

3. REPORT TITLE
FOG MODIFICATION BY USE OF HELICOPTERS

4. DESCRIPTIVE NOTES (Type of report and inclusive dates)
Scientific. Interim.

5. AUTHOR(S) (First name, middle initial, last name)
Plank, Vernon G.
Spatola, Alfred A.
Hicks, James R.

6. REPORT DATE	7a. TOTAL NO. OF PAGES	7b. NO. OF REFS
28 October 1970		12

8a. CONTRACT OR GRANT NO.		9a. ORIGINATOR'S REPORT NUMBER(S)
b. PROJECT, TASK, WORK UNIT NOS.	7605-01-01	AFCRL-70-0593
c. DOD ELEMENT	62101F	9b. OTHER REPORT NO(S) (Any other numbers that may be assigned this report) ERP No. 335
d. DOD SUBELEMENT	681000	

10. DISTRIBUTION STATEMENT
1-This document has been approved for public release and sale; its distribution is unlimited.

11. SUPPLEMENTARY NOTES	12. SPONSORING MILITARY ACTIVITY
TECH, OTHER	Air Force Cambridge Research Laboratories (CRH) L. G. Hanscom Field Bedford, Massachusetts 01730

13. ABSTRACT

Results of helicopter clearing experiments conducted at the Greenbrier Valley Airport, Lewisburg, West Virginia, during the period 7 to 29 Sept 1969, are presented and discussed. Thirty-five hover experiments and runway-clearing experiments were performed on 10 separate days with fog layers ranging from 125 to 525 ft in depth. The hover experiments, which were successful in virtually all cases, yielded clearings that varied from 400 to 2800 ft in length extent. The largest clearings occurred with the shallowest fog during tests conducted within one hour or so of the natural dissipation time of the fog. The runway-clearing experiments were successful in clearing the full 6000 ft extent of the runway on two occasions, were partially successful on four occasions and were unsuccessful on 12 occasions. Six helicopter landings were accomplished through artificially-created clearings.

Quantitative information is described concerning the wake penetration distances of the helicopters, the steady-state clearing times, the total entrainment (mixing) values and the persistence times of the clearings following helicopter departure from the test sites. The temperature, humidity and wind speed values within the cleared zones are also given for certain of the experiments.

The wake characteristics and fog-clearing capabilities of helicopters are discussed and illustrated in a separate appendix.

DD FORM 1 NOV 65 1473

Unclassified

Security Classification

14. KEY WORDS	LINK A		LINK B		LINK C	
	ROLE	WT	ROLE	WT	ROLE	WT
Fog clearing Fog modification Helicopter fog clearing Helicopter wakes Wakes, helicopter Weather modification						

Unclassified

Security Classification

☆ U. S. GOVERNMENT PRINTING OFFICE: 1970—433-274/12